DISSERTATIONES SCHOLAE DOCTORALIS AD SANITATEM INVESTIGANDAM
UNIVERSITATIS HELSINKIENSIS

VEIJO SALO

LIPOGENIC SUBDOMAINS OF THE ER: THE ROLE OF SEIPIN

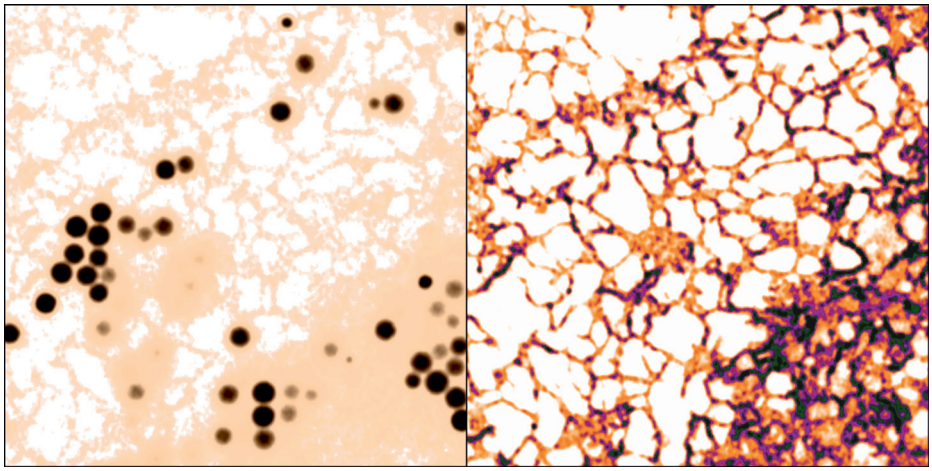

DEPARTMENT OF ANATOMY
STEM CELLS AND METABOLISM RESEARCH PROGRAM
FACULTY OF MEDICINE
DOCTORAL PROGRAMME IN BIOMEDICINE
UNIVERSITY OF HELSINKI

MINERVA FOUNDATION INSTITUTE FOR MEDICAL RESEARCH

Department of Anatomy
Stem Cells and Metabolism Research Program
Faculty of Medicine
Doctoral Program in Biomedicine
University of Helsinki

Minerva Foundation Institute for Biomedical Research

LIPOGENIC SUBDOMAINS OF THE ER: THE ROLE OF SEIPIN

Veijo Salo

DOCTORAL DISSERTATION

To be presented for public examination with the permission of the Faculty of Medicine of the University of Helsinki, in lecture hall 1 of Haartman Institute, Haartmaninkatu 3, on the 17th of April, 2020 at 12 o'clock.

ISSN 2342-3161 (print
ISSN 2342-317X (online)
ISBN 978-951-51-5956-4 (paperback)
ISBN 978-951-51-5957-1 (PDF)

Dissertationes Scholae Doctoralis Ad Sanitatem Investigandam Universitatis Helsinkiensis
No. 24/2020

Cover image: Lipid droplets and the endoplasmic reticulum.
Cover layout by Anita Tienhaara

Supervisors	Academy Professor Elina Ikonen, MD, PhD Department of Anatomy Stem Cells and Metabolism Research Programme Faculty of Medicine University of Helsinki, Finland Minerva Foundation Insitute for Medical Research Docent Maarit Hölttä-Vuori, PhD Department of Anatomy Stem Cells and Metabolism Research Programme Faculty of Medicine University of Helsinki, Finland Minerva Foundation Insitute for Medical Research
Reviewers	Professor Eeva-Liisa Eskelinen, PhD Division of Biochemistry University of Turku, Finland Professor Pedro Carvalho, PhD Sir William Dunn School of Pathology University of Oxford, United Kingdom
Opponent	Professor Robert V. Farese, Jr, MD, PhD Department of Molecular Metabolism Harvard T.H. Chan School of Public Health Department of Cell Biology Harvard Medical School, Boston, MA, United States
Custos	Professor Matti Airaksinen, MD, PhD Department of Anatomy Neuroscience Center Faculty of Medicine University of Helsinki, Finland

The Faculty of Medicine uses the Urkund system (plagiarism recognition) to examine all doctoral dissertations

TABLE OF CONTENTS

1 ABBREVIATIONS

aa	amino acid
AFM	atomic force microscopy
AGPAT	1-acylglycerol-3-phosphate acyltransferase
AH	amphipathic helix
AID	auxin-induced degradation
AKT	protein kinase B
ATGL	adipose tissue triglyceride lipase
BPY	Bodipy (boron-dipyrromethene)
BSCL	Berardinelli-Seip congenital lipodystrophy
CARS	Coherent Anti-Stokes Raman Scattering
CCT-alpha	CTP:phosphocholine cytidylyltransferase alpha,
CDP-choline	cytidine phosphatate choline
CGI-58	comparative gene identification-58
CHOP	CCAAT/enhancer binding protein
CLEM	correlative light and electron microscopy
CNS	central nervous system
Co-ip	co-immunoprecipitation
CPT	choline phosphotransferase
CRISPR	clustered regularly interspaced short palindromic repeats
DAG	diacylglycerol
DGAT	acyl-CoA:diacylglycerol acyltransferase
DGAT	diacylglycerol acyltransferase
DGK	diacylglycerol kinase
DHAP	dihydroxyacetone phosphate
DHAP	dihydroxyacetone phosphate.
dpf	days post fertilization
EM	electron microscopy
ER	endoplasmic reticulum
ERAD	ER-associated degradation
ET	electron tomography
FA	fatty acid
FACS	fluorescence-activated cell sorting
FC	unesterified cholesterol
FITM2	fat storage-inducing transmembrane protein 2
FRAP	fluorescence recovery after photobleaching
FRET	fluorescence resonance energy transfer
GDH	glycerol-3-phosphate dehydrogenase
GK	glycerol kinase
GPAT	glycerol-3-phosphate acyltransferase
GUV	giant unilamellar vesicle
HDR	homology directed repair

HH	hydrophobic helix
HPTLC	high performance thin layer chromatography
HSL	hormone sensitive lipase
IAA	indole-3-acetic acid
KO	knockout
LAL	lysosomal acid lipase
LD	lipid droplet
LPC	lyso phosphatidylcholine
LPCAT	lysophosphatidylcholine acyltransferase
LPDS	lipoprotein deficient serum
MAG	monoacylglycerol
MDH	monodansylpentane
MEF	mouse embryonic fibroblasts
MGL	monoacylglycerol lipase
NE	nuclear envelope
NL	neutral lipid
OA	oleic acid
P-choline	choline phosphatate
PA	phosphatidic acid
PAP	phosphatidic acid phosphatase
PC	phosphatidylcholine
PCR	polymerase chain reaction
PE	phosphatidylethanolamine
PELD	progressive encephalopathy with or without lipodystrophy
PEMT	phosphatidylethanolamine-N-methyltransferase
PI	phosphatidylinositol
PKA	protein kinase A
PL	phospholipid
PLA	phospholipase A
PLD	phospholipase D
PPAR-γ	peroxisome proliferator activated receptor-γ
PSD	phosphatidylserine decarboxylase
PSS	phosphatidylserine synthase
PUFA	poly-unsaturated fatty acid
SE	sterol esterase
SIM	structured illumination microscopy
siRNA	small interfering RNA
SKO	seipin knockout
SLD	supersized LD
STORM	stochastic optical reconstruction microscopy
TM	transmembrane
TAG	triacylglycerol

2 LIST OF ORIGINAL PUBLICATIONS

This thesis is based on the following publications, which are referred to in the text by their Roman numerals.

I. Hölttä-Vuori M*, **Salo VT***, Ohsaki Y, Suster ML, Ikonen E (2013). Alleviation of seipinopathy-related ER stress by triglyceride storage. *Hum Mol Genet*. 2013 Mar 15;22(6):1157-66. *Equal contribution

II. **Salo VT**, Belevich I, Li S, Karhinen L, Vihinen H, Vigouroux C, Magré J, Thiele C, Hölttä- Vuori M, Jokitalo E, Ikonen E (2016). Seipin regulates ER-lipid droplet contacts and cargo delivery. *EMBO J.* 2016 Dec 15;35(24):2699-2716.

III. **Salo VT***, Li S*, Vihinen H, Hölttä-Vuori M, Szkalisity A, Horvath P, Belevich I, Peränen J, Thiele C, Somerharju P, Zhao H, Santinho A, Thiam AR, Jokitalo E, Ikonen E (2019). Seipin facilitates triglyceride flow to lipid droplet and counteracts droplet ripening via ER contact. *Dev Cell.* 2019 Aug 19;50(4):478-493.e9. *Equal contribution.

3 ABSTRACT

With the growing obesity epidemic and associated metabolic comorbidity, molecular insights into the regulation of body fat are needed to facilitate the development of new therapeutic avenues. Cells store excess energy mostly as neutral lipids (NLs), inside fat-specialized organelles called lipid droplets (LDs). Recent research has revealed LDs to be metabolic hubs involved in many cellular processes, such as lipid metabolism, protein degradation and endoplasmic reticulum (ER) homeostasis. There is also increasing evidence for links between LD biology and many human pathologies, including cardiovascular disease, cancer progression and non-alcoholic fatty liver diseases. Thus, detailed understanding of LD biology should be beneficial for tackling these disease states.

LDs are intracellular storage organelles consisting of a core of NLs surrounded by a phospholipid monolayer. Their biogenesis begins in the ER, with accumulation of NL lenses within the ER bilayer that subsequently grow and bud into the cytosol as distinct organelles. This process is thought to occur in specialized ER subdomains with a unique lipid and protein composition, but a detailed understanding of the earliest steps of LD biogenesis is still lacking. After formation, LDs retain an intimate relationship with their mother organelle, the ER, through ER-LD contacts. Deciphering the functionalities and topological features of these specialized membrane contact sites is crucial for understanding LD biology.

Seipin is an oligomeric ER transmembrane protein implicated in LD assembly, ER-LD contacts and adipocyte development. Mutations in seipin give rise to three disease states in humans: a severe form of congenital lipodystrophy (BSCL2), a motor neuron disease called seipinopathy and a fatal neurodegenerative disease called Celia's encephalopathy. Work from various model systems has shown seipin to be crucial for LD biogenesis, and seipin has been found to localize at ER-LD contacts in yeast cells. In addition, disruption of seipin function halts the adipogenic differentiation programme at early stages. However, the molecular function of seipin remains unclear.

In this thesis, using advanced cell biological techniques in cultured human cells and zebrafish larvae, we sought to expand the understanding of the function of seipin and how mutations in seipin lead to human disease.

In the first study, we focused on the seipinopathy-linked seipin mutant, N88S-seipin, which is known to form cellular aggregates of likely misfolded protein. We found that overexpression of this variant leads to cellular ER stress, reduced NL storage and decreased voluntary swimming in zebrafish larvae. Upon increasing NL stores, these defects were alleviated and the protein was translocated from the ER to regions flanking LDs. Furthermore, increasing cellular LDs also alleviated ER stress induced

by tunicamycin, a drug which leads to the accumulation of misfolded proteins in the ER. We propose that increasing LDs may aid cells in coping with misfolded proteins.

We next focused on deciphering the function of seipin in LD formation and ER-LD contacts. Endogenously tagged seipin was found to localize stably at ER-LD contact sites, but a BSCL2-linked mutant failed to do so. Knockout (KO) of seipin led to the formation of numerous tiny LDs, which failed to grow and recruit protein and lipid cargo from the ER. Furthermore, whilst all LDs in control cells were connected to the ER, as assessed by 3D-electron microscopy, seipin KO lead to a subset of LDs completely detaching from the ER. The remaining LDs of seipin KO cells also showed morphologically aberrant and dysfunctional ER-LD contacts. As similar defects were also evident in BSCL2 patient fibroblasts, we propose that seipin is crucial for the formation of ER-LD contacts and cargo delivery.

Finally, we found that seipin can determine the site where LDs start to form, as relocalization of seipin to a subdomain of the ER, the nuclear envelope, was sufficient to relocalize LD biogenesis to that site. Utilizing electron tomography, we found that seipin-mediated ER-LD contact sites display a uniform neck-like architecture, suggesting that the seipin oligomer may structurally restrain this site. Seipin was also required for ER-LD contact maintenance, as acute removal of seipin from ER-LD contacts lead rapidly to strikingly heterogonous LD growth. Further studies revealed that this heterogeneity arises via a biophysical ripening process, with NLs partitioning from smaller to larger LDs via LD-ER contacts. These data suggest seipin-mediated ER-LD contacts function as a valve facilitating NL flux from the ER to LDs, thus allowing controlled LD growth.

Overall, this thesis provides insight into the function of the lipodystrophy protein seipin and the mechanisms of LD formation. Our data suggest that the ER-LD nexus could be considered as a joint system, with continuous bidirectional trafficking of cargo occurring via ER-LD contacts mediated by seipin. Future work will be required to investigate the molecular intricacies of the lipid flux occurring at ER-LD contacts. A deeper understanding of LD biology will aid in the development of new therapeutics for a number of pathologies, including seipin-related disorders and common metabolic disturbances.

4 REVIEW OF THE LITERATURE

4.1 LIPID DROPLET STRUCTURE AND FUNCTION

LDs are intracellular neutral lipid (NL) storage organelles. They consist of a core of NLs surrounded by a phospholipid (PL) monolayer, which also harbors LD-associated proteins. Their main function is to store NLs that can later be used for membrane constituents and energy production. In addition, they serve as protective organelles safeguarding cellular homeostasis, by acting as storage depots for reactive fatty acids and misfolded proteins (Henne et al., 2018). LDs are generated *de novo* in the endoplasmic reticulum (ER) and dynamically remodeled in size and numbers in response to the metabolic needs of the cell.

Though earliest reports of LDs in the literature stem from electron microscopy (EM) images decades ago (Angermüller and Fahimi, 1982; Kobayashi et al., 1973), LDs were long thought as passive cytosolic inclusions. The discovery and characterization of the perilipin family of proteins as LD-specific proteins in the 1990s (Brasaemle et al., 1997; Greenberg et al., 1991; U et al., 1999) and subsequent advances in live cell imaging (Martin and Parton, 2006; Targett-Adams et al., 2003) have led to the appreciation of LDs as dynamic organelles and metabolic hubs (Farese and Walther, 2009; Gao and Goodman, 2015).

Besides playing crucial roles in the regulation of intracellular energy storage and fatty acid trafficking, LDs are involved in a surprisingly wide array of intracellular processes, including modulation of the endoplasmic reticulum (ER) stress response, host-pathogen interactions and protein degradation and storage (Welte, 2015). Consequently, there is increasing evidence for the importance of LD biology in various human disease states, including metabolic disorders, non-alcoholic fatty liver disease, cardiovascular disease and neurodegenerative diseases (Henne et al., 2018; Krahmer et al., 2013a; Pennetta and Welte, 2018). Furthermore, mutations in proteins implicated in LD biology lead to rare but devastating congenital disorders such as lipodystrophy and NL storage disease (Melvin et al., 2019). Thus, understanding the basic molecular mechanisms of LD assembly could lead to new therapeutic avenues for these pathologies.

4.1.1 LDs are neutral lipid depots covered by a phospholipid monolayer

Although adipocytes are the professional fat storing cells in many eukaryotic species, virtually all eukaryotic and at least some prokaryotic cells have the capability to retain excess NLs and store them in LDs (Pol et al., 2014). The basic structure of LDs is conserved amongst species, and indeed much of current knowledge of LD biology stems from research done in model organisms such as *Saccharomyces cerevisiae*

(hereafter, yeast) and *Drosophila melanogaster* (Radulovic et al., 2013). Even bacteria store NLs in LDs, which participate in their DNA regulation (Congyan et al., 2017).

LDs vary greatly in size, from the 100-nm sized LDs of bacteria and yeast to 10-100-μm sized LDs of mammalian adipocytes (Pol et al., 2014). They are also highly dynamic in nature, shrinking and growing in size and number in response to the metabolic status of the cell (Kassan et al., 2013; Rambold et al., 2015). Furthermore, to enable efficient delivery of LD constituents to different cellular compartments, LDs are actively trafficked in the cell, with the help of microtubules, the ER and the actin cytoskeleton (Herms et al., 2015; Li et al., 2012; Pfisterer et al., 2017; Salo et al., 2016).

The basic structure of LDs consists of a NL core surrounded by a PL coat (**Figure 1**). The core is composed of hydrophobic NLs, mainly triacylglycerols (TAG) and cholesterol esters (CE). The composition of NLs in LDs varies between cell types, with adipocyte LDs harboring mainly TAG, whilst steroidogenic cell and macrophage LDs consist primarily of CE (Walther and Farese, 2012). In specialized cells, LDs may also contain high amounts of other hydrophobic compounds. For example, retinyl esters are found in high abundance in hepatic stellate cell LDs (Blaner et al., 2009). The core is devoid of proteins, which cannot be accommodated in this highly hydrophobic environment. Recent cryo-EM imaging suggest that at least in certain conditions, the NL core may be organized in various layers due to phase-separation of TAG and CE molecules (Mahamid et al., 2019).

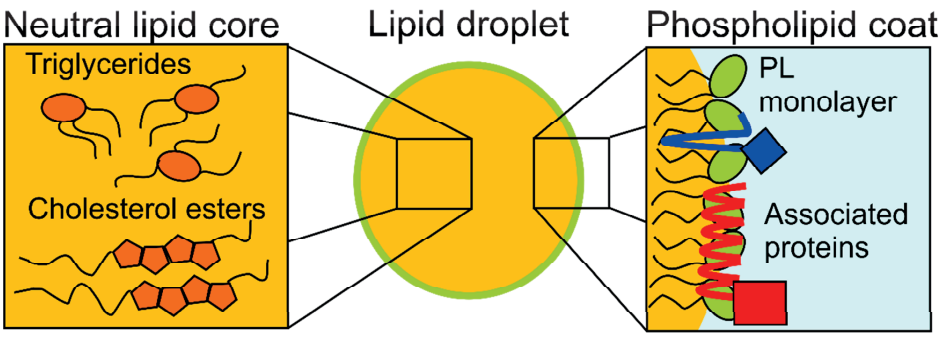

Figure 1 LDs consist of a core of NLs surrounded by a PL monolayer which harbors LD-associated proteins. Modified from (Salo and Ikonen, 2020).

In a biophysical sense, LDs can be viewed as oil-in-water emulsions, with NLs giving rise to a hydrophobic oil phase in the aqueous cytoplasm. To stabilize this emulsion, a protective surfactant layer is required to reduce the surface tension of the emulsion and stabilize it. In the context of cellular LDs, the amphiphilic PL coat acts as such a surfactant, reducing the surface tension of LDs and thus promoting their stability (Thiam et al., 2013a). Early EM studies indicated that the PL coat covering the NL

core of LDs is a single monolayer (Tauchi-Sato et al., 2002). This makes LDs unique, as they are not surrounded by a PL bilayer like other cellular organelles. In the LD monolayer, the hydrophobic acyl chains of the PLs face the NLs, whilst the hydrophilic groups face the aqueous cytoplasm, resulting in an energetically favorable system (Thiam et al., 2013a).

The PL composition of the LD monolayer affects the properties of the LDs, regulating LD stability and protein recruitment to LDs (Fei et al., 2011a; Thiam et al., 2013a). In most cell systems, the LD monolayer is mainly composed of phosphatidylcholine (PC), phosphatidylethanol (PE) and phosphatidylinositol (PI) as well as other, less-abundant phospholipids and lyso-phospholipids. The LD monolayer also harbors diacylglycerol (DAG), although due to its hydrophobicity this lipid may also be stored in the LD core. The cylindrical PC, with no intrinsic curvature preference, is a more stabilizing surfactant than PE, which has a small headgroup compared to its acyl chains and thus exposes more of the hydrophobic phase of the LD to the aqueous cytoplasm. Decreasing the PC/PE ratio of the PL monolayer would then result in a less stable emulsion. Indeed, reducing LD PC levels leads to increased LD coalescence, and this is one mechanism governing LD growth (Haider et al., 2018; Krahmer et al., 2011). Interestingly, the LD monolayer differs in lipid composition from that of its mother organelle, the ER, likely due to different activities of PL remodeling enzymes in these compartments (Tauchi-Sato et al., 2002).

4.1.2 Proteins are embedded in the LD monolayer

While the NL core of LDs is devoid of proteins, the LD monolayer can accommodate proteins. Due to their high lipid content and the ensuing low density, LDs are relatively easy to isolate from cells using centrifugation: they tend to float (Goodman, 2018). Studies utilizing subcellular fractionation techniques followed by mass spectrometry have yielded information on the proteome of LDs (Beller et al., 2008; Bersuker et al., 2018; Guo et al., 2008; Krahmer et al., 2013b). Although the LD proteome is diverse and dependent on the cell type in question and the metabolic status of the cells, a common set of circa 100-150 high-confidence LD proteins in mammalian cells has emerged (Olzmann and Carvalho, 2019). In line with the key role of LDs in lipid metabolism, a many of these proteins are involved in lipogenesis and lipolysis, including enzymes and their accessory proteins. However, LDs also harbor proteins involved in a wide spectrum of other processes, including ER-associated degradation (ERAD), host-pathogen interactions, cytoskeleton regulation and vesicular trafficking (Goodman, 2018).

4.1.3 Proteins target to LDs from the ER and the cytoplasm

It is currently unclear what mediates protein targeting specifically to LDs. In contrast to proteins localized to other cellular compartments, such as the ER or mitochondria, LD proteins lack a specific targeting signal embedded in their sequence (Farese and Walther, 2009). However, though no universal “zip code” for LD associated proteins

has been identified, proteins targeting to LDs can roughly be separated into two classes (class I and class II LD proteins, **Figure 2**) based on their mode of association with the LD monolayer (Kory et al., 2016).

Class I proteins are typically found in both the ER and the LD monolayer. They harbor hydrophobic helical sequences, which typically adopt a "hairpin" topology with both N- and C-termini facing the cytoplasm. These proteins lack bulky luminal domains, allowing for both ER *bilayer* and LD *monolayer* localization, and the trafficking between the two organelles could thus occur via diffusion on ER-LD membrane bridges (Wilfling et al., 2014). Proteins in this category include many lipogenic enzymes, such as ACSL3, DGAT2 and GPAT4 (Jacquier et al., 2011; Kassan et al., 2013; Kory et al., 2016; Wilfling et al., 2013). In the absence of LDs, these proteins typically reside in the ER, but upon LD generation they become highly enriched at LDs. How this LD enrichment arises is unclear, but may involve selective removal of ER-associated proteins by proteasomal degradation (Bersuker et al., 2018; Ruggiano et al., 2016). The hydrophobic hairpin topology alone is not sufficient to ensure LD-targeting, as many proteins containing such motifs are not recruited to LDs, implicating other, so far undiscovered regulatory mechanisms (Olzmann and Carvalho, 2019).

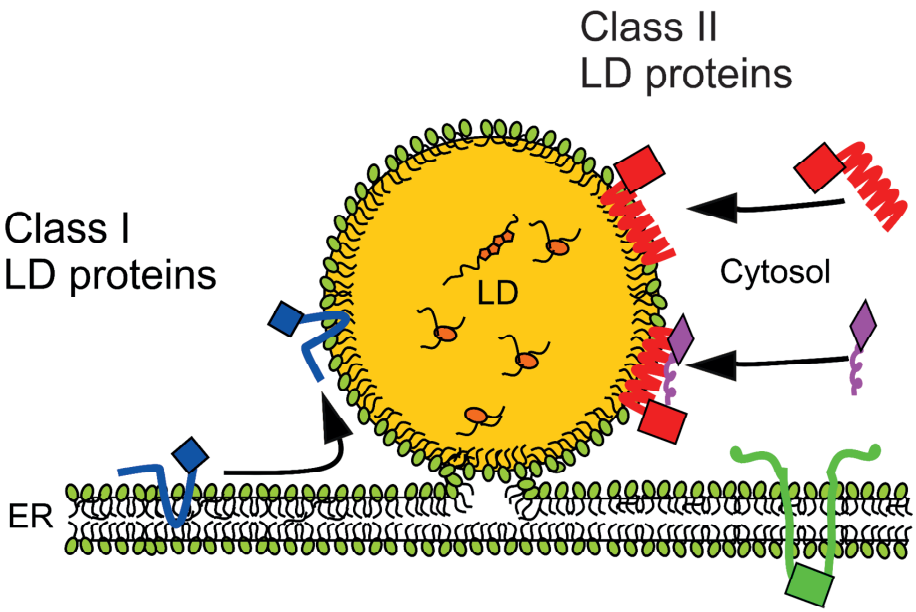

Figure 2 Class I LD proteins (blue) target to LDs via ER-LD contact and often harbor hairpin topology. Class II LD proteins target to LDs from the cytoplasm via AHs (red), or via protein-protein interactions with other LD proteins (magenta). Transmembrane proteins with ER luminal domains (green) cannot target to the LD surface.

Class II proteins target LDs directly from the cytosol. These include proteins such as the PC-synthesizing enzyme CCT-alpha and members of the perilipin family (Kory et al., 2016; Krahmer et al., 2011; Rowe et al., 2016). These typically associate with the LD monolayer through amphipathic helices (AH), which are characterized by a segregation of hydrophobic and polar residues to the opposite sides of the helix (Giménez-Andrés et al., 2018). When bound to the LD monolayer, the hydrophobic side of the AH is presumed to face the acyl chains of the monolayer, while the hydrophilic side faces the cytosol, resulting in an energetically favorable situation. However, many AH containing proteins do not target to LDs and even LD-targeting AHs differ in length and other biophysical properties, raising the question what ultimately determines their localization to LDs (Olzmann and Carvalho, 2019).

Finally, some class II proteins associate with LDs through their interactions with other LD proteins. Examples include the lipase HSL, which associates with LDs through interaction with perilipin 1 (Sztalryd and Brasaemle, 2017), and *Drosophila* histones, which are recruited to LDs by the protein Jabba (Li et al., 2012). Furthermore, a subset of LD proteins likely interact with LDs through lipid anchors or lipid modifications, examples including the palmitoylated protein ELMOD2 (Suzuki et al., 2015), the small GTPase Rab18 (Martin et al., 2005) and the phosphatidic acid (PA) sensing LD-LD contact site protein CIDEA (Barneda et al., 2015).

4.1.4 LD functions

The main function of LDs is to store energy in the form of energy-dense NLs in times of excess and release upon demand. This is especially evident in adipocytes, the professional fat-storing cells, whose entire cytoplasm is often filled up by 1-2 giant LDs. Upon lipolysis of TAG to free fatty acids (FA) and beta-oxidation of the FAs in mitochondria, a high amount of energy in the form of ATP can be generated. Besides energy storage, liberated FAs and glycerol moieties can be converted to PL molecules to be used for membrane biosynthesis. In addition to these crucial tasks, LDs are also engaged in numerous other cellular processes (**Figure 3).**

4.1.4.1 LD are fatty acid buffering organelles

Free FAs are reactive molecules, and as such they are detrimental to cellular functions and membranes at high concentrations (De Carvalho and Caramujo, 2018). Buffering of intracellular FA levels by esterification and storage in LDs helps cells to be protect themselves from such high concentrations and the ensuing lipotoxicity (Listenberger et al., 2003; Petschnigg et al., 2009). Indeed, numerous studies have demonstrated LDs to be crucial for lipotoxicity alleviation in various systems, ranging from yeast to human liver cells (reviewed in (Gluchowski et al., 2017; Kohlwein, 2010)).

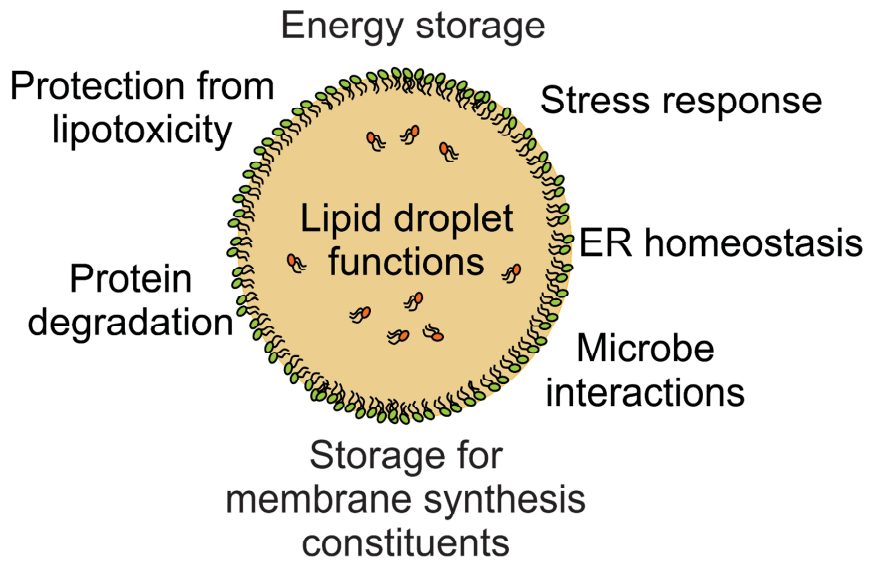

Figure 3 LDs are involved in many cellular processes. Modified from (Salo and Ikonen, 2020).

A recent example of this at a cellular level comes from studies of adipocytes. During active lipolysis high amounts of FAs are rapidly liberated and, somewhat surprisingly, high fractions of these free FAs are actually quickly re-esterified into *de novo* generated LDs to protect the ER from lipotoxic stress (Chitraju et al., 2017). Analogously, on the organismal level, neuronal glial cells have been shown to protect nearby neurons from cellular stress by channeling reactive, easily oxidizable polyunsaturated FAs (PUFAs) and other FAs to be stored in LDs (Bailey et al., 2015; Ioannou et al., 2019).

LDs can also be viewed as sensors of cellular nutrient status, which has been most studied in yeast (Henne et al., 2018). In yeast, during plentiful nutrient availability, LD abundance somewhat counterintuitively decreases, as cells shuffle lipids to membrane synthesis to enable active cell proliferation (Markgraf et al., 2014). Upon switch to nutrient-depleted conditions, LD abundance initially increases, and lipids are now shuffled to storage in LDs, which can later aid cell survival in the ongoing nutrient-poor environment (Barbosa et al., 2015; Seo et al., 2017). Similarly, in mammalian cells, amino acid starvation leads to increased LD generation concomitantly with the activation of autophagy (Nguyen et al., 2017; Rambold et al., 2015). The FAs required for the *de novo* LD generation in these nutrient-poor conditions likely arise from membrane hydrolysis by the autophagic machinery (Nguyen et al., 2017; Rambold et al., 2015), and the cells are again utilizing LDs as a way to robustly buffer intracellular FA levels. Thus, LDs allow cells to cope with changes in the energy availability of their milieu.

4.1.4.2 LDs and ER homeostasis

As a separate, but intimately ER-connected membrane compartment (Salo and Ikonen, 2019), LDs also play important roles in ER homeostasis and have been linked to ER stress pathways (Hapala et al., 2011). Activation of ER stress has been shown to induce LD formation and LD-deficient cells are more sensitive to perturbations of ER membrane homeostasis (Chitraju et al., 2017; Fei et al., 2009; Velázquez et al., 2016). In line with this, ERAD machinery components have often been detected in LD proteomes (Bersuker and Olzmann, 2017) and LDs constitute an additional compartment for ER proteostasis (Bersuker et al., 2018; Olzmann et al., 2013). For some proteins, such as human C18orf32 and yeast Dga1, localization to LDs may help to prevent their degradation by ERAD, whilst their ER-localized pool is more susceptible to degradation (Bersuker et al., 2018; Ruggiano et al., 2016). Thus, as a separate membrane compartment LDs allow an additional layer of control for membrane protein homeostasis.

It has also been postulated that LDs may serve as sequestration sites for misfolded ER proteins and/or aid in their translocation from the ER lumen to the cytosol (Hölttä-Vuori et al., 2013; Ploegh, 2007). However, thus far this has been shown only for a small subset of ERAD substrates (Hartman et al., 2010; Ohsaki et al., 2008) and recent studies suggest that LD biogenesis is not a general requirement for ERAD (Olzmann and Kopito, 2011; To et al., 2017). Overall, however, LDs appear to aid in keeping up ER homeostasis, and this likely stems from the fact that they provide an additional, biophysically unique and rapidly malleable membrane compartment, expanding the cell's repertoire for homeostasis.

4.1.4.3 LDs are involved in apoptosis and pathogen control

Besides being a storage organelle for NLs needed for energy production, recent studies have demonstrated LDs to serve as storage site for other lipophilic compounds. The most studied of these is the role of LDs for retinyl ester storage in hepatic stellate cells (Blaner et al., 2009), where dynamic remodeling of these stores is involved in stellate cell activation after liver injury (Molenaar et al., 2017). LDs were also shown to store acylceramide, a hydrophobic ceramide metabolite, linking LD homeostasis to apoptosis control (Senkal et al., 2017). A recent study also reported that macrophage LDs sequester the lipophilic anti-tubercular antibiotic bedaquiline, and thus facilitate its delivery to *Mycobacterium tuberculosis,* which consumes cellular LDs for its needs (Greenwood et al., 2019). Interestingly, increasing LD abundance improved the efficacy of the drug in clearing out *Mycobacterium* infection, suggesting avenues for improving therapeutics in the future.

LD biology has been linked to numerous pathogens, both bacteria and viruses (Melo and Dvorak, 2012). Typically, infection with these pathogens, ranging from viruses (e.g. hepatitis C virus), to bacteria (e.g. *E. Coli* and *Mycobacterium tuberculosis)* and parasites (e.g. *Toxoplasma gondii)* lead to an increase in LD formation. The molecular

mechanisms leading to this phenomenon are still under investigation, but LDs likely play a dual role: they are both part of the host defense mechanism and advantageously used by the invading pathogen (Pereira-Dutra et al., 2019). Examples of the former include the role of LD-associated histones helping developing *Drosophila* embryos in fighting off bacterial infection (Anand et al., 2012). On the other hand, especially intracellular bacteria and parasites appear to use *de novo* generated LDs as a nutrient source (Barisch and Soldati, 2017). Finally, viruses also use the LD, and nearby LD-associated ER membranes as platforms for virus assembly and replication (Laufman et al., 2019; Lee et al., 2019; Miyanari et al., 2007).

4.2 LIFE CYCLE OF LDS

LDs are dynamic organelles, constantly changing in size and number in response to the metabolic status of the cell (**Figure 4)**. LD life cycle can be segregated into a series of discrete steps, starting with initial biogenesis in the ER, followed by further growth and finally, breakdown (Thiam and Beller, 2017). In cellular studies, to harmonize these processes and enable quantitative study, cells are often treated with high concentrations of extracellular lipids (such as oleic acid, OA) to facilitate LD biogenesis and, conversely, switched to nutrient-poor conditions to facilitate LD breakdown. However, even in these conditions individual LDs within cells are variable in size and can be thought of as being in a different stage of their life cycle, and this is likely even more pronounced *in vivo*.

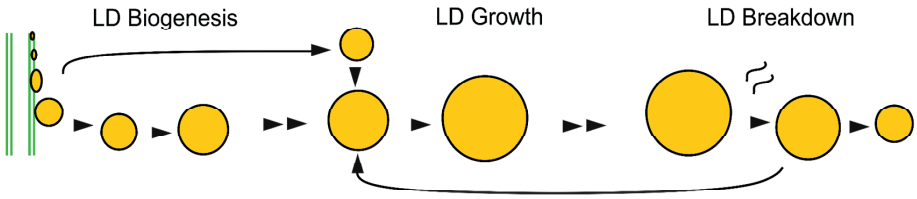

Figure 4 Life cycle of LDs. Modified from (Salo and Ikonen, 2020).

4.2.1 Lipid biosynthesis pathways

LD biology is closely linked to the intertwined NL and PL synthesis pathways (summarized in **Figure 5**) (Pol et al., 2014). These biochemical pathways are regulated at each step by numerous factors, including substrate availability, enzymatic activities and specificities as well as subcellular localization of the enzymes, leading to a complex regulatory network. This matter is further complicated by the fact that typically, a number of enzymes can catalyze each enzymatic step, albeit at different efficiencies. As most of our knowledge on specific enzymes stems from *in vitro* work, it is a future challenge to characterize the reaction rates of these pathways *in vivo* (Takeuchi and Reue, 2009).

This aforementioned complexity is well exemplified in the pathway for *de novo* TAG generation (**Figure 6)**. Here, enzymes of GPAT, AGPAT, PAP/lipin and DGAT families work in concert to esterify glycerol and activated FAs to finally form TAG. Many of the intermediates, such as DAG and PA can instead be reshuffled to alternative metabolic fates, including PL synthesis, or utilized as secondary messenger molecules (Vance, 2015). For each enzymatic step, 2-10 putative enzymes exist in mammalian cells, although there likely exists a high degree of cell-type and subcellular localization dependent variation (Takeuchi and Reue, 2009). Except for the primarily cytosolic lipins, these enzymes are mostly membrane-bound proteins,

residing in the ER, mitochondrial membranes and, in some cases, on the LD monolayer (Wang et al., 2017).

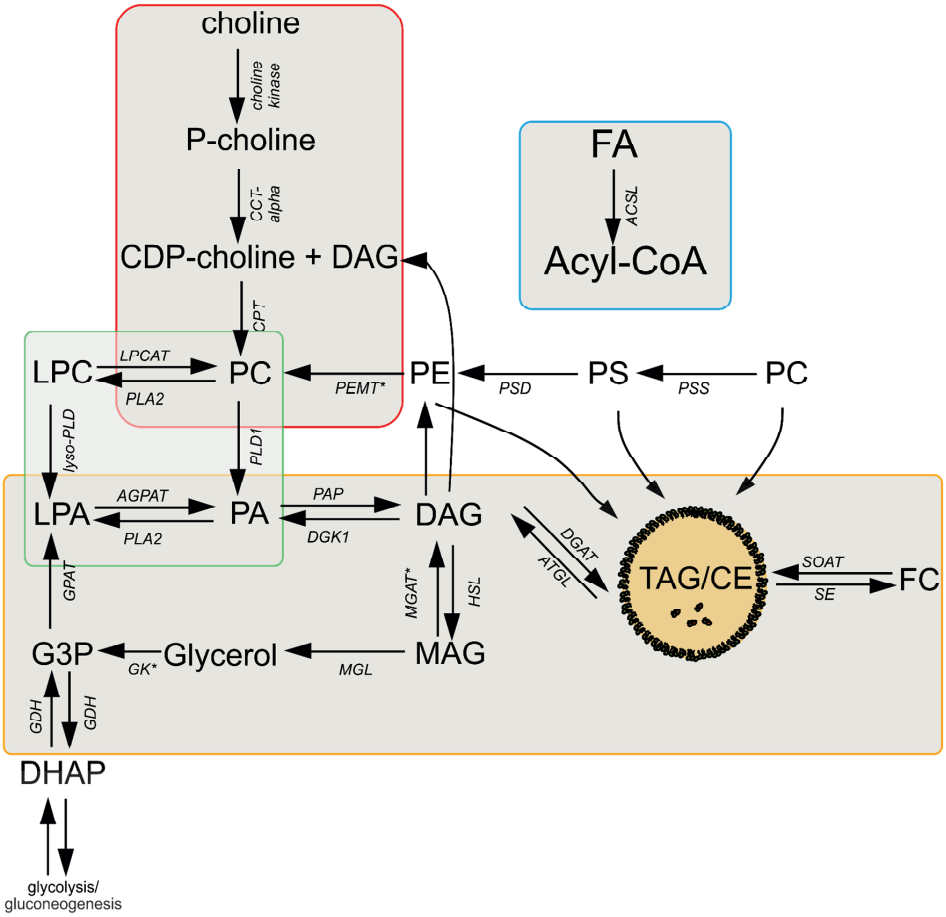

Figure 5 An overview of NL and PL pathways involved in LD biology in mammalian cells, including *de novo* NL synthesis (orange), FA activation (blue), Kennedy pathway of PC biosynthesis (red) and the Lands cycle of PL remodeling (green). Enzymatic steps are in italics, multiple enzymes may exist for each step. Asterisk indicates steps only active in specialized cell types, such as adipocytes or liver cells. Although not indicated, many of the steps shown here require or release activated FAs. PEMT, phosphatidylethanolamine-N-methyltransferase (this pathway is mostly active in liver); PSD, phosphatidylserine decarboxylase; PSS, phosphatidylserine synthase; PLA, phospholipase A; PLD, phospholipase D; GDH, glycerol-3-phosphate dehydrogenase; GK, glycerol kinase (mostly active in liver and kidney); DGK diacylglycerol kinase; SE, sterol esterase; CDP-choline, cytidine diphosphatase choline; P-choline, choline phosphatase; LPC lysophosphatidylcholine; FC, unesterified cholesterol, MAG (monoacylglycerol); DHAP, dihydroxyacetone phosphate; SOAT, sterol-o-acyltransferase CCT-alpha, CTP:phosphocholine cytidylyltransferase alpha. Adapted from (Pol et al., 2014).

Many PL and NL generating reactions require activated FAs in the form acyl-coenzyme A (acyl-CoA) as substrates. FA activation occurs via an ATP-dependent, two-step reaction catalyzed by ACSL enzymes. Remarkably, at least 11 ACSL enzymes have been documented in mammalian cells (Takeuchi and Reue, 2009), but whilst these all catalyze the same reaction, they differ in their subcellular localization and affinities for FAs with different acyl chain lengths and saturation. The compartmentalization of ACSL as well as other lipid biosynthesis enzymes is likely crucial for efficient cellular metabolism but is still incompletely understood (Ellis et al., 2010; Young et al., 2018). Of the ACSL enzymes, the ER and LD localized ACSL3 appears to be especially important in NL synthesis for LD generation (Kassan et al., 2013; Poppelreuther et al., 2018).

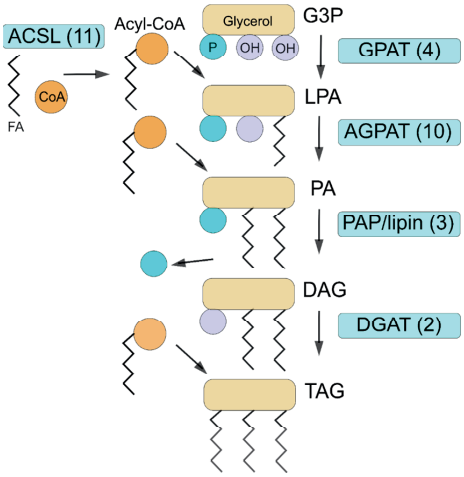

Figure 6 Schematic of *de novo* TAG generation pathway. Acyl-CoA synthetase (ACSL) enzymes catalyze Acyl-CoA formation, a substrate for many subsequent steps. Glycerol-3-phosphate (G3P) is converted to lysophosphatidic acid (LPA) via the activity of 1-glycerol-3-acyltransferase (GPAT) enzymes. LPA is converted to phosphatidic acid (PA) via the activity of 1-acylglycerol-3-phosphate-acyltransferase (AGPAT) enzymes. PA is dephosphorylated to DAG by phosphatidic acid phosphatase (PAP/lipin) enzymes. DAG is esterified to TAG by diacylglycerol acyltransferase (DGAT) enzymes. Numbers in parentheses indicate the number of putative isoforms in mammalian cells (Takeuchi and Reue, 2009)

4.2.2 LD biogenesis

De novo LD biogenesis begins in the ER, which also harbors the terminal enzymes of both TAG and CE synthesis, namely DGAT1, DGAT2, SOAT-1 and SOAT-2 (Chang et al., 2009; Yen et al., 2008). With the exception of DGAT2, these are integral multispanning ER transmembrane (TM) proteins, which thus cannot be accommodated on the LD monolayer (Walther et al., 2017). DGAT2, on the other hand, harbors a hairpin-like motif instead of a true TM domain, allowing for dual localization to the ER and LDs (Kuerschner et al., 2008; McFie et al., 2018; Wilfling et al., 2013). Besides NL synthesizing enzymes, various accessory proteins, such as seipin, FITM2, Rab18 and perilipins, have been shown to play roles in the early steps of LD biogenesis (Walther et al., 2017).

Initial LD biogenesis is thought to occur within the bilayer of the ER (Pol et al., 2014). Newly synthesized NLs are deposited within the leaflets of ER bilayer and are initially likely freely diffusing. To date, there is no direct evidence indicating that this early NL synthesis would occur on any specific ER subdomains, as in the absence of pre-

existing LDs, the TAG synthesizing machinery appears to be dispersed all around the ER, although detailed studies are lacking (Jacquier et al., 2011; Stone et al., 2009). Nevertheless, a bilayer can only accommodate minute concentrations (~3 mol% according to *in vitro* studies (Hamilton et al., 1983)) of TAG without biophysical forces driving the oil phase to nucleate, i.e. form a nm-sized lens (Walther et al., 2017). These lens-like aggregations have been predicted by molecular dynamic simulations (Khandelia et al., 2010; Pezeshkian et al., 2017) and observed in yeast by EM (Choudhary et al., 2015). Subsequent growth of such lens like-structures is postulated to lead to the deformation of the ER bilayer, resulting in a budding out of a small nascent LD towards the cytoplasmic side (**Figure 7**). After further growth, these structures become clearly identifiable LDs that may subsequently detach from the ER (Olzmann and Carvalho, 2019; Wilfling et al., 2013), although recent studies indicate that this is rarely, if ever, the case in normal cells (discussed in detail below and reviewed in (Salo and Ikonen, 2019)).

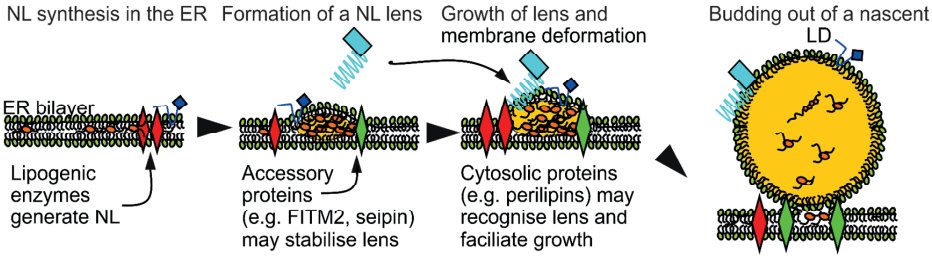

Figure 7 Early steps of LD biogenesis. Modified from (Salo and Ikonen, 2020).

There are still a number of unanswered questions regarding this model of LD biogenesis. Due to their small size and possible instability, nascent LD lenses have been difficult to identify and study in cells or *in vitro*. Though ~40-60 nm sized lens-like structures were detected in yeast (Choudhary et al., 2015), we detected budded out LDs in the size range of 30 nm in mammalian cells (Salo et al., 2019), whilst theoretical studies suggested a budding size of circa 12 nm (Zanghellini et al., 2010). Thus, the size limit of smallest forming LDs is yet unknown and may vary between cell types.

The forces leading to the budding of LDs are also unclear, and especially intriguing is the observation that LDs almost exclusively bud out to the cytoplasmic side of the ER. These processes likely involve both facilitating protein machinery and a favorable local lipid environment (Choudhary et al., 2018; Jackson, 2019; Ben M'barek et al., 2017). Thus, LD biogenesis is thought to occur in specialized, but yet poorly characterized ER subdomains where these factors come together to collaborate in LD budding and nascent LD growth (Pol et al., 2014). Of note, separating these two seemingly distinct steps experimentally is difficult, as the nascent LDs are well below conventional microscopy resolution and biochemical detection limits. Thus, deductions on how protein and lipid composition effects early LD formation steps are often made based on observed LD alterations at a later time point, i.e. how LDs appear

after they have already formed. To date, no single protein has been found indispensable for LD formation (Guo et al., 2008). Indeed, theoretical work suggests that with rising NL concentrations, LD-like structures will eventually bud out of the ER even in the absence of any dedicated protein machinery, due to the biophysical properties of NLs in an aqueous environment (Deslandes et al., 2017). However, within cells, a collaboration of proteins such as seipin, FITM2, ACSL3 and perilipins controls nascent LD formation (Chen and Goodman, 2017).

Seipin, discussed in detail below, may regulate the local PL composition and/or structurally control nascent ER-LD contacts to enable nascent LD growth (Salo et al., 2019). FITM2, an ER TM protein which was shown to be capable of directly interacting with TAG, may shuffle TAG to the nascent LD and regulate local DAG levels to enable LD budding (Choudhary et al., 2018; Gross et al., 2011). FITM2 was also proposed to harbor PL remodeling enzymatic capabilities, leading to the suggestion that it may modulate the surface tension of the luminal leaflet of the ER at LD formation sites and thus facilitate directional budding of LDs to the cytoplasmic side (Becuwe et al., 2018; Hayes et al., 2018). ACSL3, an acyltransferase shown to mark nascent LD formation sites (Kassan et al., 2013), likely plays a role by increasing the local concentration of activated FAs, necessary for PL and TAG synthesis (Poppelreuther et al., 2018). Cytoplasmic perilipin proteins, especially perilipin-3, may sense the increased local concentration of NLs or DAG at the ER. By accumulating at these sites perilipins may aid in nascent LD stabilization and, possibly through protein crowding effects, facilitate bilayer deformation to enable LD budding (Bulankina et al., 2009; Gao et al., 2017b; Skinner et al., 2009; Thiam and Beller, 2017). Finally, multiple ER-shaping proteins have been shown to affect LD assembly (Falk et al., 2014; Klemm et al., 2013; Papadopoulos et al., 2015; Renvoisé et al., 2016). A reason for this may be modulation of the local ER surface tension, leading to alterations in LD formation and/or growth (Deslandes et al., 2017; Wang et al., 2018b).

Indeed, multiple lines of evidence suggest that local ER membrane lipid composition at LD forming sites plays an important role in regulating LD emergence, and the role of proteins may be to primarily control this parameter. In a recent study, the intrinsic curvature of PLs was found to regulate ER budding: negatively curved lipids (e.g. DAG), facilitated LD embedding in the ER whilst positively curved lipids (e.g. lysolipids) facilitated budding out of the ER (Choudhary et al., 2018). Besides inducing curvature, various PLs also differentially modulate the surface tension of the ER bilayer, and this was shown to effect the size of emerging LDs in a study primarily utilizing model membranes and artificial LDs (Ben M'barek et al., 2017).

Asymmetrical distribution of PLs between the ER bilayer leaflets and the consequential difference in surface tension may also aid in ensuring LD budding towards the cytoplasmic side of the membrane (Chorlay and Thiam, 2018). This could arise via certain PLs showing a preference for the luminal vs cytoplasmic side of the bilayer, as has been shown previously for phosphatidylserine (PS) at the plasma

membrane and more recently also at the ER (Tsuji et al., 2019). Indeed, membrane asymmetry, resulting in different surface tensions, achieved either via an excess of PLs or proteins on one side vs the other has been proposed to impose directionality on LD emergence from the ER (Chorlay et al., 2019). Overall, local lipid composition likely plays a key role in nascent LD formation and budding and studies utilizing fluorescent lipid sensing proteins have implicated local increases of PA and DAG at LD forming sites in the yeast ER (Choudhary et al., 2018; Wolinski et al., 2015). However, direct proof of LD-forming ER subdomains having a different lipid composition than that of the bulk ER is lacking and would require advances in subcellular lipidomic techniques.

4.2.3 LD growth

After formation, a LD can grow in size via acquisition of more NLs to its core and concomitant expansion of the LD monolayer. This occurs via at least three different pathways acting in parallel: via lipid deposition from the ER to LDs via ER-LD contacts; via localized lipid synthesis on the LD monolayer; and via transfer of lipid constituents between neighboring LDs through fusion or ripening (Barneda and Christian, 2017) (**Figure 8**). In principle, more lipids could also be delivered to LDs via vesicular transport, but thus far direct evidence for this is lacking (Penno et al., 2013).

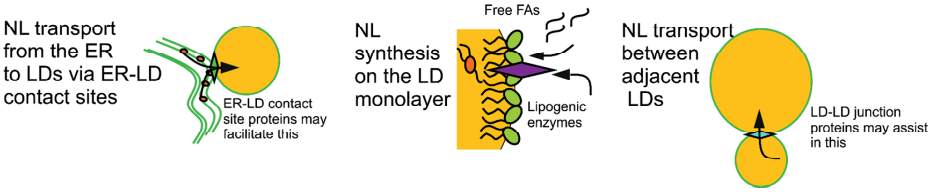

Figure 8 Modes of LD growth. Modified from (Salo and Ikonen, 2020).

4.2.3.1 LD growth via ER-LD contacts

The notion that LD expansion may be driven by lipid transport via ER-LD contacts is not surprising considering that most of the machinery for NL synthesis is ER-resident. Furthermore, whilst the rate-limiting enzyme for the major PL, PC, synthesis (CTT-alpha) can localize to the LD monolayer in some cell types (Krahmer et al., 2011), although not in others (Aitchison et al., 2015; Haider et al., 2018), the terminal enzymatic steps of PC synthesis occur solely at the ER or Golgi (Henneberry et al., 2002)**.** Thus, a likely source for additional material for LD expansion is the ER, with newly synthesized lipids transported to the LD via ER-LD contacts. Indeed, although traditionally it was assumed that after their formation, most LDs would detach from ER membranes to become isolated cytoplasmic organelles, recent studies have shown that most – if not all – LDs appear to stay in touch with their mother organelle throughout their lifetime (Salo and Ikonen, 2019).

A subset of ER-LD contact sites are postulated to be unique in terms of their topology, with direct membrane continuity between the ER bilayer and LD monolayer, with the ER-LD contact site being a membranous bridge (Salo and Ikonen, 2019). This is in contrast to traditional membrane contact sites, where tethering proteins bring organelles within nm distances of each other, but the individual membranes remain separated (Schuldiner and Bohnert, 2017). This topology would ensure rapid diffusion of lipid constituents between the two cellular compartments. Hints of such membranous bridges have been seen in EM images of ER and LDs (Kassan et al., 2013; Romanauska and Köhler, 2018; Salo et al., 2019; Wilfling et al., 2013). This aspect was thoroughly investigated in a landmark yeast study, where FRAP experiments demonstrated movement of proteins from the ER to the LD surface in a temperature and energy independent manner, suggesting direct connectivity (Jacquier et al., 2011). Since then, FRAP has demonstrated rapid exchange of both lipid and protein cargo between the ER and LDs in multiple cell types (Kimura et al., 2018; Salo et al., 2016; Wilfling et al., 2013). The lipodystrophy protein seipin has been implicated in the formation and maintenance of such bridges (Grippa et al., 2015; Romanauska and Köhler, 2018; Salo et al., 2019).

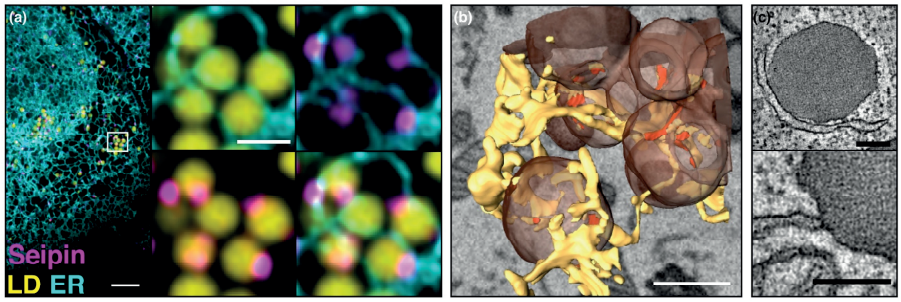

Figure 9 Examples of ER-LD contacts from light microscopy (a), 3D-EM (b) and electron tomography images. Note both discrete and extended ER-LD contacts in c. Scale bars: 1 µm and 5 µm (a), 1 µm (b), 200 nm (c). Reproduced from (Salo and Ikonen, 2019).

In addition to membranous bridges, proteinaceous tethers between the ER and LDs also exist, and structures reminiscent of these have been detected in EM images (Salo et al., 2019; Wang et al., 2016a). Candidates for forming these tethers include ER and LD resident proteins coming together to form a bridging complex. These include a complex of FATP1 (ER) and DGAT2 (LD) (Xu et al., 2012), Rab18 (LD) together with members of the NRZ complex and associated SNARE proteins (ER) (Xu et al., 2018), and Orp2 (LD) and VAPA (ER) (Weber-Boyvat et al., 2015). Recently, Snx14 was also shown to be capable of tethering LDs to the ER, by binding to both organelles simultaneously (Datta et al., 2019) and a similar topological arrangement has been proposed for DGAT2 (McFie et al., 2018). Interestingly, in all these cases, tethering of the two organelles was proposed to facilitate LD growth, although the exact mechanisms underlying this are unknown. Finally, LDs are also frequently detected

to touch the ER membrane for extended lengths, in an egg-in-a-cup conformation (Jacquier et al., 2011; Mishra et al., 2016; Robenek et al., 2006), but the significance for this kind of conformation for LD growth is unknown. Examples of ER-LD contacts are shown in **Figure 9.**

4.2.3.2 LD growth via lipid synthesis on the LD

Besides lipid deposition from the ER via ER-LD contacts, TAG synthesis can also occur at the LD monolayer, independent of the ER. In an landmark study, it was demonstrated that at least one member of all the enzymes required for *de novo* TAG generation – such as ACSL3, GPAT3, AGPAT2, DGAT2 - can relocate from the ER to LDs, where they facilitate LD expansion by catalyzing TAG synthesis (Wilfling et al., 2013). Interestingly, this DGAT2-dependent pathway typically targets only a subset of cellular LDs, termed "expanding LDs" which consequently grow larger than other LDs in the same cell (Walther et al., 2017).

It is presently unclear how this LD diversity is achieved, i.e. what precludes from all LDs acquiring the TAG synthesizing enzymes, but the Arf1/COPI machinery was shown to be necessary for GPAT3 localization to LDs (Wilfling et al., 2014). This is thought to arise via COPI-mediated budding of small nano-LDs from the LDs, resulting in an increase in LD surface tension (Thiam et al., 2013b; Wilfling et al., 2014). Alteration of the LD surface tension could then allow these enzymes to diffuse from the ER to LDs via ER-LD bridges as described above. In the original study, COPI-mediated alteration of the LD surface tension was suggested to result in *de novo* ER-LD bridge formation (Wilfling et al., 2014), but it appears plausible that such bridges may exist independent of COPI activity, and the trafficking of proteins via these bridges is controlled by COPI machinery. Seipin has also been implicated in this process, as seipin perturbation in *Drosophila* cells leads to an increase of the expanding LD population, with earlier and increased targeting of the TAG synthesis machinery to a subset of LDs (Wang et al., 2016a). Together with data proposing that seipin acts as a diffusion barrier controlling LD surface tension (Grippa et al., 2015), these findings suggest that the expanding LDs likely differ in their monolayer properties from those of other LDs.

Of note, as discussed above, currently there is no evidence for *de novo* phosphatidylcholine synthesis on the LD monolayer. The last step of PC synthesis, the conversion of CDP-choline to PC, is catalyzed by choline phosphotransferase, CPT, an ER resident enzyme (Henneberry et al., 2002). Furthermore, isolated LDs lack this enzymatic activity (Moessinger et al., 2011). The substrate for this enzymatic step, CDP-choline, can be generated at LDs in at least some cell types, by the activity of CCT-alpha, and LD growth has been shown to facilitate the relocation and activation of this enzyme at LDs (Aitchison et al., 2015; Krahmer et al., 2011). Thus, during LD expansion, local activation of CCT-alpha may lead to local increases in CDP-choline levels, which could rapidly be transferred to the ER, converted to PC and then transferred back to the LD. The delivery of these compounds could arise via diffusion

through ER-LD contacts or via transfer by lipid transfer proteins, and allow for LD monolayer expansion (Penno et al., 2013).

Interestingly, VPS13, a recently described lipid transfer protein capable of PC transfer *in vitro,* was shown to localize to multiple ER contact sites, including those between the ER and LDs (Kumar et al., 2018). Furthermore, PC-remodeling lysophosphatidylcholine acyltransferase (LPCAT) enzymes have been localized to LDs and shown to be important for LD growth (Moessinger et al., 2011, 2014). As their substrates (lyso-PC and activated FAs) are relatively water soluble molecules, they might be transferred to LDs independent of ER-LD contacts, and PC could thus be generated at the LD directly (Penno et al., 2013).

Overall, it is clear that LDs can grow both via ER-derived NL transfer and LD-autonomously via generation of TAG at the LDs. However, their relative contribution to LD growth is presently unclear. Indeed, this is likely dependent on both the cell types in question and the metabolic status of the cells. A major contributing factor may be the relative activities of DGAT1 and DGAT2, the former being a permanently ER-localized protein whilst the latter can be localized to both ER and LDs (Barneda and Christian, 2017; Olzmann and Carvalho, 2019; Wilfling et al., 2013). Of note, CE synthesis is permanently restricted to the ER (Chang et al., 2009), implicating ER-to-LD lipid transport as the main mode of expansion for exclusive CE containing LDs.

4.2.3.3 LD growth via lipid transfer between LDs

LDs can also grow by lipid transport from one LD to another, typically between adjacent LDs. This can be achieved via two biophysically distinct mechanisms with different time scales: LD-LD fusion, which is a rapid merging or coalescence of droplets (occurring within seconds); and Ostwald ripening, a molecular diffusion process by which smaller droplets continuously leak material to bigger ones through a connecting phase (occurring over minutes-hours) (Thiam and Forêt, 2016; Thiam et al., 2013a). Somewhat confusingly, both processes are often referred to simply as "fusion" in the literature. As these processes are facilitated by LD-LD contacts and proximity, they can be modulated by factors influencing LD-LD clustering, such as microtubule and actin cytoskeleton networks (Boström et al., 2007; Pfisterer et al., 2017) and proteins inducing LD clustering (Jambunathan et al., 2011; Lohmann et al., 2013). Upon LD coalescence, the total volume of fusing LDs remains the same, whilst the surface area decreases. In line with this, cells deficient in PL synthesis often contain larger LDs via an increased rate of LD-LD fusion (Guo et al., 2008; Krahmer et al., 2011).

Rapid fusion of two nearby LDs to become a single LD appears to be relatively rare in intact cells, as cells often contain clusters of relatively similar-sized LDs, stable for long periods of time. This is due to the surfactant properties of the LD monolayer, which efficiently protects the LDs from coalescence (Thiam et al., 2013a). However, rapid merging of adjacent LDs within seconds has been observed *in vivo* (for example,

in (Pfisterer et al., 2017)) and can be induced by addition of surface-reactive molecules that disrupt the LD monolayer and thus induce coalescence (Murphy et al., 2010).

Slower LD-LD fusion process, termed ripening, has more frequently been observed in cells, and is a major contributor to the growth of LDs during adipogenic differentiation (Jüngst et al., 2013; Paar et al., 2012). In this process, the larger LD acquires lipids from the smaller LD due to a difference in the internal pressure of the LDs, which is dependent on the size difference of the LDs (Thiam et al., 2013a). This process is facilitated by Fsp27, a protein mutated in congenital lipodystrophy (Rubio-Cabezas et al., 2009). Fsp27 is enriched at LD-LD contact sites, where it facilitates the growth of the larger LD at the expense of the smaller LD, possibly by increasing the local PL barrier permeability, allowing NL transfer (Barneda et al., 2015; Gao et al., 2017a; Gong et al., 2011). Our studies have recently indicated that ripening can also occur between nearby LDs via the connecting ER bilayer, and this process is controlled by seipin, probably through modulation of ER-LD contact site functionality (discussed in detail in Results and Discussion) (Salo et al., 2019).

4.2.4 Breakdown of LDs

The canonical function of LDs is energy storage. Upon times of cellular demand, the NLs of the LD core can be broken down to release free FAs for energy production and membrane synthesis. This is achieved via lipolytic enzymes, hydrolyzing NLs at the LD monolayer, or via engulfment of LD constituents into degradative vesicles in a specialized form of selective autophagy, termed lipophagy (Zechner et al., 2017) (**Figure 10**). Both processes result in the breakdown of the ester bonds in NLs by enzymatic hydrolysis, resulting in the liberation of free FAs.

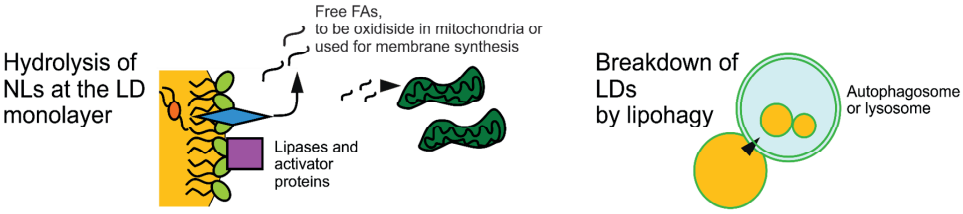

Figure 10 Modes of LD breakdown. Modified from (Salo and Ikonen, 2020).

The main mammalian lipases acting on TAG are ATGL (adipose tissue triglyceride lipase), HSL (hormone sensitive lipase) and MGL (monoacylglycerol lipase) (Kraemer and Shen, 2002; Schweiger et al., 2006; Zimmermann et al., 2004). ATGL has higher *in vitro* activity on TAG, whilst HSL is more efficient at hydrolyzing the resulting DAG, but both enzymes co-operate in a cell-type specific manner (Zechner et al., 2009). The product of DAG hydrolysis, MAG, is further broken down by MGL. ATGL and HSL act at the LD monolayer, whilst MGL is cytoplasmic, and their

activities are regulated by various cellular cues, including perilipin proteins (Sztalryd and Brasaemle, 2017; Zechner et al., 2017).

For example, in adipocytes during basal conditions, perilipin-1 is enriched at the LD surface, binding CGI-58, a potent cofactor of ATGL (Lass et al., 2006; Subramanian et al., 2004; Yamaguchi et al., 2004). Upon increased demands for energy, catecholamines activate protein kinase A (PKA), which phosphorylates perilipin-1, resulting in release of CGI-58 to activate ATGL (Sztalryd and Brasaemle, 2017). Concomitantly, phosphorylated perilipin-1 also more efficiently recruits HSL to the surface of LDs (Miyoshi et al., 2006; Sztalryd et al., 2003). Acting in concert, these lipases then catalyze efficient TAG degradation into free FAs, to be used for membrane synthesis or ATP production in mitochondria through beta-oxidation pathways.

The fate of the LD-liberated FAs may further be regulated by spatiotemporal control of LD-mitochondria proximity. Indeed, during energy depleted conditions, LDs are recruited to the vicinity of mitochondria (Herms et al., 2015; Rambold et al., 2015; Valm et al., 2017), likely leading to more efficient usage of liberated free FAs for energy production. This relocalisation of LDs is regulated by transport along tyrosinated microtubules in a process regulated by the cellular energy sensor, AMPK (Herms et al., 2015). Mitochondria-LD contacts are also facilitated by perilipin-5, which has been proposed to act as a tether between these two organelles (Kimmel and Sztalryd, 2014; Wang et al., 2011).

Whilst lipases on the LD monolayer brake down NLs one molecule at a time, LDs can also be degraded in larger portions via lipophagy (Singh et al., 2009). In this process, entire small LDs or portions of larger LDs are engulfed into autophagosomes, which subsequentially fuse with lysosomes and NLs are hydrolyzed by the lysosomal enzyme LAL (lysosomal acid lipase) (Zechner et al., 2017). Molecular cues marking LDs for degradation by autophagosomes are currently under investigation, but may involve direct, transient interaction of lysosomes with LDs in a process regulated by Rab7 (Schroeder et al., 2015). Whilst the molecular details and regulatory loops involved in lipophagy are only beginning to be unraveled, it is currently accepted that both lipolysis at the LD surface and lipophagy are required for maximal LD breakdown efficiency in most cell types (Schulze et al., 2017). Interestingly, recent studies in hepatocytes suggest LD size may determine which mode of breakdown dominates, with larger LDs being more susceptible to breakdown by lipases and smaller LDs to lipophagy (Schott et al., 2019).

Overall, a major outstanding question in understanding LD size changes in cells is deciphering how cells can efficiently couple LD core NL changes with the expansion and shrinkage of the LD monolayer. Seipin has been implicated in this process (Grippa et al., 2015; Salo et al., 2019; Wang et al., 2016a), but its precise role still remains unclear.

4.3 SEIPIN

Seipin is an oligomeric ER TM protein, implicated in LD formation and adipogenesis. Seipin was first identified as the gene defective in BSCL2, a severe form of congenital lipodystrophy (Magré et al., 2001), whilst subsequent studies have documented other seipin mutations giving rise to hereditary spastic paraplegias (Windpassinger et al., 2004) and a severe form of encephalopathy with fatal outcomes at a young age (Guillén-Navarro et al., 2013). Seipin is required for adipogenesis, and studies in a wide variety of model organisms have implicated an evolutionary conserved role for seipin in LD assembly, with a typical loss of function/knockout (KO) phenotype of supersized and tiny LDs (Cartwright and Goodman, 2012; Dollet et al., 2014; Sarmento et al., 2018). However, despite considerable effort, including recent cryo-EM structural studies, the molecular mechanism of seipin function(s) remains unclear (Gao et al., 2019; Henne et al., 2020).

4.3.1 Seipin structure and conservation

Seipin is an integral ER membrane protein, with two TM domains, a luminal loop and amino- and carboxyterminal cytoplasmic ends (Lundin et al., 2006; Windpassinger et al., 2004) (**Figure 11**). In humans, *BSCL2*, the gene coding seipin, is ubiquitously expressed, with highest expression levels in the brain and testes (Magré et al., 2001; Windpassinger et al., 2004). *BSCL2* gives rise to three transcripts, isoform 1 (398 amino acids (aa)), isoform 2 (287 aa) and isoform 3 (462 aa) (Sarmento et al., 2018). Isoforms 1 and 3 contain the intraluminal loop and both TM domains, but isoform 3 has an extended N-terminal sequence compared to isoform 1. Isoform 2 differs from the others in its C-terminal sequence and may lack the second TM completely. Its expression appears to be limited to the central nervous system and to date there is no evidence at the protein level of its existence (Magré et al., 2001; Sánchez-Iglesias et al., 2016; Windpassinger et al., 2004). Indeed, the functional relevance of these various isoforms is unclear. Isoform 1 is the most commonly studied in the literature and subsequent aa numberings refer to that.

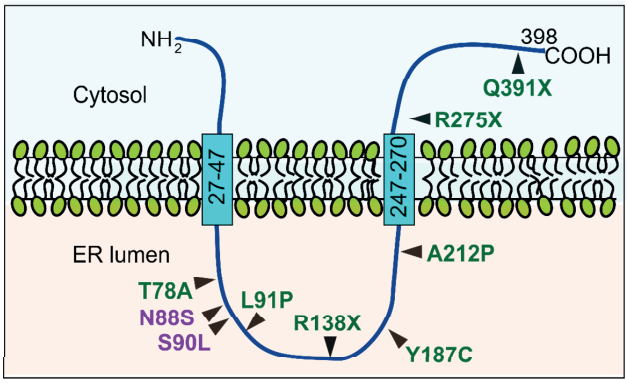

Figure 11 Schematic of seipin isoform 1. Select missense and truncation mutations implicated in BSCL2 (green) and seipinopathy (magenta) are shown. X denotes introduction of premature stop codon. Seipin is N-glycosylated at N88-S90. Adapted from (Wee et al., 2014).

Two genome-wide screens conducted in *S. cerevisiae* found seipin to be essential for proper LD morphology, with a phenotype of supersized and tiny LDs in its absence (Fei et al., 2008; Szymanski et al., 2007). In accordance with a lipodystrophic phenotype in humans, seipin was found to be essential for proper adipogenesis in mice (Chen et al., 2009; Cui et al., 2011; Payne et al., 2008), *Drosophila* (Tian et al., 2011), rat (Ebihara et al., 2015) and human cells (Mori et al., 2016; Victoria et al., 2010). Furthermore, studies have revealed a crucial role for seipin in LD morphology in multiple model organisms, including various non-adipogenic human cell lines (Boutet et al., 2009; Salo et al., 2016; Wang et al., 2016a), *A. thaliana* (Cai et al., 2015), *C. elegans* (Cao et al., 2019), *D. amoebae* (Jessica M. Kornke, 2017) and *R. toruloides* (Coradetti et al., 2018).

The intraluminal region and the two flanking TM segments are the most conserved domains of seipin between different species (Fei et al., 2008; Sarmento et al., 2018; Szymanski et al., 2007). This region has thus been denoted as the conserved core sequence, hypothesized to relate to seipin's core function in LD formation, while the extended cytoplasmic regions (found in multicellular organisms) may relate to a more complex role for seipin in specialized fat-storing cells, such as adipocytes (Yang et al., 2013). This hypothesis stems from the fact that the LD phenotype of yeast seipin KO cells can be rescued by human seipin, even a truncated form lacking the cytoplasmic C-terminus (Fei et al., 2008), whilst rescue of defective adipogenesis in seipin depleted cells requires the full-length protein (Yang et al., 2013). Furthermore, some BSCL2-causing truncation mutants only lack small portions of the C-terminus, implying significance of this domain for fat storage (Talukder et al., 2015).

In yeast, seipin interacts with ldb16, an ER TM protein with no known mammalian homologues (Grippa et al., 2015; Wang et al., 2014). Depletion of either yeast seipin, ldb16 or both result in largely indistinguishable phenotypes, which can be rescued by expression of human seipin, including a variant only containing the core sequence (Grippa et al., 2015; Wang et al., 2014). In line with this, also LD biogenesis defects in *Drosophila* cells could be rescued with constructs lacking both N- and C-termini (Wang et al., 2016a). Overall, these data suggest that the (currently unresolved) function of seipin in LD-formation is accomplished by its core sequence, and the cytoplasmic termini may have additional roles, putatively important for adipogenesis. This model is challenged, however, by the intriguing finding that fat storage defects in *Drosophila* fat body can be rescued by *Drosophila* seipin lacking the C-terminus, whilst rescue of ectopic lipid storage in non-adipose tissues in this model requires the full-length protein (Tian et al., 2011).

4.3.1.1 The structure of the seipin oligomer

Seipin forms homo-oligomers in the ER. Early reports of purified yeast seipin, analyzed via negative staining EM, suggested a toroid conformation of circa 9 subunits (Binns et al., 2010), whilst atomic force microscopy (AFM) of immuno-purified human seipin suggested a complex of 12 subunits in a circular conformation (Sim et

al., 2013). In line with this, endogenously fluorescently tagged *Drosophila* and human seipin appear as discrete, mobile foci in the ER (Salo et al., 2019, 2016; Wang et al., 2016a). Finally, recent cryo-EM structures of the luminal region of *Drosophila* and human seipin reported oligomers of 12 and 11 subunits, respectively (Sui et al., 2018; Yan et al., 2018), and a preliminary report suggests yeast seipin to be composed of 9 subunits (Henne et al., 2020). Oligomerization is instrumental for seipin function, and several BSCL2-causing point mutants appear to impair seipin oligomerization and function. The best studied example is the BSCL2-causing point mutant A212P (Magré et al., 2001), which has been shown to exist as smaller oligomers than WT seipin, as assessed by EM and AFM of purified preparations (Binns et al., 2010; Sim et al., 2013) and super resolution microscopy of intact cells (Salo et al., 2016). Finally, a mutant designed based on the seipin cryo-EM structure to hinder oligomerization, failed to complement seipin function in cells (Yan et al., 2018). However, the exact number of subunits in the oligomer appears not to be critical for seipin function, as human seipin (11 subunits) has been shown to rescue both yeast (9) and *Drosophila* (12) seipin-depleted phenotypes in LD formation (Henne et al., 2020; Wang et al., 2014, 2016a).

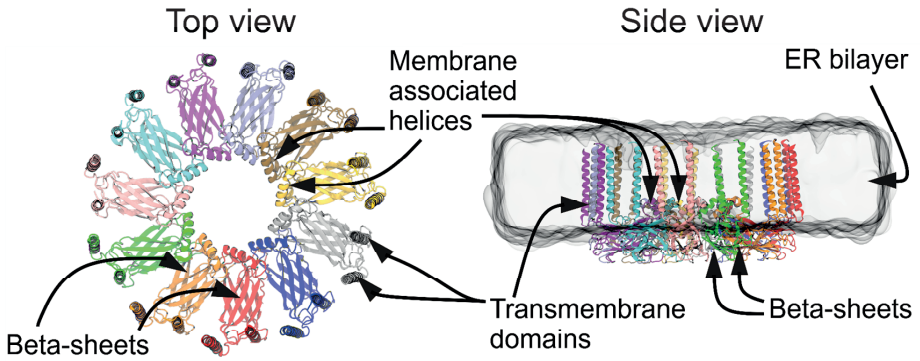

Figure 12 Seipin oligomer structure. The TM regions were modelled into the cryo-EM structure of the luminal domains of human seipin (Yan et al., 2018) using PyMol software. Image credit: Xavier Prasanna.

Besides providing insight into the oligomerization status of seipin, the cryo-EM structures of human and *Drosophila* seipin revealed several notable structural features (**Figure 12**). Interestingly, neither study could resolve the structures of the cytoplasmic regions of seipin, which likely reflects structural flexibility in these regions (Sui et al., 2018; Yan et al., 2018). The luminal structures of both species showed a ring-like structure of circa 15 nm in diameter, consisting of 11-12 seipin monomers closely intertwined. Each monomer harbors two notable features: several hydrophobic helices in very close proximity to the bilayer membrane, and two beta sheets, each consisting of four beta-strands, with an overall fold reminiscent of lipid binding domains of proteins such as NPC2 (Sui et al., 2018; Yan et al., 2018).

The hydrophobic, putatively membrane-anchored helices were found to be able to bind NL-covered monolayers *in vitro* and localized to LDs in cells, when expressed as individual peptides (Sui et al., 2018). Upon mutation of several hydrophobic residues in these helices to aspartic acid, LD-localization could be inhibited. Whilst mutating the hydrophobic helices was not alone sufficient to block seipin function in cells, together with an additional deletion of the N-terminus of seipin, shown previously to localize to LDs when expressed alone (Wang et al., 2016a), seipin function in LD formation was impaired. Thus, the hydrophobic or amphipathic helices of seipin, either in the luminal region or at the cytoplasmic N-terminus, may function in recognizing the packing defects induced by local NL lenses in the ER bilayer and thus allow for seipin stabilization at nascent LD formation sites (Sui et al., 2018). During subsequent LD growth, this would place the seipin oligomer at the necks between the ER and LDs, with a small part of the LD monolayer therefore derived from the luminal leaflet of the ER, as suggested by EM tomography of seipin-mediated ER-LD necks (study III, (Salo et al., 2019).

The bulk of the seipin luminal region consist of two beta sheets, which form a beta-sandwich-like fold. This is structurally similar to many lipid-binding domains, including that of NPC2 (Xu et al., 2007), a sterol binding protein in the lumen of the lysosome, where it functions to bind cholesterol and aids in cholesterol export together with NPC1 (Ikonen, 2018). Other proteins containing such domains include PKC, which has a similar fold involved in PS binding (Lemmon, 2008). These structural similarities suggest that seipin may be an ER luminal lipid-binding protein. Indeed, *in vitro* work indicated that both purified full-length seipin and a truncated variant containing only the putative lipid binding domain could bind anionic PLs, such as PA, but not other PLs, such as PC, PS or PE (Sui et al., 2018). Interestingly, the binding for PA was dependent on the acyl-chains of PA, with seipin showing high affinity for PA containing oleate and palmitate. The putative lipid binding domain is important for seipin function, as a designed mutant, harboring two aa substitutions in the hydrophobic cleft of the beta sandwich, was unable to complement the seipin KO LD phenotype in cells (Sui et al., 2018). However, which lipids seipin binds or interacts with in intact cells remains to be determined.

The luminal region of human seipin also contains a conserved, experimentally verified N-glycosylation site (aa N88-S90, a N-X-V/S site). Although the detailed functional significance of this site is unclear, mutations in it result in motor neuronal disease in humans (discussed below in more detail). Furthermore, N-glycosylation deficient seipin mutants have been shown to aggregate in cells, with increased localization to ER domains adjacent to LDs (Hölttä-Vuori et al., 2013; Ito and Suzuki, 2007; Windpassinger et al., 2004). The cryo-EM structures of seipin did not resolve the glycan groups, so it is unclear how glycosylation may modify the structural properties of the seipin oligomer.

4.3.2 Seipin associated diseases

Mutations in seipin give rise to at least three distinct disease states in humans **(Table 1)**. Various recessively inherited, loss-of-function of mutations give rise to BSCL2, the most severe form of congenital lipodystrophy in humans (Magré et al., 2001). Dominantly inherited, gain-of-function mutations in the N-glycosylation site of seipin give rise to motor neuron disorders, hereditary spastic paraplegias with variable phenotypes, collectively termed seipinopathies (Ito and Suzuki, 2009; Windpassinger et al., 2004). Finally, mutations resulting in skipping of exon 7 of seipin, either homozygously or in combination with a BSCL2-causing mutant, cause an early-onset, fatal neurodegenerative disorder called Celia's encephalopathy (Guillén-Navarro et al., 2013).

Table 1. *Mutations in seipin leading to disease. Fs denotes frameshift, numbered by first affected aa, X denotes introduction of premature stop codon.*

Disease	Mutation	Inheritance	Notes	Reference
BSCL2 lipodystrophy (select mutations)				
	T78A	Recessive	Only described in patients with Q319X. Rescues LD defect in yeast.	(Miranda et al., 2009; Wang et al., 2014)
	L91P	Recessive	Does not rescue LD defect in yeast.	(Miranda et al., 2009; Wang et al., 2014)
	R138X	Recessive		(Magré et al., 2001)
	Y187C	Recessive	Does not rescue LD defect in yeast.	(Nishiyama et al., 2009; Wang et al., 2014)
	A212P	Recessive	Does not rescue LD defect in yeast.	(Fei et al., 2008; Magré et al., 2001)
	L214fs	Recessive		(Magré et al., 2001)
	Y225fs	Recessive		(Magré et al., 2001)
	I262fs	Recessive		(Wu et al., 2009)
	R275X	Recessive	Does not rescue LD defect in yeast.	(Ebihara et al., 2004; Wang et al., 2014)
	Q391X	Recessive	Only described in patients with T78A.	(Miranda et al., 2009)
Seipinopathy motor neuron disease				
	N88S	Dominant	Rescues LD defect in yeast.	(Fei et al., 2008; Windpassinger et al., 2004)
	S90L	Dominant	Rescues LD defect in yeast.	(Fei et al., 2008; Windpassinger et al., 2004)
Celia encephalopathy, PELD				
	c.985C>T; Y289LfsX64	Recessive/ Compound		(Guillén-Navarro et al., 2013)

4.3.2.1 Lipodystrophies and BSCL2

Lipodystrophies are a group of disorders characterized by loss of adipose tissue, with concomitant metabolic disturbances such as insulin resistance, diabetes and hyperlipidemia (Garg, 2004). Lipodystrophies are grouped into acquired and congenital forms. Acquired lipodystrophy is most typically caused by HIV drug treatments, especially protease inhibitors, and often involves adipose tissue loss from the face, arms and legs together with insulin resistance and hyperlipidemia (Carr et al., 1999). The molecular mechanisms behind HIV-related lipodystrophy are unclear but may involve modulation of major adipogenic transcription factors (Garg, 2004; Vigouroux et al., 2011). In rare cases, acquired lipodystrophy may also arise via autoimmune mechanisms (Garg, 2004).

Congenital lipodystrophies are rare, monogenic diseases and they are further categorized into partial (familial partial lipodystrophy, FPL) and generalized (congenital generalized lipodystrophy, CGL) based on the severity and age-of-onset of adipose tissue loss. CGL patients display generalized loss of body fat already at birth, whilst FPL patients start to display partial loss of body fat during the first decades of life (Garg and Agarwal, 2009). Besides lack of adipose tissue, CGL patients typically develop severe insulin resistance, hypertriglyceridemia, hepatosteatosis and may also display *acanthosis nigricans,* muscular hypertrophy, hepatomegaly and a reduced life span (Magré et al., 2001). CGL diseases are also called Berardinelli-Seip congenital lipodystrophies (BSCL), named after the researchers who first identified the disease in the 1950s (Berardinelli, 1954; Seip, 1959). The estimated global prevalence of BSCL lipodystrophies is around 1 per 10 million, with certain geographic regions showing up to hundred-fold higher local prevalence (De Azevedo Medeiros et al., 2017; Garg, 2004).

Although some affected loci likely still remain to be identified, most congenital lipodystrophies are caused by mutations in genes encoding proteins involved in lipid metabolism and LD biology (**Table 2**). (Krahmer et al., 2013a; Melvin et al., 2019; Vigouroux et al., 2011)**.** For example, mutations in AGPAT2, an enzyme catalyzing LPA to PA conversion, leads to CGL (Agarwal et al., 2002). Interestingly, mutations in lipin-1, an enzyme catalyzing PA to DAG conversion, lead to lipodystrophy in mice, but not humans (Péterfy et al., 2001; Temprano et al., 2016; Zeharia et al., 2008). Recently, mutations in the rate-limiting PC synthesis enzyme CCT-alpha were shown to lead to a severe form of congenital lipodystrophy (Payne et al., 2014). Somewhat counterintuitively, also putative loss-of-function mutations in the lipase HSL have recently been linked to FPL (Zolotov et al., 2017). These data highlight the importance of PL and TAG metabolism in adipose tissue biology.

Mutations in several non-enzymatic proteins implicated in LD growth and stability, such as perilipin-1, FSP-27 and seipin, lead to lipodystrophy (Gandotra et al., 2011; Magré et al., 2001; Rubio-Cabezas et al., 2009). Mutations in Cav1 and Cavin1, proteins implicated in caveolae assembly and possibly involved in intracellular FA trafficking in adipose cells, also lead to forms of GCL (Cao et al., 2008; Dwianingsih

et al., 2010; Hayashi et al., 2009; Kim et al., 2008; Shastry et al., 2010). Mutations in proteins likely directly influencing adipocyte differentiation, rather than LD biology, can also lead to congenital lipodystrophies. These include mutations in peroxisome proliferator activated receptor-γ (PPAR-γ), a major adipogenic transcription factor (Agarwal and Garg, 2002; Broekema et al., 2019) and mutations in proteins involved in nuclear envelope integrity and insulin signaling, such as Lamin-A, ZMPSTE24 and AKT (Melvin et al., 2019).

Table 2. *Proteins implicated in congenital lipodystrophies.*

Gene/Protein	Protein function	Disease	Reference
AGPAT2/AGPAT2	Lipogenic enzyme, LPA to PA conversion	CGL	(Agarwal et al., 2002)
BSCL2/Seipin	Unknown, ER-LD contact regulator	CGL	(Magré et al., 2001)
Cav1/Caveolin-1	Caveloae formation	CGL	(Kim et al., 2008)
PTRF/Cavin-1	Caveloae formation	CGL	(Hayashi et al., 2009)
PLIN1/Perilipin-1	LD coat protein, regulator of lipolysis	FPL	(Gandotra et al., 2011)
CIDEC-C/FSP-27	LD-LD contact protein, facilitates LD growth	FPL	(Rubio-Cabezas et al., 2009)
LMNA/Lamin-A	NE structural protein	FPL	(Cao, 2000)
PPARγ/ PPAR-γ	Adipogenic transcription factor	FPL	(Agarwal and Garg, 2002)
ZMPSTE24/ ZMPSTE24	Lamin processing	FPL	(Agarwal et al., 2003a)
AKT2/AKT2	Involved in insulin signaling	FPL	(Tan et al., 2007a)
LIPE/HSL	Lipase	FPL	(Zolotov et al., 2017)
CCT-alpha	Rate-limiting enzyme of PC synthesis	Unclassified	(Payne et al., 2014)

The phenotype of seipin-caused BSCL2 is considered to be the most severe of the known lipodystrophies. Whilst all CGL patients lack metabolically active adipose tissue (e.g. subcutaneous, visceral, and bone marrow fat), BSCL2 patients typically also lack “mechanical” fat deposits (e.g. retro-orbital and periarticular fat) and show earlier onset of diabetes and other metabolic comorbidities (Agarwal et al., 2003b; Van Maldergem et al., 2002; Simha and Garg, 2003). BSCL2 patients also have an increased risk of hypertrophic cardiomyopathy and mild to moderate mental retardation in comparison with other CGL patients (Agarwal et al., 2003b; Cartwright and Goodman, 2012; Van Maldergem et al., 2002; Simha and Garg, 2003). Furthermore, BSCL2 has been linked to teratospermia (Jiang et al., 2014) and mitochondrial dysfunction (Jeninga et al., 2012). These unique characteristics of BSLC2 lipodystrophy compared to other forms of CGL may relate to seipin function outside of adipocytes, in line with high expression level of the protein in brain tissues and testes (Cartwright and Goodman, 2012; Magré et al., 2001).

4.3.2.2 Seipin and neuronal disorders

Whereas loss-of-function mutations in seipin give rise to BSCL2, gain-of-function mutations in the ER luminal N-glycosylation motif of seipin (N88S and S90L) give rise to dominantly inherited motor neuronal disorders, collectively now termed seipinopathies (Ito and Suzuki, 2009; Windpassinger et al., 2004). The clinical spectrum of this disease is broad and heterogenous, with upper and/or lower motor neurons affected to varying degrees in lower and/or upper extremities, typically without major afflictions in sensory neurons (Auer-Grumbach et al., 2005; Ito and Suzuki, 2009; Windpassinger et al., 2004). Thus, though seipinopathy refers to the genetic diagnosis, patients may clinically be diagnosed with Silver syndrome (main phenotype: weakness and wasting in the small hand muscles and spasticity of the lower limbs), distal hereditary motor neuropathy type V (weakness and wasting in the small hand muscles), hereditary spastic paraplegia (spastic paraplegia in the lower limbs) or Charcot-Marie-Tooth disease type 2 (distal muscle weakness, wasting of the upper and lower limbs) (Ito and Suzuki, 2009). A subset of patients harboring a mutation may be asymptomatic or display only minor abnormalities and the penetrance and severity of the disease varies even within a common pedigree (Auer-Grumbach et al., 2005). Seipinopathy patients have not been reported to display signs of lipodystrophy.

Whilst the molecular pathogenesis of seipinopathy is unclear, cell biological work has shown that the seipin N-glycosylation mutants lead to UPR, protein aggregation and ER stress (Hölttä-Vuori et al., 2013; Ito and Suzuki, 2007; Ito et al., 2012; Windpassinger et al., 2004). Overexpression of N88S seipin also leads to motor neuron dysfunction and ER stress in mice and a swimming defect in developing zebrafish embryos (Hölttä-Vuori et al., 2013; Yagi et al., 2011). In these studies, neuronal cell death was not observed, suggesting ER stress alone is sufficient to induce symptoms. However, another study in transgenic mice reported N88S overexpression to induce cell death in the spinal cord together with increased autophagy (Guo et al., 2013). Overall, seipinopathy may arise via toxic accumulation of the protein which could be especially harmful in sensitive cells, such as motor neurons.

Seipin may also play important physiological roles in neuronal cells, which could be disrupted by the N-glycosylation mutations. Indeed, mouse studies have linked seipin function to neuronal function via control of PPAR-γ, with neuronal-specific seipin KO mice displaying increased susceptibility to beta-amyloid induced neuroinflammation and tau aggregation (Chang et al., 2019; Wang et al., 2018a). Loss of seipin in mice also increased cerebral ischemia/reperfusion damage (Chen et al., 2016), decreased excitatory post-synaptic currents in neuronal mouse model (Wei et al., 2013), and reduced axonal regeneration in a *Drosophila* model (Rao et al., 2016). Together with the frequently observed cognitive impairment in BSLC2 patients, these studies suggest that seipin may play a neuroprotective role. Considering that both N88S- and WT-seipin can readily co-immunoprecipitate with each other (Fei et al., 2011b), it may be that seipinopathy arises via a loss-of-function mechanism exacerbated by the propensity of N88S to form protein aggregates.

Further implications for the role of seipin in neuronal function comes from the recent discovery of Celia's encephalopathy, also called progressive encephalopathy with or without lipodystrophy (PELD) (Guillén-Navarro et al., 2013; Ruiz-Riquelme et al., 2015). Patients suffering from this extremely rare disease (less than 10 cases described so far in the literature) are initially healthy, but start to show signs of psychomotor delay by the age of two years, with subsequent progressive encephalopathy and complex neurological symptoms, leading to death in the first decade of life (Guillén-Navarro et al., 2013). PELD is caused by a mutation in the coding DNA of seipin (c.985C>T), resulting in aberrant splicing leading to the skipping of exon 7 and the production of a new aberrant protein, called Celia-seipin, which lacks the second TM domain and distal C-terminal cytoplasmic region. Heterozygous carriers of this variant are healthy, whilst homozygotes are inflicted. Interestingly, this variant also leads to the disease in patients carrying a BSCL2-lipodystrophy (loss-of-function) linked-mutation in the other allele, and these patients also show classic signs of CGL (Guillén-Navarro et al., 2013). Subsequent analysis has documented that also other nearby mutations may interfere with this splicing site, leading to various clinical phenotypes, ranging from PELD to BSCL2 with various levels of cognitive impairment and neurological symptoms (Sánchez-Iglesias et al., 2019).

Cell biological studies have suggested that Celia seipin can form larger oligomers than WT-seipin, whilst co-overexpression of WT- and Celia-seipin reduces oligomer sizes to normal (Ruiz-Riquelme et al., 2015). Aggregates of Celia-seipin were detected in a PLD patient brain biopsy by immunohistochemistry, and these are postulated to lead to ER stress in neurons (Ruiz-Riquelme et al., 2015). These data suggest a toxic gain-of-function, which may be prevented in heterozygote carriers by the presence of WT seipin (Ruiz-Riquelme et al., 2015; Sarmento et al., 2018), although further studies into the pathogenesis of this devastating disease are needed.

4.3.3 Seipin function

Despite a clear role in both adipogenesis and LD formation, the molecular role(s) of seipin remains to be identified. Indeed, considering the pleiotropic diseases associated with seipin mutations and its tissue-wide expression pattern, seipin likely has multiple different functions, perhaps in a cell-type dependent manner. Seipin appears to have a primary and evolutionary conserved role in LD formation and perhaps an additional role specific to adipocyte differentiation. However, as these processes are intimately linked and yet incompletely understood, a common molecular function could be in play at both phenomena. Indeed, whether impaired LD biogenesis and/or LD maintenance leads to impaired adipogenesis, is thus far unresolved (Qi et al., 2017).

Many interaction partners have been proposed for seipin, including lipogenic enzymes, calcium channels, ER-shaping proteins and cytoskeleton regulators (**Table 3**) indicating involvement in multiple cellular pathways. With the exception of GPAT and promethin (Castro et al., 2019; Pagac et al., 2016), these interactions have not

been documented in both yeast and mammalian systems, raising the question how relevant they are for the function of seipin in LD formation. Indeed, the striking ability of human seipin to rescue the yeast seipin KO LD phenotype suggests that if this is function requires a specific seipin-protein interaction, it should also be broadly conserved. This would be somewhat surprising, considering the large deviation in primary sequences between human and yeast seipin, and the fact that the yeast seipin complex is composed of two distinct proteins and loss of both can be compensated by human seipin (Wang et al., 2014). Indeed, some of the proposed seipin interactions in mammalian cells may relate to seipin function outside of LD formation, such as regulating adipogenesis. Some proposed functions for seipin are reviewed below.

Table 3. *Proposed interaction partners of seipin. Yeast protein names in italics. Co-ip, co-immunoprecipitation.*

Protein name	Protein function	Main evidence for interaction	Proposed function of interaction	Reference
Ldb16	Regulator of LD morphology	Co-ip: endogenous proteins in yeast	Forms a complex with seipin to regulate LDs	(Cartwright et al., 2015; Wang et al., 2014; Wolinski et al., 2015)
Promethin/ *Ldo45* *Ldo16*	Regulator of LD identity (yeast)	Co-ip: endogenous proteins (yeast), overexpressed proteins (human cells)	Unclear, seipin may regulate localization	(Castro et al., 2019; Eisenberg-Bord et al., 2018; Teixeira et al., 2018)
GPAT3-4/ *Get1-2*	Catalyzes G3P to LPA converstion	Co-ip: endogenous proteins (yeast), overexpressed proteins (murine cells)	Seipin negatively regulates GPAT enzyme activity	(Pagac et al., 2016)
SERCA	ER calcium pump, transports Ca+2 into ER lumen	Co-ip: endogenous proteins (human cells), overexpressed proteins (*Drosophila* cells)	Seipin positively regulates SERCA activity	(Bi et al., 2014)
Lipin-1	Catalyzes PA to DAG conversion	Co-ip and AFM: overexpressed proteins (murine cells)	Seipin recruits lipin to the ER membrane	(Sim et al., 2012; Talukder et al., 2015)
AGPAT-2	Catalyzes LPA to PA conversion	Co-ip and AFM: overexpressed proteins (murine cells)	Scaffolding of lipogenic enzymes	(Sim et al., 2012; Talukder et al., 2015)
14-3-3-β	A scaffolding protein, signal transduction	Co-ip: overexpressed proteins (murine and human cells)	Cytoskeleton remodeling	(Yang et al., 2014)
Perilipin-2	LD coat protein, lipolysis regulator	Co-ip: overexpressed proteins (human cells)	Seipin regulates perilipin-2 localization to LDs	(Mori et al., 2016)
Perilipin-1	LD coat protein, lipolysis regulator	Co-ip and AFM: overexpressed proteins (human cells)	Seipin regulates perilipin-1 localization to LDs	(Jiao et al., 2019)
Reep-1	Regulates ER morphology	Co-ip: overexpressed proteins (murine cells)	Unclear	(Renvoisé et al., 2016)

4.3.4 Seipin, adipogenesis and metabolic dysfunction

Several independent KO mouse models for BSCL2 lipodystrophy have been generated. These all exhibit a phenotype mostly consistent with that observed in humans, with lipodystrophy, insulin resistance and fatty liver (Chen et al., 2012; Cui

et al., 2011; Prieur et al., 2013). However, in contrast to BSLC2 patients, hypertriglyceridemia is not observed in mice, which has been attributed to increased uptake of TAG-rich lipoproteins and FAs by the liver (Dollet et al., 2014; Prieur et al., 2013). Indeed, seipin may play different roles in liver function in humans vs rodents, as liver-specific seipin-ablated mice displayed no metabolic phenotype (Chen et al., 2014), whilst cellular studies have shown a role for seipin in hepatocyte lipid metabolism (Amine et al., 2017; Li et al., 2019a).

Several adipocyte-specific KO mouse models for seipin have also been investigated. These all develop lipodystrophy with greatly reduced fat mass (Liu et al., 2014; Mcilroy et al., 2018; Zhou et al., 2015), suggesting seipin is tissue-autonomously crucial for adipose tissue development and maintenance. It is somewhat unclear to what extent the other metabolic phenotypes can be attributed to adipose tissue loss only. Constitutive ablation of seipin in mature mouse adipose tissue was sufficient to induce both progressive adipose tissue loss, insulin resistance and hepatic steatosis (Liu et al., 2014) and these phenotypes in a global seipin KO model could be rescued by re-expression of seipin in adipose tissue alone (Gao et al., 2015). However, in inducible adipose-tissue specific KO mouse, the authors observed only severe fat loss without insulin resistance or hepatic steatosis (Zhou et al., 2015). Finally, a recent study employing constitutive seipin depletion specifically in developing mouse adipocyte tissue described early-onset, generalized lipodystrophy and altered fuel utilization without severe metabolic disturbances (Mcilroy et al., 2018). Overall, these studies suggest that whilst seipin is critical for adipocyte function and adipose tissue plays a major role in organismal energy homeostasis, seipin plays important metabolic roles also in other tissues.

Indeed, seipin KO mouse models have proved to be a valuable tool to dissect the contributions of adipose tissue loss to the pathogenesis of other diseases, such as cardiomyopathy and atherosclerosis (Joubert et al., 2017; Wang et al., 2016b). For example, the cardiomyopathy associated with BSCL2 patients and also detected in seipin KO mouse could be alleviated by efficient treatment of hyperglycemia via dapagliflozin, suggesting hyperglycemia plays a key role in the development of this cardiac dysfunction (Joubert et al., 2017). Furthermore, seipin KO exacerbated the development of atherosclerotic lesions in several atherogenic mouse models (Liao et al., 2018; Wang et al., 2016b), highlighting the importance of adipose tissue and seipin in this common disease.

The reasons behind impaired adipogenesis in the absence of seipin are unclear. Early studies utilizing cultured mouse preadipocyte cells (3T3-LI) and mesenchymal stem cells found seipin to be upregulated during adipogenesis and indispensable for adipogenic differentiation (Chen et al., 2009; Payne et al., 2008). Impaired adipogenic capacity has also been documented in seipin KO mouse embryonic fibroblasts (MEFs) and induced pluripotent stem cells from BSCL2 patients (Chen et al., 2012; Mori et al., 2016). Mechanistically, this defect appears to be evident not during stem cell commitment to preadipocyte lineage, but rather during the early stages of preadipocyte

differentiation (Chen et al., 2009). Interestingly, LD biogenesis is impaired (with supersized and tiny LDs) also during early time points of adipogenesis differentiation in BSCL2 KO MEFs, and this morphological defect precedes alterations in canonical adipocyte differentiation marker levels (such as PPAR-γ, see below) (Chen et al., 2012).

Multiple studies have suggested PPAR-γ signaling to be affected via seipin ablation, with seipin required to activate and/or sustain PPAR-γ signaling during adipogenesis (Chen et al., 2009; Prieur et al., 2013). In line with this, supplementation with PPAR-γ agonists has been shown to partially rescue the adipogenic defects in seipin knockdown 3T3-LI cells and seipin KO MEFs in some studies (Chen et al., 2009; Prieur et al., 2013), but not in others (Chen et al., 2012). PPAR-γ agonists also improved metabolic disturbances, including insulin resistance, in seipin KO mouse models (Liu et al., 2014; Prieur et al., 2013). These findings, together with evidence from various cellular models implicating seipin in PA metabolism (see below), have led to a hypothesis suggesting that seipin may function during early adipogenesis to prevent a toxic metabolite, probably PA, from accumulating at an undesired cellular localization and interfering with PPAR-γ (Gao et al., 2019; Liu et al., 2014). However, induced pluripotent stem cells from BSCL2 patients failed to develop into adipocytes in the presence of PPAR-γ activator (Mori et al., 2016).

Unrestrained cAMP/PKA signaling and increased lipolysis has also been documented in seipin KO adipocyte-differentiating MEFs and mature adipocytes (Chen et al., 2012; Prieur et al., 2013; Zhou et al., 2015). Indeed, in adipocyte-differentiating seipin KO cells, lipolysis mediators such as perilipin-1 and HSL were hyper-phosphorylated at PKA-mediated sites concomitant with increased lipolysis. Thus, through currently unclear mechanisms, seipin deficient cells exhibit constitutive and unrestrained lipolysis, leading to breakdown in TAG storage (Chen et al., 2012). In line with this, studies have proposed seipin to interact directly with Perilipin 1 and Perilipin 2, both known regulators of lipolysis (Jiao et al., 2019; Mori et al., 2016). A recent study also demonstrated partial alleviation of lipodystrophy in seipin KO mice via inhibition of ATGL (Zhou et al., 2019). Unrestrained PKA-signaling has also previously been reported to perturb adipogenesis, independently of seipin (Li et al., 2010).

However, increased lipolysis is not a universal feature of seipin depleted cells. It was not observed in *Drosophila* seipin KO fat body nor in non-adipogenic human seipin-ablated cells (Ding et al., 2018; Liu et al., 2014; Salo et al., 2019) and lipolysis was conversely decreased in mature seipin-deficient adipocytes and yeast seipin KO cells (Fei et al., 2011c; Liu et al., 2014; Wolinski et al., 2011). Overall, these data implicate the effect of seipin on lipolysis is likely tissue/cell-type specific or it may be indicative of a yet unidentified up-stream phenomenon. However, lipolysis may well be a major culprit of the defective adipogenesis and as such a potential therapeutic target in lipodystrophy patients.

4.3.5 Seipin as a regulator of actin dynamics and calcium flux

Seipin has also been proposed to regulate adipogenesis via remodeling of the actin cytoskeleton, through a direct interaction with 14-3-3-β through seipin's cytoplasmic termini (Yang et al., 2014). In this model, seipin would transfer ER-derived lipid storage signals to the actin cytoskeleton through the scaffold protein 14-3-3-β and its client cofilin-1, enabling the extensive remodeling of actin required for adipocyte development (Yang et al., 2014). Whilst a number of recent studies have linked actin remodeling to adipogenesis, insulin resistance and LD storage (Kim et al., 2019; Pfisterer et al., 2017; Tharp et al., 2018), the precise role of seipin in regulating cytoskeleton elements is unclear.

Seipin has also been proposed to regulate fat storage via modulation of intracellular calcium levels (Bi et al., 2014; Ding et al., 2018). Seipin was found to physically interact with the sarco/endoplasmic reticulum Ca2+-ATPase (SERCA) in both *Drosophila* and human cells (Bi et al., 2014). SERCA activity and ER calcium levels were reduced in seipin KO flies and SERCA disruption in *Drosophila* fat body cells led to reduced lipid storage similar to seipin KO. Interestingly, the reduced lipid storage of seipin KO flies could partially be alleviated by concomitant disruption of an ER-to-cytosol calcium pump, RyR, suggesting reduced ER calcium levels are important for fat storage. In a follow-up study, seipin was also found to be important for the maintenance of mitochondrial calcium homeostasis (Ding et al., 2018). Seipin KO fat body cells displayed altered mitochondrial function, and reducing mitochondrial calcium export could partially alleviate the lipid storage defects in seipin mutants (Ding et al., 2018). Although the molecular mechanisms by which seipin influences SERCA activity and/or mitochondrial calcium levels are unclear, a recent study also linked seipin to alterations in calcium metabolism in human liver cancer cells (Li et al., 2019b).

4.3.6 Seipin and LDs

Seipin perturbation leads to impaired LD assembly in multiple model systems, with a phenotype of small and supersized LDs. Other features include delayed LD formation, aberrant LD protein composition and dysfunctional and morphologically abnormal ER-LD contacts (Chen and Goodman, 2017). Two emerging hypotheses have been proposed to account for these observed effects. Seipin may primarily function to control LD formation via modulation of PL metabolism and/or PL distribution at the ER, or ascertain its function via control of ER-LD contacts and LD forming sites, perhaps acting as a structural component and/or diffusion barrier (Chen and Goodman, 2017; Gao et al., 2019). Data for these hypotheses, which are naturally not mutually exclusive, is briefly discussed below.

4.3.6.1 Seipin as a modulator of cellular lipid metabolism

Seipin is likely a non-enzymatic protein, as no enzymatic domains have thus far been identified in it. However, the dramatic effects of seipin loss on LDs and adipogenesis have led to thorough investigation of the consequences of seipin ablation on cellular lipid metabolism. Unfortunately, consistent, robust aberrations in seipin depleted lipidomes have not yet been uncovered, except for the global decrease of NLs in lipodystrophy patients and BSCL2 animal models lacking adipose tissue. For example, considering the cellular levels of TAG in the absence of seipin, some yeast studies have reported increased levels (Fei et al., 2008, 2011c), whilst others have detected a decrease ((Gao et al., 2017b; Han et al., 2015) or no alterations (Grippa et al., 2015; Wang et al., 2014). Similarly in mammalian studies of non-adipocyte cells, seipin depletion leads to both decreased (Boutet et al., 2009; Hölttä-Vuori et al., 2013; Salo et al., 2016) and increased (Fei et al., 2011b) levels of TAG, and other studies have detected no change (Wang et al., 2016a). Also robust alterations in cellular PL levels have not been detected in response to acute or chronic seipin depletion (Fei et al., 2008, 2011c; Grippa et al., 2015; Salo et al., 2019; Wang et al., 2014, 2016a). Studies have documented alterations in yeast and human lipidome saturation indexes in seipin deficiency (Boutet et al., 2009; Fei et al., 2008), implicating decreased SCD1 activity, while other studies have failed to uncover robust changes in these parameters (Salo et al., 2019; Wang et al., 2016a).

An especially interesting lipid in this context is PA, a putative binding client for seipin (Yan et al., 2018). PA levels are increased in the absence of seipin in many model systems, such as yeast microsomes (Fei et al., 2011c), *Drosophila* larvae (Tian et al., 2011), mouse testes (Jiang et al., 2014), mature seipin depleted mouse adipose tissue (Liu et al., 2014) and 3T3-Li preadipocyte microsomes (Pagac et al., 2016). On the other hand, others have failed to detect differences in cellular PA levels even in the presence of a robust LD phenotype, arguing that global PA handling may not be the culprit of seipin deficiency (Grippa et al., 2015; Wang et al., 2016a). However, this does not rule out a role of seipin in locally controlling PA metabolism at the ER. This notion is supported by the discovery that multiple PA-sensing fluorescent probes accumulate at distinct LD-associated ER foci in yeast seipin KO cells, suggesting localized PA accumulation (Grippa et al., 2015; Han et al., 2015; Wolinski et al., 2015). It should be noted, however, that such accumulates were not observed in mammalian seipin KO cells (Wang et al., 2016a), and Grippa and colleagues postulated that these PA-probes may in fact be reporting localized PL packing defects, rather than PA accumulation (Grippa et al., 2015; Horchani et al., 2014).

Seipin has been proposed to control cellular PL and/or TAG metabolism via direct interactions with multiple lipogenic enzymes, including AGPAT2 (Talukder et al., 2015), lipin-1 (Sim et al., 2012) and GPATs (Pagac et al., 2016). Through immuno-purification of co-overexpressed proteins and AFM studies, single seipin oligomers were shown to be able to bind both AGPAT2 and lipin-1 at the same time. In developing adipocytes, the seipin-lipin-1 interaction was increased in response to exogenous FAs, and a forced stabilization of the AGPAT2-seipin interaction increased

cellular PPAR-γ expression in the nucleus (Sim et al., 2012; Talukder et al., 2015). These data indicate that seipin may act as a scaffold for these enzymes, facilitating lipid flux from enzyme to enzyme, which would be essential during conditions of high lipogenesis, such as adipogenesis (Talukder et al., 2015). This mechanism may not be involved in regulating the core function of seipin in LD formation, as the cytoplasmic N- and C-termini of seipin (crucial for lipin-1 binding in human cells) are evolutionarily poorly conserved and not necessary for seipin function in yeast (Wang et al., 2014; Yang et al., 2013). However, disrupted lipid flux between AGPAT and lipin enzymes could explain the increased levels of local PA. Importantly, AGPAT2 mutations also lead to lipodystrophy in humans, similar to seipin, and loss of lipin-1 function leads to lipodystrophy in mice (Melvin et al., 2019).

In contrast to a facilitatory role for seipin in AGPAT2-lipin1 mediated lipid flux, the interaction between seipin and GPAT is proposed to be inhibitory in nature (Pagac et al., 2016). In this study, the authors demonstrated that GPAT activity is altered/increased in multiple seipin depleted systems. Seipin was proposed to control GPAT activity and thereby prevent aberrant LD expansion. Whilst the molecular underpinnings of this interaction are unclear, inhibiting GPAT activity was also shown to partially alleviate defective adipogenesis in seipin-deficient cells (Pagac et al., 2016). Importantly, this interaction was observed in both yeast and mammalian preadipocyte systems, arguing for a conserved role in both LD formation and adipogenesis. These data lend further support for the model (discussed above) of a toxic lipid ligand, dependent on the inhibitory action of seipin on GPAT activity, being the culprit of defective adipogenesis in the absence of seipin (Pagac et al., 2016). Furthermore, this model is supported by seipin's capability of binding anionic PLs, such as PA (Yan et al., 2018) and observations that overexpression of seipin can inhibit LD formation in mammalian cells (Fei et al., 2011b; Yang et al., 2013). However, why seipin would directly need to inhibit GPATs to allow for growth of seipin-associated LDs, as reported recently (Cao et al., 2019; Salo et al., 2019), remains to be uncovered.

4.3.6.2 Seipin as a stabilizer of LD formation sites and ER-LD contacts

In the absence of robust global lipidomic changes in seipin deficient cells, a more discrete role for seipin in structurally regulating ER-LD contacts and the identity of LDs has been proposed. In this model, seipin may not primarily control lipid synthesis or degradation, but rather controls the flow of lipids (NLs, PLs or both) between these two organelles. This notion is supported by the localization of the seipin complex at ER-LD contact sites and the defects of LDs and ER-LD contacts in its absence (Fei et al., 2008; Grippa et al., 2015; Salo et al., 2019, 2016; Szymanski et al., 2007; Wang et al., 2016a). However, what exactly seipin regulates at ER-LD contacts is unclear. Indeed, although recent studies have clearly shown a LD-autonomous growth-promoting function for both *C. elegans* and human seipin (Cao et al., 2019; Salo et al., 2019), this could be achieved via many different mechanisms.

In yeast, seipin KO leads to a phenotype where some cells accumulate supersized LDs (SLDs), whilst others display aggregated small LDs often entangled in the ER network (Cartwright et al., 2015; Grippa et al., 2015; Szymanski et al., 2007; Wolinski et al., 2011). A number of other yeast mutants also display SLDs, and these have been attributed to alterations in PE/PC ratios and increased PA levels (Fei et al., 2011c). However, the LD phenotype of seipin KO is different from these mutants, as the LD morphology cannot be rescued by supplementation with PL precursors. Instead of reverting to normal sized LDs of WT cells, stimulation of PL synthesis in seipin mutants leads to a higher fraction of small, aggregated LDs (Cartwright et al., 2015; Grippa et al., 2015; Wang et al., 2014). These data suggest seipin may function to uncouple LD growth from ER PL pools, as the excess PL leads to numerous tiny LDs. It has thus been proposed that in the absence of seipin LD morphology is solely dependent on available PLs in the ER (Grippa et al., 2015; Wang et al., 2018b).

This elegant notion is further supported by observations that the SLDs and small aggregated LDs appear to have different monolayer features, with small LDs displaying monolayer packing defects recognized by typically non-LD resident proteins, whilst the SLDs have a higher surface tension, more similar to normal WT LDs (Grippa et al., 2015). Indeed, defective targeting of various LD-localized proteins have been noted in multiple seipin KO models, including mammalian cells (Salo et al., 2016; Wang et al., 2016a). For example, a subset of LDs in seipin depleted *Drosophila* cells acquire machinery for local TAG synthesis prematurely, leading to their aberrant expansion (Wang et al., 2016a), whilst growth-abortive tiny LDs of human seipin KO cells fail to acquire ACSL3, a key acyltransferase important for LD growth (Salo et al., 2016). These targeting defects may arise due to alterations in LD monolayer properties. Overall, seipin may function to control the monolayer surface tension of LDs via ER-LD contacts by acting as a diffusion barrier (Grippa et al., 2015). Whilst this function would explain many of the observed LD defects in seipin deficient cells, whether it controls primarily PL, NL or protein flux, is unclear.

Seipin has recently been linked to control of LD diversification in yeast cells. During nutritional stress, yeast cells expand their ER-vacuole contact sites, which also serve as a site for LD production in these conditions (Hariri et al., 2017). These ER-vacuole contact site-associated LDs, which represent a unique LD subpopulation, can be modulated by protein factors Ldo45/Ldo16, which interact with seipin (Eisenberg-Bord et al., 2018; Teixeira et al., 2018). A human homolog of Ldo45/Ldo16 called promethin could also be co-immunoprecipitated by seipin in co-overexpression experiments, and its localization to LDs was regulated by seipin expression levels (Castro et al., 2019). As the Ldo45/Ldo16 proteins are modulated by nutritional conditions (Teixeira et al., 2018), they may assert an additional layer of control over seipin-mediated ER-LD contacts.

Seipin may also physically help to tether the ER and LDs together, facilitating the formation of membrane bridges (Salo et al., 2019). This notion is supported by the observation that a subset of LDs detach completely from the ER in the absence of

seipin in both yeast and mammalian cells (Chen and Goodman, 2017; Han et al., 2015; Salo et al., 2016), a phenomenon not described in WT cells or any other mutants. In line with this, LD inheritance between yeast mother and daughter cells is disturbed in seipin KO, owing likely to disrupted ER-LD connections (Wolinski et al., 2011). However, most LDs even in the absence of seipin retain contacts with the ER (Salo et al., 2016; Wang et al., 2016a), likely due to other tethering factors, such as Rab18 and snx14. However, these remaining contacts are apparently not sufficient to ensure controlled LD growth in the absence of seipin.

The defective LDs of seipin KO cells may also be a consequence of defective initial LD biogenesis. Indeed, in a yeast system where NL synthesis was held constant, LD biogenesis was severely delayed in seipin deficient cells (Cartwright et al., 2015). The authors also observed a defect in NL partitioning between the ER and LDs, with relative accumulation of TAG in membranes, concomitant with appearance of tiny, de-novo LDs. Tiny, growth-abortive LDs are also generated in seipin KO mammalian cells during *de novo* lipogenesis (Salo et al., 2016; Wang et al., 2016a). These data suggest that in the absence of seipin, LDs may spontaneously "oil out" of the ER, suggesting seipin could regulate NL flux from the ER to LDs. This notion is supported by FRAP experiments of FA analogs in acutely seipin depleted cells (Salo et al., 2019) as well as ultrastructural evidence of electrolucent (i.e. lipid-like) material accumulating in LD-proximal ER regions (Grippa et al., 2015) and a widening of ER width in lipid-challenged mammalian seipin KO cells (Salo et al., 2016). This "oiling out", could be a consequence of deficient platform assembly for LD formation in the absence of seipin (discussed in more detail in Results and discussion).

Whilst the LD phenotype of seipin deficient yeast cells is overall similar to what has been reported in mammalian cells, there are a few notable differences. In mammalian cell systems both SLDs and aggregated LDs are typically seen in the same cell, whilst in yeast there is more cell-to-cell heterogeneity (Chen and Goodman, 2017). A possible explanation is the more complex architecture and larger size of mammalian ER, where more diverse lipid subdomains may exist within single cells. Furthermore, yeast seipin mutants typically display tangles of ER networks in close proximity to aggregated LDs, a phenotype not reported in mammalian cells (Grippa et al., 2015; Salo et al., 2016; Wolinski et al., 2011). Similar aggregates could also be induced in WT yeast cells via forcing increased LD generation by growing cells in OA-containing medium (Chorlay et al., 2019; Wolinski et al., 2015). As the ER morphology is normal in seipin KO mammalian cells (Wang et al., 2016a), these differences may stem from differences in ER regulating factors, indicating higher adaptivity of the mammalian ER network. In line with this, seipin deficiency sensitizes yeast, but not mammalian cells to ER stress (Wang et al., 2016a; Wolinski et al., 2015). It should be noted, however, that seipin has been proposed to interact with ER-shaping proteins in both yeast and mammalian systems (Renvoisé et al., 2016; Wang et al., 2018b).

Perhaps the most striking difference between yeast and mammalian systems in relation to seipin biology is the observation that in yeast systems almost all seipin foci localize

at ER-LD contacts (Wang et al., 2014), whilst in mammalian cells there are typically many more seipins than LDs, and a high fraction of seipins reside in the ER, outside of ER-LD contacts (Salo et al., 2016; Wang et al., 2016a). This strongly suggests that at least in mammalian cells, seipin likely plays roles outside of ER-LD junctions, possibly modulating Ca2+ flux, ER PL metabolism or other functions. The specific function of non ER-LD-junction associated seipin foci has thus far not been clarified.

5 AIMS OF THE STUDY

The aim of this study was to elucidate the role of seipin in organizing lipogenic subdomains of the ER and decipher how its function is disrupted in diseases caused by seipin mutations. Specific aims of the study are listed below:

In the first study, we aimed to shed light on the pathogenesis of seipinopathy, caused by the N-glycosylation defective N88S-seipin. We utilized cells of CNS origin and developing zebrafish larvae to ectopically overexpress N88S and characterize its subcellular localization and effects on NL storage. We also investigated the interplay between LDs and ER stress pathways in these systems.

In the second study, we sought to characterize the role of seipin in LD formation and investigate mechanisms leading to lipodystrophy in its absence. By employing CRISPR/Cas9 mediated genome editing in combination with advanced imaging techniques, we investigated the subcellular localization of endogenous seipin and the consequences of seipin loss in human cells.

In the third study, we aimed to define the ultrastructure of seipin-mediated ER-LD contacts sites and investigate seipin's role in regulating NL flux between the ER and LDs.

6 METHODS

Methods used in this thesis are summarized in **Table 4**. Detailed Materials and Methods are presented in the original publications (I-III), and some methodical considerations are presented here.

Table 4. *List of main methods used in this thesis.*

Method	**Study**
3D-SIM microscopy	II
Adenovirus-mediated silencing	III
Airyscan super resolution live and fixed cell microscopy	II, III
Auxin-induced degradation of intracellular proteins	III
CLEM	III
Click-chemistry analyses of FA flux	II, III
Electron tomography	II, III
Fluorescence recovery after photobleaching (FRAP)	II, III
Generation of stable cell lines	II, III
GUV preparation and model membrane studies	III
HPTLC lipid analysis	I, II, III
Image analysis (ImageJ, Huygens, iIlastik, MatLab, CellProfiler, Icy)	I, II, III
Immuno-EM	II
Immunoblotting	I, II, III
Immunofluorescence	I, II, III
Laser scanning confocal microscopy	I, II, III
LD isolation	I, III
Lipid mass spectrometry	III
Mammalian cell culture and transfection	I, II, III
Molecular cloning	I, II, III
PCR	II, III
Retrovirus-mediated ectopic expression	II
Statistical analysis	I, II, III
Stochastic optical reconstruction microscopy (STORM)	II
Widefield live and fixed cell microscopy	II, III
Zebrafish maintenance, microinjections and swimming experiments	I

6.1.1 Model systems

In these studies, we utilized multiple immortalized cell lines, including human astrocytoma (U251 MG), murine neuronal-like (NSC-34) and human epidermoid carcinoma cells (A431). Most extensively we employed A431 cells. These are fast growing, genetically malleable and metabolically active cells, and have extensively been used for LD studies by us and others (Heybrock et al., 2019; Moessinger et al., 2011; Salo et al., 2016). Using highly proliferative cells was necessary as many of our techniques (such as CRISPR-mediated gene KO and endogenous tagging) involve the generation of stable, genetically modified cell lines. The duration of stable cell line generation via limiting dilution is dependent on the growth rate of the cell lines used.

Whilst drawing conclusions for normal physiology from cancer cells is always risky, the mechanisms involved in LD assembly appear broadly conserved amongst cell types. Furthermore, we also validated our key findings using non-transformed cells, primary and BSCL2 patient-derived fibroblasts. In study I, we also employed an *in vivo* system, developing zebrafish and in study III, an *in vitro* system of giant unilamellar vesicles (GUVs).

An important aspect of the studies presented here is tight control of the metabolic status of the cells. Typically for LD studies in mammalian cells, cells are treated with high concentrations of extracellular FAs (Guo et al., 2008; Kuerschner et al., 2008) and we used oleic acid (OA) for this purpose (I-III). OA treatment readily induces LD formation. However, as we were especially interested in the early steps of LD biogenesis (II-III), it was important to create a starting condition where the cells would not initially contain any pre-existing LDs. To achieve this, we first stringently starved the cells by culturing them for several days in a medium which lacked extracellular FAs (i.e. lipoprotein deficient serum containing medium, LPDS). During this treatment, cells efficiently metabolize their pre-existing LDs, presumably to use the liberated FAs for energy production and as membrane precursors for cell proliferation. Thus, upon pre-treatment of cells with LPDS and subsequent OA treatment, we could ensure the LDs we were observing were generated *de novo*. To further improve the stringency of the starvation, we also employed DGAT1 and DGAT2 inhibitors in study III.

Previous studies have utilized starvation protocols in serum free medium to reduce LD numbers (Kassan et al., 2013). However, as serum starvation induces autophagy and other cellular adaptations which interfere with LD biogenesis (Rambold et al., 2015; Shpilka et al., 2015), we chose to use LPDS starvation instead.

6.1.2 Gene perturbation studies

Loss-of-function techniques are key to obtaining information about the function of proteins. To achieve gene/protein perturbation, we used multiple techniques, including small interfering RNA (siRNA, I-III), gene ablation via CRISPR/Cas9 technology (II-III), adenovirus-mediated silencing (III) and auxin-mediated degradation of proteins

(III). All these techniques have their advantages and disadvantages and some of these in relation to our studies are discussed here.

siRNAs are easily obtainable commercially and easy to use. However, they only allow for transient knockdown of the gene of interest and are never 100% efficient. As they target the mRNA of the protein of interest, it takes time to achieve protein level depletion, and this time is dependent on the half-time of the protein. In the case of seipin, our studies suggested that even upon depletion of a substantial amount of the protein, the remaining seipin oligomers remain functional as LD-autonomous, LD-growth promoting units (III). Thus, to reveal the "true" phenotype of seipin KO, i.e. the tiny, growth abortive LDs with a few supersized ones (Salo et al., 2016; Wang et al., 2016a), more efficient seipin removal is necessary. To this end, we utilized CRISPR/Cas9-mediated gene ablation (Ran et al., 2013).

CRISPR-techniques (II-III) are more labor intensive and time consuming than siRNAs, requiring cloning and often limiting dilution to obtain single clonal cell lines. However, using CRISPR it is possible obtain cells with permanent and total disruption of the gene of interest. In the case of seipin, the phenotype of tiny and supersized LDs is evident in A431 seipin KO cells, recapitulating the phenotype observed in BSCL2 patient cells (II). However, CRISPR-mediated gene KO is not an acute manipulation, and cells have ample time to adapt to the loss of the protein of interest. Thus, the phenotypes observed in chronic KO cells may be the result of adaptations and may not reveal the direct function of the protein of interest. To overcome this limitation, we adapted the plant-based auxin-induced degradation system (AID) (Nishimura et al., 2009) to examine the effects of acute seipin removal (III).

The AID system allows for rapid depletion of a protein of interest (Nishimura et al., 2009). In this system, a degron tag is fused to a target protein and cells are genetically engineered to exogenously express a plant-derived protein of the auxin receptor F-box protein TIR1/AFB class. Upon addition of a molecule of the auxin class, such as indole-3-acetic acid (IAA), these proteins form a complex which recruits the ubiquitination machinery of the cell to the target protein, resulting in rapid polyubiquitination and proteasomal degradation of the protein of interest (Nishimura et al., 2009; Tan et al., 2007b). Although previously used primarily for cytosolic proteins, we found this system also works for transmembrane proteins (Li et al., 2019c). In study III, we used this system to characterize the phenotypes of acute seipin removal. Of all the aforementioned techniques, AID system is by far the most laborious, as it requires generation of homozygous knock-in clones. However, it allows for examination of acute phenotypes.

6.1.3 Protein localization studies

A common method to decipher a protein's function is to observe its intracellular localization with microscopy. To facilitate this, proteins can be tagged with fluorescent molecules or easily recognizable epitopes. In study I, we used GFP-tagged

constructs to observe the localization of seipin and its mutants. However, overexpression is often problematic as this typically involves a substantial overproduction of the protein of interest, which may mask the proteins true localization. In the case of seipin, high overexpression reveals no specific enrichment at any ER subdomain. Thus, to obtain information about a protein's preferred intracellular localization, it would be optimal to examine the protein at endogenous levels. Whilst this can sometimes be achieved via antibody staining, this technique is highly dependent on obtaining functional antibodies for immunofluorescence and is mainly limited to fixed cells.

To overcome these issues, we utilized several approaches. In study II, we generated low-level overexpressing cells (using retrovirus-mediated overexpression) of GFP-tagged WT- and A212P-seipin, which we generated on top of a seipin KO background. This allowed for detailed characterization of the proteins' subcellular localization, although we were still observing circa 4-fold overexpressed levels of the protein. To examine the localization and dynamics of seipin at endogenous levels, we utilized CRISRP-mediated endogenous tagging via homology-directed repair (HDR) (Pinder et al., 2015) (II-III). In this system, cells are transfected with plasmids containing Cas9 and sgRNAs targeted to loci of interest, together with a plasmid containing homology arms flanking the targeted genomic locus and a tag of interest. After transient selection with antibiotics and limiting dilution to obtain single clones, cell lines with homozygous knock-in of the gene of interest with the tag of interest can be obtained. In study II, we used this technique to tag seipin with sfGFP at its genomic locus and image its localization in relation to LDs in both live and fixed cells.

In study III, we expanded the usage of this technique, by tagging multiple genes of interest (seipin, ACSL3, Rab18) with various tags (SNAPf-tag, split GFPx7, degron tag to be used with the AID system). To facilitate obtaining homozygously tagged clones, we used fluorescence-activated cell sorting (FACS) prior to single cell cloning. Whilst initially labor intensive, this technique is highly useful, as overexpression-induced mislocalization artifacts can be avoided. Furthermore, these cells can be easily further used to manipulate the subcellular localization of the protein of interest or achieve its rapid removal on-demand with the AID system (III).

It should be noted that prior to embarking on endogenous tagging of a protein of interest, it will be vital to know where (e.g. N- or C-terminus) the protein can be tagged without interfering its function. Seipin appears to tolerate C-terminal tagging quite well, with no apparent loss of function even upon tagging the protein with a split-GFPx7 tag, which will result in a high number (up to 7) of GFP-molecules/protein.

6.1.4 Lipid biochemistry

To gain insight into the lipid levels of cells and tissues, we utilized several techniques, such as high-performance thin layer chromatography (HPTLC) (I-III) and mass spectrometry (III). Prior to analysis, lipids of the samples were isolated via traditional

solvent-based lipid extraction techniques (Bligh, E.G. and Dyer, 1959). This technique takes advantage of the physicochemical properties of lipids and allows for their separation into an organic phase, distinct from the water phase containing other macromolecules, such as proteins and carbohydrates.

The distinct physicochemical properties of LDs vs other organelles also form the basis for LD isolation techniques, which we used extensively in these studies (I, III). Lipid-filled LDs are lighter than other cellular organelles, and after mechanical homogenization of cell lysates they can easily be separated from other organelles via sucrose gradient centrifugation as they end up floating to the top of the centrifuge tube (Brasaemle and Wolins, 2006). Isolated cellular LDs can then further be subjected to various analyses, including immunoblotting (I), imaging (III) and lipid analysis (III).

We also examined the FA flux of cells utilizing click-chemistry methods (II-III) (Thiele et al., 2012). With this technique, we could examine the fate of an exogenously added lipid. In our studies, we utilized alkyne-OA, which is very similar to OA, but contains an additional triple bond at its tail. This alkyne moiety is typically not found in biological systems but is unlikely to grossly affect the biological properties of the lipid. After incubation of cells with alkyne-FA, lipids are extracted and a fluorogenic "click"-reaction is performed, allowing for subsequent detection of the metabolites using HTPLC or similar techniques. This enables examining into what lipid groups alkyne-OA is metabolized within cells. This is akin to using radiochemically- or isotope-labelled lipids but allows for using micromolar concentrations of the labelled lipid and thus greatly increases specificity. In other words, when examining LD biogenesis using alkyne-FA, there is no need to add unlabeled lipid, and thus we are in fact tracing the entire exogenous FA pool.

6.1.5 Light microscopy

In these studies, we utilized multiple light microscopy techniques, including confocal laser scanning microscopy (I-III), widefield imaging (II-III), Airyscan imaging (II-III), 3D-structured illumination microscopy (3D-SIM, II) and stochastic optical reconstruction microscopy (STORM, II). Within these modalities, we performed both live and fixed cell imaging as well as FRAP studies. Whilst technical details are found in the methods of the articles, a few considerations are discussed here.

In all these studies, we were imaging cellular LDs. Due to their high NL content, they are easily stainable by organic dyes, such as Bodipy (BPY), commercial LipidTox dyes, monodansylpentane (MDH) and the bright, BPY-derived LD540 (Spandl et al., 2009). LDs can also be visualized by fluorescently tagged protein markers, such as the LD coat protein perilipin-2 (Salo et al., 2016) and the ER-LD model peptides HPOS (Kassan et al., 2013) and LiveDrop (Wang et al., 2016a), which accumulate on LDs due to the unique physiochemical properties of the LD monolayer. Of all these probes, we found LD540 to be superior in terms of signal-to-noise ratio and sensitivity, as it could detect even the tiny LDs of seipin depleted cells similarly to LiveDrop or HPOS,

but with less background. Furthermore, nascent LDs became detectable with both dyes at roughly same time points (III). An important consideration in LD imaging is to avoid glycerol-based mountants, as these will lead to post-fixation artifacts such as fusion. To minimize these artifacts, we typically mounted samples in PBS or similar water-based mountants.

The key to successful imaging is to utilize the correct technique for the question at hand. For example, to observe quantitatively LD morphology within cell populations and individual cells, it is not necessary to utilize the high resolution of confocal systems and super resolution techniques, as widefield imaging gives adequate resolution, but is more rapid, enabling higher number of cells to be sampled for quantitative analysis. On the other hand, minute details such as estimates of the seipin oligomer size in the ER could only be approached with super resolution techniques such as STORM.

For live cell imaging, the main consideration is to obtain sufficient signal for analysis but without causing phototoxicity or bleaching. When imaging low-abundance objects, such as endogenously tagged proteins, an important aspect to consider is the "photon budget" and how to spend it. Microscopy settings (such as laser intensity, detector gain, times between acquisitions in a time series etc.) have to be set accordingly so that adequate data can be obtained to answer the question at hand. Thus, to examine a rapid (seconds timescale) process such as nascent LD formation in the dynamic ER network or rapid LD motility, acquisition rates of 1 frame/second and less have to be used. On the other hand, to observe slower processes (minutes-hours time scales), such as LD size changes over time, imaging at such high frame rates for prolonged periods of time would result in phototoxicity and bleaching, hampering detailed analysis.

It is also essential to optimize all possible parameters, since the actual biological events (such as LD biogenesis) cannot easily be speeded up or slowed down according to your needs. These optimizable parameters include using appropriate phenol-red free imaging medium, anti-fade reagents and, most importantly, bright and photostable dyes and fluorescent proteins. To this end, we moved from traditional eGFP to using tags such as split7x-GFP (Kamiyama et al., 2016) (which allows multiple copies of sfGFP to tag one molecule) and SNAPf (Sun et al., 2011) (which allows to label proteins with bright organic dyes). In studies II-III we performed the majority of live cell imaging using a Zeiss Airyscan system, which due to its unique detector architecture allows for higher resolution and, most importantly, higher sensitivity than traditional confocal microscopes (Korobchevskaya et al., 2017). It should be noted, however, that we did not have access to spinning disk microscopes or advanced modalities like lattice light sheet imaging during these studies. It would be highly interesting to use these techniques for imaging of nascent LD biogenesis.

In studies II-III, we used FRAP techniques to address molecule motility in cells. In this technique, a portion of fluorescently labelled molecules are bleached and

fluorescence recovery to that bleached region of interest is followed over time. As bleaching of common fluorophores is essentially irreversible, recovery then gives an indication of molecule mobility (Lippincott-Schwartz et al., 2001). To trace ER-to-LD protein trafficking we bleached HPOS-mCherry signal within individual LDs and LD clusters and followed recovery of the fluorescence (II). Since LDs are motile organelles, we simultaneously imaged an additional LD marker, a LipidTox dye, to ensure that we could trace fluorescence recovery to the bleached LD, even if that moved during time lapse image acquisition. Using this technique, we found HPOS recovery to LDs to be impaired in seipin KO cells, whilst HPOS recovery in the ER was unchanged, suggesting impaired ER-to-LD trafficking (II).

We also performed BPY-C12 FRAP in LDs (II-III). BPY-C12 is a commonly used fluorescent FA analog and can thus be thought to trace lipid trafficking within the cell (Ohsaki et al., 2016; Rambold et al., 2015; Salo et al., 2016). In line with this, we and others have found that it is metabolized in cells and can also be esterified. However, a major issue in this technique is that for each observable fluorophore, we have no way of knowing in what kind of lipid it is. Thus, whilst we found that a majority of BPY-C12 appeared to be as esterified NL molecules in isolated cellular LDs, it doesn't directly indicate we are observing NL trafficking when performing BPY-C12 FRAP. Furthermore, the BPY side chain is likely a major contributor to BPY-C12's intracellular behavior, and thus kinetic parameters obtained with FRAP cannot be considered as direct indicators of NL trafficking. Further developments in fluorescent lipid dyes are necessary to overcome this limitation.

For image analysis, we performed multiple different analyses, including co-localization studies (I-II), feature-based image analysis (II-III), FRAP analysis and tracking of objects and their intensities (II-III). These were performed using software such as Image J FIJI, Huygens, Matlab, CellProfiler, Ilastik and ICY. We aimed to automate as much of the analysis as possible to speed up the work flow and to avoid unintentional bias. For example, for analysis of LD size distributions and localizations in cells, extensive automated workflows were developed to analyze hundreds-thousands of cells automatically. For more difficult tasks, such as tracking of objects, we were partially forced to rely on manual tracking of objects to ascertain reliable tracking results.

In image analysis, an important consideration is how to develop a workflow where the data (images) are analyzed accurately, but without having to make "judgement calls" during the analysis, to ensure unbiased results. Automation, scripting and blinding are excellent tools to facilitate this. For example, for LD motility analysis in study II, we used two parallel approaches. We manually quantified the motility of dozens of droplets, which was labor-intensive, but accurate. We additionally used co-localization analysis of adjacent time frames to measure a similar parameter, but for a much larger number of objects, with the idea that the less overlap between subsequent frames, the more the objects had moved. As both techniques gave matching results regarding the general phenotype (i.e. LDs moved more rapidly in seipin KO cells than

in WT cells), we could use the automated, more rapid technique for similar analyses in many different conditions.

An important aspect of the image analysis techniques we used in studies II-III was the detailed analysis of LD size distributions on a single-cell level. Using automated scripts developed for detecting single LDs in cells, we could assess the effects of acute seipin removal on the size distributions of cellular LDs. Whilst overall LD coverage of cell areas was not dramatically affected, the size heterogeneity of small and large LDs became apparent. This indicates complex regulation of LD sizes and suggests that single averaged parameters, such as total LD numbers/cell or mean LD sizes/cell, which are typically used for this kind of analyses in the literature, are not necessarily sufficient to completely describe the phenotypes observed.

7 RESULTS AND DISCUSSION

7.1 ALLEVIATION OF SEIPINOPATHY RELATED ER STRESS BY TRIGLYCERIDE STORAGE (I)

Mutations in the luminal N-glycosylation site of seipin (N88S, S90L) lead to a dominantly inherited form of motor neuron disease, a form of spastic paraplegia (SPG17 or Silver syndrome), termed collectively as "seipinopathies" (Ito and Suzuki, 2009). Previous work had suggested the pathogenesis of seipinopathy to involve aggregation of misfolded seipin mutants, leading concomitant ER stress activation (Ito and Suzuki, 2007; Yagi et al., 2011). However, in HeLa cells N88S-seipin aggregates were in fact found to be protective against ER stress (Ito et al., 2012), although the detailed nature of these cytoplasmic inclusions remained unclear. Importantly, previous work had not explored links between NL metabolism and seipinopathy causing seipin mutants.

7.1.1 N88S-Seipin localizes to LDs

In this study we set out to investigate the subcellular localization of N88S-seipin and its effects on lipid status of cells of CNS origin (human astrocytoma U251 MG cells and murine NSC-34 motor neuron-like cells). We ectopically expressed GFP-tagged WT- and N88S-seipin proteins and found that overexpression of the mutant protein decreased the TAG content of cells, whilst WT-seipin overexpression had no effect (**I, Fig. 1**). siRNA-mediated knockdown of seipin also lead to decreased TAG storage (**I, Fig. S1**), suggesting N88S-seipin asserts a dominant negative effect on the lipid status of the cells. WT-seipin was localized to the ER, whilst in a high fraction of cells, N88S-seipin formed distinct, often ring-like inclusions (**I, Fig. 2**). Co-staining with lipophilic dyes revealed these inclusions to be LDs, and the segregation of N88S-seipin from bulk ER to LDs could be increased via OA treatment of cells (**I, Fig. 2-3**). Using biochemically isolated LDs from cells, we found a higher fraction of N88S-seipin than WT-seipin copurifying with LDs (**I, Fig. 3**). These data suggest that N88S-seipin, in contrast to WT-seipin, readily accumulates at LDs or ER regions juxtaposed to LDs and this segregation can be increased by LD induction.

7.1.2 Alleviation of N88S-seipin and tunicamycin induced ER stress by triglyceride storage

In agreement with previous reports in non-neurogenic cell models (Ito and Suzuki, 2007), we found that N88S-seipin overexpression lead to increased ER stress also in neuronal cells (**I, Fig. 3**). We measured ER stress by immunoblotting of CCAAT/enhancer binding protein (CHOP), a commonly used ER stress marker (Hetz, 2012). CHOP levels were also increased by treatment of cells with the ER-stressor tunicamycin, a general inhibitor of N-glycosylation, which leads to

accumulation of misfolded proteins in the ER (**I, Fig. 4**). Importantly, ER stress levels induced by both N88S-seipin and tunicamycin could be alleviated by increasing LD abundance, either via OA treatment or ATGL knockdown (**I, Fig 3-4, S2**). These results suggest that increasing TAG storage at LDs may protect neuronal cells from ER stress induced by protein misfolding.

7.1.3 Zebrafish model of seipinopathy

Finally, we utilized zebrafish, a common model system in lipid metabolism studies (Hölttä-Vuori et al., 2010), to generate an *in vivo* model for seipinopathy. We induced human WT or N88S-seipin overexpression by mRNA microinjection at a two-cell stage and characterized the ensuing phenotypes during the first days post fertilization (dpf). We found that N88S- but not WT-seipin overexpression induced lipid abnormalities in the developing zebrafish (**I, Fig. 5**). A marked reduction of TAG levels in 2-4 dpf zebrafish heads was observed, with a concomitant increase in TAG levels in the trunks of the larvae, suggesting defective yolk lipid mobilization to the developing brain (**I, Fig. 5, S3)**. This was accompanied by a decrease in free swimming of the N88S-expressing zebrafish larvae at 4-6 dpf, without obvious morphological abnormalities or loss of motor neurons (**I, Fig. 5, S3-S4**). This defect could be rescued by supplementation with exogenous OA, which also decreased CHOP levels in the developing zebrafish (**I, Fig 5**). These results suggest that N88S-seipin expression can modulate lipid levels and motor neuron function also *in vivo*.

7.1.4 LDs and ER stress

In this study, we found that overexpression of N88S-seipin decreases cellular and nervous tissue TAG content. Restoration of defective TAG storage lead to reduced ER stress and improved the motility defect caused by N88S-seipin. We propose that increase in LDs is protective against ER stress, possibly via sequestration of misfolded proteins, such as N88S-seipin, to LDs or LD-associated ER subdomains. Increasing LD content has since been found to be protective against ER stress in several other studies (Bosma et al., 2014; Qiu et al., 2016). In one study, ATGL knockout mouse livers were robustly protected against tunicamycin induced ER stress (Fuchs et al., 2012). However, in those studies the protective effect of increased LDs against ER stress was mostly attributed to sequestration of toxic lipid metabolites within the LDs. Whilst it is clear that the monounsaturated OA is beneficial for membrane homeostasis, especially in combating saturated FA induced lipotoxicity (for a recent review, see (Palomer et al., 2018)), we postulate additionally that the presence of LDs as such may be protective. More specifically, LDs may offer large hydrophobic surfaces that help to reduce the concentration of misfolded proteins in the ER and prevent their toxic ER aggregation, as exemplified by the N88S mutant (see below for details). In line with this, a recent study found LDs to be necessary for inclusion body clearance in a yeast model of proteotoxicity (Moldavski et al., 2015).

Besides providing mechanistic insight into seipinopathy and ER stress, our study also suggested a link between motor neuron disease and NL storage, a notion strengthened in the past years (Pennetta and Welte, 2018). In particular, also other proteins whose mutations lead to inherited forms of spastic paraplegias, have extensively been linked to LD metabolism (Blackstone, 2018; Eastman et al., 2009; Klemm et al., 2013; Papadopoulos et al., 2015; Renvoisé et al., 2016). Indeed, it can be envisioned that cells with an intrinsically low NL content, such as neuronal cells, are particularly vulnerable to perturbations of LD assembly and functions. Remarkably, a treatment regime including PUFAs has recently been shown to alleviate neurological symptoms of a patient suffering from the devastating seipin-related Celia's encephalopathy (Araújo-Vilar et al., 2018).

An interesting, thus far unresolved question raised in this study is the detailed localization of N88S-seipin in relation to LDs. Whilst our immunofluorescence imaging clearly demonstrates N88S-seipin aggregates juxtaposed to LDs, due to the large luminal domains of seipin it seems unlikely that this protein could escape the ER bilayer and be accommodated on the LD monolayer. Rather, it may be that N88S mutation compromises seipin oligomer assembly in such a way that larger patches of the ER are in close proximity to the LD. Indeed, perhaps these LDs are partially embedded in the ER, as has been proposed for NL-lipoprotein accumulations in the ER induced by misfolded ApoB (Morishita et al., 2019; Ohsaki et al., 2008). How N88S-seipin may affect the seipin-mediated ER-LD neck structure, as described in detail in study III, awaits further characterization and would require EM studies of ER-LD necks in N88S-seipin expressing cells.

7.2 SEIPIN REGULATES ER-LD CONTACTS AND CARGO DELIVERY (II)

Loss-of-function mutations in seipin lead to BSCL2, the most severe form of lipodystrophy in humans, characterized by near complete lack of adipose tissue (Magré et al., 2001). Seipin appears to play a critical, yet poorly understood, role in LD biogenesis, as its disturbance results in morphologically aberrant LDs in a wide variety of model systems (Chen and Goodman, 2017). Work in yeast has suggested that seipin localizes to ER-LD contacts, wherein it may modulate LD protein and/or lipid composition (Cartwright et al., 2015; Fei et al., 2008; Grippa et al., 2015; Szymanski et al., 2007; Wang et al., 2014). In this study, we sought to investigate the function of seipin in LD formation in human cells, utilizing both metabolically active and genetically malleable human epidermoid carcinoma cells (A431) as wells as control and BSCL2 patient fibroblasts.

7.2.1 Aberrant LD biogenesis in seipin knockout cells

We first knocked out seipin from A431 cells using CRISPR/Cas9 technology and characterized the LD phenotype. As we were interested in the earliest defects of LD assembly, we first depleted cells of pre-existing LDs and then added OA to cells for short periods of time. We observed that *de novo* generated LDs in seipin knockout (SKO) cells were more numerous and heterogeneous in size, with some supersized LDs and a massive accumulation of tiny LDs (**II, Fig. 1A-B**). By EM, these tiny LDs were in the size range of circa 100-200 nm in diameter, and live cell imaging revealed they displayed highly increased motility and aberrant, multidirectional trajectories (II, **Fig. 2**). Tiny LDs were also observed upon longer OA incubations in SKO A431 cells and were readily detectable in BSCL2 patient fibroblasts (**II, Fig. 6-7**). The LD phenotype could be rescued by re-introduction of GFP-tagged WT-seipin to the cells, whilst a BSCL2-causing point mutant, A212P-seipin, failed to do so (**II, Fig. 1A-B**).

7.2.2 Seipin is stably localized at ER-LD contacts

We next investigated the subcellular localization of WT- and A212P-seipin. Both proteins formed discrete puncta in the ER network, likely representing individual seipin oligomers (**II, Fig. 1C**). The oligomers formed by A212P appeared smaller in size as assessed by super resolution STORM imaging, in agreement with previous *in vitro* work (**II, Fig. 1D**) (Binns et al., 2010; Sim et al., 2013). WT-seipin foci were found to be enriched at ER-LD contacts, with typically one such foci per LD, whilst A212P-seipin was not enriched at ER-LD contacts, arguing for the functional relevance of this location (**II Fig. 1C-G)**. The associations of WT-seipin with LDs was found to be stable, with seipin foci hovering around the LDs or moving together with them (**II, Fig 2A)**. We also examined endogenous seipin localization by tagging the protein chromosomally with sfGFP and found a similar localization pattern of stable ER-LD contact enrichment (**II, Fig. 1H, EV2)**. As a TM ER protein, seipin

cannot escape the ER and these data thus reveal that LDs exhibit a close physical relationship with the ER, with seipin stably localizing at the ER–LD junctions.

A similar localization at ER-LD contacts had previously been reported for the yeast seipin complex (Fei et al., 2008; Grippa et al., 2015; Szymanski et al., 2007). However, previous studies in mammalian systems had failed to detect ER-LD contact enrichment of seipin (Fei et al., 2011b; Hölttä-Vuori et al., 2013; Payne et al., 2008; Sim et al., 2012; Talukder et al., 2015; Tian et al., 2011; Yang et al., 2013), likely due to the use of protein overexpression in those studies. These data exemplify the importance of investigating protein subcellular localization at physiological expression levels.

7.2.3 Seipin regulates ER-LD contact morphology

The stable localization of seipin at ER-LD contacts prompted us to examine the association of SKO LDs with the ER. Using 3D-EM and live cell Airyscan imaging, we found that whilst WT LDs were always in contact with the ER and moving along ER elements, a subset of the tiny, fast-moving LDs in SKO cells were completely detached from the ER (**II, Fig 2**). We also assessed the detailed morphology of ER-LD contacts in WT and SKO cells by electron tomography. WT ER-LD contacts were often regular in appearance, with a foot-like ER process that touched the LD (**II, Fig 3).** 3D modeling revealed several discrete patch-like ER contacts per LD. In SKO cells, however, some LDs displayed no ER contacts or only narrow string-like bridges to the ER, whilst others had very extensive ER contacts, with modelling showing a web-like ER attachment (**II, Fig 3**). Together, these data suggest that seipin controls the extent of ER–LD contacts, as seipin loss is accompanied by missing, rudimentary, or very large ER–LD contacts. LDs without ER connections were also observed in BSCL2 patient fibroblasts, but not in control fibroblasts.

7.2.4 Seipin regulates ER-LD protein and lipid trafficking

We next assessed the consequences of abnormal ER-LD connectivity by examining protein and lipid cargo recruitment from the ER to LDs. The trafficking of ACSL3, a key acyltransferase implicated in early LD assembly (Kassan et al., 2013), from ER to LDs was disrupted in SKO cells and BSCL2 patient cells **(II, Fig. 4, 7F-G)**. Whilst all WT LDs displayed enrichment of this class I LD protein, in SKO cells ACSL3 accumulated at ER-LD junctions instead. Using heterologous cells fusions, we found that for efficient ACSL3 transfer to the LD monolayer, seipin needs to be present during LD formation, as reintroducing seipin to SKO cells with pre-existing LDs failed to facilitate ACSL3 LD recruitment **(II, Fig. 4C)**. In contrast, exogenously expressed perilipin-2, a class II LD protein which targets to LDs from the cytoplasm (Brasaemle et al., 1997), displayed no targeting defects in SKO cells (**II, Fig. 4**, **EV4**). Also HPOS, a model ER-LD peptide employing the LD-targeting sequence of caveolin-1 (Kassan et al., 2013), could initially reach virtually all WT and SKO LDs (**II, Fig. 5, EV5**). However, FRAP studies revealed that subsequent trafficking of this

model peptide from the ER to LDs was substantially hampered in SKO cells. In WT cells, FRAP suggested bidirectional, continuous transfer of HPOS between the ER and LDs, but in SKO cells trafficking to pre-existing LDs was compromised (**II, Fig. 5A-B)**. Together, these data suggest that trafficking of protein cargo from the ER to LDs is impaired in SKO cells.

To probe the lipid transport capabilities of ER–LD junctions, we utilized BPY-C12, a fluorescent FA analog used to monitor cellular FA trafficking in cells (Ohsaki et al., 2016; Rambold et al., 2015), which we found could be esterified to NLs and stored in LDs (**II, Fig EV6)**. FRAP experiments and longer time lapse imaging suggested WT cells could continuously transport NL cargo to LDs, whilst this transport was hindered in SKO cells **(II, Fig 5D-H)**. Metabolic labeling experiments with alkyne-labelled FA and click chemistry showed no difference in initial FA flux between WT and SKO cells during the earliest stages of LD formation **(II, Fig 6H)**. However, in cells with pre-existing LDs, FA incorporation into NLs was impaired in SKO cells and BSCL2 patient fibroblasts (**II, Fig 5H, 7H)**. Overall, in seipin deficient cells initial protein and lipid trafficking to nascent LDs is at least partly preserved and NL synthesis during early LD assembly is intact, but subsequent trafficking of cargo between ER and more mature LDs is compromised, and this is accompanied by decreased net NL synthesis.

Finally, we examined LDs of cells after longer periods of FA incubation, probing LD motility, ER-LD proximity and protein exchange between ER and LDs **(II, Fig 6)**. We found that the connectivity of LDs to the ER is continuous over time in WT cells, whilst in the absence of seipin, tiny "nascent-like" LDs with dysfunctional and missing ER contacts are continuously present. Over time, in SKO cells, some LDs become strikingly supersized, and these LDs displayed heterogeneous ER connectivity, with some showing no recovery of the HPOS peptide in FRAP experiments, whilst in others the recovery was accelerated, suggesting more efficient/more numerous ER-LD contacts, or unrestrained transport.

7.2.5 Seipin and ER-LD contacts

Overall, in this study we described a role for seipin in ensuring functional ER–LD contacts of LDs in human cells (**II, Fig. 8**). In the absence of seipin, cells accumulated high numbers of tiny LDs, which failed to grow. These data may suggest that the initial formation of LDs in the ER does not depend on seipin, but in the absence of seipin, growth of most LDs beyond a size of circa 100-200 nm becomes abortive. Similar results were obtained in another study at the same time, employing primarily *Drosophila* cells, where the authors suggested seipin is required for converting nascent LDs to more mature ones (Wang et al., 2016a). However, our data suggested that seipin may instead be required for the very earliest steps of LD assembly, as adding back seipin via heterologous cell fusions failed to rescue ACSL3 recruitment to LDs *initially* formed in the absence of seipin. Indeed, assessing what role, if any, seipin plays in LD maintenance *after* LD formation is hindered by the fact that the early steps

of LD biogenesis are so severely compromised in the absence of seipin. This question we subsequently tackled in our follow-up study (III).

Based on our data, we propose seipin may structurally contribute to ER-LD junctions by stabilizing them. Indeed, we found more heterogeneous ER-LD contacts in its absence together with impaired ER-LD junction functionality. Morphologically aberrant ER-LD contacts in the absence of seipin have been observed by EM also in seipin mutant yeast cells (Grippa et al., 2015; Romanauska and Köhler, 2018; Wolinski et al., 2015). However, our data analysis was hampered by the fact that also WT LDs often contained more than one zone of ER-LD proximity in ET stacks, whilst seipin was most often present as only a single foci/LD. Thus, LDs likely have multiple different types of connections with the ER, of which only a subset may be regulated by seipin. Other regulators of ER-LD contacts include Rab18 (Ozeki et al., 2005; Xu et al., 2018), FITM2 (Choudhary et al., 2015), DGAT2-FATP2 (Xu et al., 2012) and Snx14 (Datta et al., 2019). Pinpointing the morphology and functionality of seipin-mediated ER-LD contacts was the topic study III.

The most striking finding of this study was the realization that at least in the mammalian cell types under study, virtually all LDs of WT cells appeared to be connected to the ER membrane. Similar findings had been reported in yeast model systems (Jacquier et al., 2011), but in mammalian cells it was commonly presumed that most LDs would detach from the ER after their initial biogenesis (Pol et al., 2014). Indeed, in single section EM images LDs can often be found to exist in isolation in the cytosol. However, when systematically assessing ER-LD proximity using 3D-EM and live cell imaging, all LDs in WT cells appeared to be in the proximity of the ER. Motility of LDs is also thought to indicate detachment from the ER (Pol et al., 2014), but we found LDs to be motile along ER profiles, suggesting on-going connectivity with the ER. Finally, our FRAP studies revealed on-going lipid and protein cargo exchange between LDs and the ER. These processes were seipin-mediated, demonstrating that seipin is important in maintaining ER-LD contacts. This is best exemplified by the fact that in the absence of seipin some LDs were completely detached from ER membranes. However, as most LDs were still proximal to the ER even in the absence of seipin, but failed to adequately grow, seipin's role is not limited to acting as an ER-LD tether, but it likely controls ER-LD junction functions in a more intricate manner.

7.3 SEIPIN FACILITATES TRIGLYCERIDE FLOW TO LIPID DROPLET AND COUNTERACTS DROPLET RIPENING VIA ENDOPLASMIC RETICULUM CONTACT (III)

Work from numerous model systems has shown that LD biogenesis is severely hampered in the absence of the ER-LD contact protein seipin (Chen and Goodman, 2017), with a phenotype of numerous tiny LDs and a few supersized LDs, without robust changes in cellular lipid profiles (Salo et al., 2016; Wang et al., 2016a). LD growth arises via TAG transfer from the ER to LDs, via localized TAG generation at the LD surface or via TAG transfer between LDs (Walther et al., 2017). Biophysically, LDs are oil-in-water emulsion droplets expected to undergo spontaneous destabilization processes (Thiam et al., 2013a), such as fusion and ripening, which, if left unrestricted, would lead to the development of supersized LDs (Thiam and Beller, 2017). However, cells have developed protein machineries to regulate LD growth, and seipin is likely a key player in this regulation. In this study we continued our investigation of seipin in mammalian A431 cells, using techniques to manipulate seipin subcellular localization and rapidly deplete it from ER-LD contacts, to uncover the role of seipin in ER-LD contact maintenance.

7.3.1 Seipin can determine the site of LD formation

In mammalian cells, seipin exists as discrete, motile ER-associated foci, a subset of which associate with LDs (Salo et al., 2016; Wang et al., 2016a). Previous work suggested that seipin associates with budded out LDs, and upon encountering such a nascent LDs, enables its growth (Wang et al., 2016a). Using live cell super-resolution imaging in cells where seipin is chromosomally tagged with bright fluorophores, we found LD-destined seipin foci to be immobilized prior to accumulation of well-known nascent LD markers (**III, Fig. 1A-H**). Indeed, correlative light and electron microscopy (CLEM) tomography of cells first stringently delipidated and then treated with OA for short periods of time revealed small LD-like structures circa 30-100 nm in diameter at sites marked by seipin (**III, Fig. 1I-J**). These data challenge the previous view that seipin associates with preformed nascent LDs (Wang et al., 2016a), and suggest that seipin may determine where an LD starts to develop. Interestingly, live cell imaging of LD biogenesis also revealed that nascent LDs typically form at ER structures around the cell in a highly dispersed manner, with distances between newly forming LDs higher than expected by chance **(III, Fig. 1C)**. In other words, a growing LD appeared to inhibit new LDs from forming in its vicinity.

To test whether seipin may define a subdomain of the ER that is destined for LD formation, we artificially targeted seipin to the nuclear envelope (NE), a subdomain of the ER. To achieve this, we employed GFP-nanobody, a peptide which binds to GFP in cells with high affinity (Rothbauer et al., 2006), and the intrinsic interaction of KASH2 and SUN2 at the NE (Sosa et al., 2012). We fused GFP-nanobody to the

SUN2-interacting fragment of KASH2, and co-expressed this GFP-nanobody-KASH fusion protein and SUN2 in cells with endogenously GFP-tagged seipin **(III, Fig. 2A)**. Using this system, we could restrict most endogenous seipin to localize exclusively at the cytoplasmic leaflet of the NE **(III, Fig. 2B)**. In these seipin NE-trapped cells, the vast majority of LDs now formed at the NE, in contrast to the dispersed manner observed in control cells (**III, Fig. 2C-D**). Thus, seipin can determine the site of LD formation.

7.3.2 Architecture of seipin-mediated ER-LD contacts

We next assessed the ultrastructure of seipin-mediated membrane-LD contact sites by ET and CLEM. LDs in A431 cells typically harbor only a single seipin foci, but multiple proximities with the ER, reflecting heterogeneity in ER-LD contact machinery and function (Salo and Ikonen, 2019; Salo et al., 2016). The uniform architecture of the NE, as compared to the rest of the ER, enabled us to more accurately investigate the structure of *seipin*-mediated membrane-LD contacts in the seipin NE-trapped cells. We found the NE-trapped LDs to exhibit typically 1-2 clear NE contacts, with a strikingly uniform appearance and dimensions (**III, Fig. 2E-F)**. At these circa 15 nm-in-diameter neck-like contacts, a small fraction of the LD monolayer appeared to be in direct contact with the ER lumen. Similar necks could be seen by CLEM at seipin sites of cells without NE-trapping of seipin, and in WT A431 cells and primary human fibroblasts (**III, Fig. 2G, S2**). Finally, their appearance could be disrupted via acute removal of seipin (see below) (**III, Fig. S2)**. Together, these data suggest that seipin-mediated ER-LD membrane contacts display a uniform neck-like architecture.

The architecture of the seipin-mediated ER-LD contact sites fit well with the structural insights into the seipin oligomer (Sui et al., 2018; Yan et al., 2018). Indeed, the cryo-EM structures of the luminal domains of human and *Drosophila* seipin oligomers revealed a 15- to 20-nm-wide ring-shaped structure intercalating into the bilayer of the ER (Sui et al., 2018; Yan et al., 2018), which is well in-line with our measurements of the ER-LD necks. Moreover, Sui et al found that the luminal domain of seipin contains a hydrophobic helix which showed high affinity for a NL covered monolayer. Together with our findings, these data suggest that nm-sized NL lenses in the ER may be detected and stabilized by seipin oligomers, thus marking the site where LDs start to develop. Seipin may itself restrict the budding size of forming LDs and perhaps stabilize the high local curvature of the ER-LD neck, as previously proposed (Han et al., 2015). Interestingly, an ER-LD neck with very similar dimensions (circa 15 nm diameter with apparent contact of the ER lumen with the LD monolayer), was recently observed in a HeLa cell using *in situ* cryo-ET (Mahamid et al., 2019).

7.3.3 Acute depletion of seipin via auxin-induced degradation

We next investigated the functionality of seipin-mediated ER-LD contacts. We had previously described defective cargo transfer between the ER and LDs in the absence of seipin (II), but these could relate to secondary effects due to aberrancies in earliest

steps of LD assembly. Thus, to investigate the function of seipin at pre-existing ER-LD contacts we generated cells in which endogenously tagged seipin could be acutely depleted by adapting the AID-system (Nishimura et al., 2009) **(III, Fig. 3A)**. In these seipin degron cells, seipin could be rapidly and efficiently (>95% reduction of seipin protein in 30 min) depleted via addition of the degradation inducer IAA (**III, Fig. 3B)**. Importantly, using this system seipin could also be rapidly depleted from pre-existing ER-LD contacts (**III, Fig. 3C**). Depletion of seipin prior to LD biogenesis resulted in the familiar phenotype of small and supersized LDs (**III, Fig. 3D)**, common for SKO cells (Salo et al., 2016; Wang et al., 2016a), validating the system for studying the effects of acute seipin depletion.

7.3.4 Ripening-mediated heterogenous growth of LDs upon acute seipin removal

Using seipin degron cells, we assessed the effects of acute seipin removal on the growth of pre-existing LDs. Upon acute seipin removal, larger LDs began to grow faster, whilst smaller nearby LDs started to shrink, giving rise to the seipin phenotype of small and supersized LDs within a few hours **(III, Fig 3E, 4A-B)**. These changes appeared to be due to defective aliquoting of lipids between the ER and LDs, as they occurred even in the presence of DGAT2 inhibition, lipolysis inhibition or concomitant inhibition of both *de novo* lipogenesis and lipolysis **(III, Fig. 4E, S3-S5)**. Importantly, despite clear changes in LD size distributions, we could not detect differences in net lipolysis, overall FA flux or the lipidomic profiles of LDs (**III, Fig. 4C-D, S3B)**. Finally, FRAP studies utilizing BPY-C12 strengthened the notion that upon acute seipin removal, larger LDs started to gain relatively more NLs from the ER, whilst smaller LDs did not (**III, Fig. 4F-I, S5E-H)**. In control cells both small and larger LDs gained NLs in a similar manner. These data demonstrate that seipin is required for LD size maintenance and homogenous growth also after initial LD biogenesis.

These LD size alterations were reminiscent of what had been previously observed for LD-LD lipid transfer mediated by FSP-27/CIDE-C, i.e. they occurred according to the principles of ripening, with larger LDs gaining content at the expense of smaller LDs (Gong et al., 2011). However, the inhomogeneous growth of LDs upon acute seipin removal was not dependent on direct LD-LD contacts (**III, Fig. 4F)** and CIDE family proteins are not detectable at LDs of A431 cells (Moessinger et al., 2011). As NL transport through the aqueous cytosol is likely to be extremely slow, we thus postulated that this ripening process may occur through the connecting lipid phase, i.e. the ER. Indeed, utilizing a previously described *in vitro* system with artificial LDs connected to flattened giant unilamellar vesicles (GUVs) (Ben M'barek et al., 2017), we could demonstrate ripening-mediated growth and shrinkage of artificial LDs through the connecting bilayer (**III, Fig. 5, S5)**. In this system, growth and shrinkage of LDs was absolutely dependent on their connection with the bilayer, as LDs not in contact with the bilayer did not change in size (**III, Fig. 5K-N)**.

Our data thus far suggested that seipin may help to prevent ripening-induced changes of LDs, and acute removal of seipin revealed a principle of LD ripening via the ER. To test this more directly, we combined isolated cellular LDs +/- fluorescently tagged seipin with flattened GUV bilayers and performed time lapse imaging of LD size changes **(III, Fig 6A)**. In this setup, similar to artificial LDs, also cellular membrane-connected LDs experienced ripening-mediated LD size changes, with smaller LDs shrinking and larger LDs growing. At the same time, LDs not on the membrane did not change in size, as expected **(III, Fig. 6B-C)**. Importantly, upon analyzing membrane-associated LDs, we found that seipin containing LDs shrunk less or grew more than similar sized LDs devoid of seipin **(III, Fig. 6D-E, S7B-C)**. This suggests that seipin can facilitate LD growth and prevent ripening-induced shrinkage of small LDs *in vitro*.

7.3.1 Seipin at the ER-LD neck facilitates continuous NL transfer to the LD

We next analyzed the growth promoting function of seipin at ER-LD contacts in detail in cells. By limiting the number of seipin foci either globally via partial knockdown or locally via NE-trapping, we found that seipin promotes LD growth LD-autonomously in cells. In cells with few remaining seipins, these were invariably enriched at ER-LD contacts and the seipin-associated LDs grew more rapidly than LDs in cells with higher seipin content (**III, Fig. 7A-C)**. Similarly, in the periphery of seipin NE-trapped cells, where local seipin density was low, seipin associated LDs grew faster than in the NE, where seipin content was high **(III, Fig. 7D-F)**. These data suggest that seipin promotes the growth of the LD it is associated with. Furthermore, the growth of a LD appears to inhibit the growth rate of other nearby LDs. Finally, we performed competition experiments in cells, where via cell-fusions we could simultaneously examine the size changes of LDs which still harbored seipin at their ER contact and LDs where seipin had been acutely depleted. In line with our *in vitro* results, LDs containing seipin grew, whilst LDs where seipin had been depleted, shrunk in size (**III, Fig. 7G-H)**.

Overall, the findings in this study suggest that seipin is critical for LD growth by partitioning TAG from the ER to LDs. Upon acute seipin removal, a principle of LD ripening via the ER becomes apparent, with larger LDs acquiring NL at the expense of smaller ones via the connecting lipid phase, the ER **(III, Fig. 7J)**. At the ER-LD neck, seipin may thus actively transfer NLs to the LD or modulate the structure of the contact site to enable such transfer. Whilst the molecular mechanism behind this phenomenon is still unclear, our data together with recent structural insights into seipin complex (Sui et al., 2018; Yan et al., 2018), and the uniform membrane architecture of ER-LD necks raise the possibility that seipin restricts the diameter of the LD neck and controls lipid diffusion at this site.

7.3.2 Seipin as an organizer of NL flux at the ER-LD network

The notion that LDs may grow via ripening through the ER is a new concept, which will require further investigation in the future. Whilst ripening-mediated growth through the connecting phase is a clearly observable phenomenon *in vitro*, cells have developed machinery, such as seipin, to counteract it. Upon LD biogenesis in the absence of seipin, some LDs become supersized, likely due to ripening-mediated growth via the ER, whilst other LDs fail to do so, as they may have already detached from the ER (II). Upon seipin removal from pre-existing LDs, all LDs become susceptible to ripening, as they are in contact with the ER. However, the LD size changes we observed were most obvious in conditions of sustained LD growth, i.e. with new TAG generation in the ER, suggesting that even upon seipin removal, the rate of TAG backflow from LDs to the ER is likely to be quite low. Thus, our data generally favor a model wherein seipin promotes NL deposition to the LDs, rather than prevents it backflow. It is intriguing to speculate that the role of seipin is thus most important for smaller LDs to grow, as they have to "fight against" the ripening-mediated tendency to shrink.

In our study, we could not find defects in overall cellular lipid metabolism or FA flux upon acute seipin removal, suggesting seipin's primary role may not be related to control of enzymatic activities or lipolysis, as has been suggested (Boutet et al., 2009; Chen et al., 2012; Pagac et al., 2016; Talukder et al., 2015). However, our data cannot rule out a more localized defect in for example PA handling or desaturase activities. Furthermore, we could not detect changes in the lipidomes of isolated LDs upon acute seipin removal. This could be thought as evidence against a role for seipin in regulating LD monolayer properties (Grippa et al., 2015). However, we only analyzed bulk LD preparations, and thus whether the tiny (shrinking or detached) LDs would show an altered lipid profile vs the larger (aberrantly growing) LDs is not known.

Regulated growth of LDs via the ER is likely also crucial for adipogenesis, as in BSCL2 knockout preadipocytes, LD heterogeneity preceded their eventual disappearance and defective adipogenesis (Chen et al., 2012). Furthermore, whilst uncontrolled ripening would eventually be presumed to lead to supersized unilocular LDs, the hallmark of mature adipocytes, this is not a spontaneous process as proper adipogenesis requires both seipins and CIDE proteins (Chen et al., 2009; Slayton et al., 2019). In this scenario, seipin facilitates growth of LDs via the ER, whilst CIDE proteins promote their coalescence. Also in a recent yeast study, loss of seipin function and overexpression of exogenous CIDE-A had similar effects on droplet morphology, suggesting they work in the same pathway, but with antagonistic roles (Lv et al., 2018).

Our findings further strengthen the notion that seipin may define a subdomain of the ER primed for LD generation. Indeed, seipin has previously been proposed to modulate PA metabolism at a ER subdomain primed for LD formation and control of local DAG levels has been proposed to be vital for LD emergence (Cartwright et al.,

2015; Choudhary et al., 2018; Wolinski et al., 2015). Seipin is localized at LD forming domains during the earliest observable steps of LD formation in mammalian cells (III and (Wang et al., 2016a)), and the hydrophobic AHs of the seipin oligomer seem well-suited for detection of small NL aggregates between the ER leaflets (Sui et al., 2018). In line with this, LD budding was almost completely abolished in a double yeast mutant of seipin and the putative ER-shaping protein Pex30, with toxic levels of TAG proposed to accumulate in the ER (Wang et al., 2018b). Remarkably, LD budding was partially restored by modulation of the ER PL composition, suggesting that seipin and Pex30 may normally function to regulate local PL composition of ER domains primed for LD formation (Wang et al., 2018b). Interestingly, at least in yeast cells, peroxisomes may also be formed at these seipin-defined subdomains (Joshi et al., 2018; Wang et al., 2018b), suggesting seipin may modulate the organization of lipogenic subdomains primed for both LD and peroxisome generation.

Finally, the findings in study III strongly indicate that seipin can dictate where an LD forms, as relocalisation of seipin to a subdomain of the ER, the NE, was sufficient to relocalize LD biogenesis to that site. However, defects in LD machinery localization and/or lipid organization within the ER *prior* to LD biogenesis induction have not thus far been observed in the absence of seipin, suggesting that at least *pre-defined* subdomains required for LD assembly may not exist. Rather, the driving force for LD biogenesis appears to be the local increases of NLs within the ER, but seipin may help to concentrate this TAG for LD formation to occur.

8 CONCLUSIONS AND FUTURE PROSPECTS

In this thesis, using a plethora of cell biological approaches, we sought to understand the molecular function of seipin. Whilst advances in this field have been made by us and others, the molecular function of seipin still remains mysterious (Gao et al., 2019; Henne et al., 2020). Understanding seipin would greatly broaden our insight on how cells handle excess energy in LDs and would be beneficial for developing new therapeutics for seipin-associated diseases and other metabolic diseases owing to altered NL storage. Furthermore, detailed insight into the basic cellular mechanisms of LDs could also lead to advances in a wide variety of fields, including infection control and food/oil production (Libbing et al., 2019; Pyc et al., 2017; Vieyres and Pietschmann, 2019) .

In study I, we linked the pathogenesis of seipinopathy to NL storage, and found that modulation of cellular NL stores could decrease ER stress. As ER stress is implicated in the pathogenesis of multiple disease states, further investigation of the pathways by which increasing NL storage in LDs alleviates ER stress is warranted. Indeed, new insights into neuronal NL storage and its complex implications have been made recently (Bailey et al., 2015; Fanning et al., 2019; Ioannou et al., 2019). Our work fits well with the emerging notion that neuronal cells and tissues might be especially sensitive to perturbation of cellular NL stores (Pennetta and Welte, 2018). Further insight into the pathogenesis of seipinopathies and Celia's encephalopathy would benefit from both detailed structured investigations of these mutants and further *in vivo* work.

In studies II-III, we investigated the function of seipin in ER-LD contact site formation and maintenance. We found seipin to be vital for both LD biogenesis and LD maintenance and suggest it facilitates LD growth via ER-LD contacts. Together with recent findings from other labs (Grippa et al., 2015; Sui et al., 2018; Wang et al., 2016a, 2018b), our data support a model where seipin defines an ER-LD contact primed for supporting controlled LD growth. Indeed, seipin may itself structurally limit the neck of the ER-LD contact and maintain its correct topology and function. Seipin also appears crucial during the very earliest stages of LD biogenesis, although we and others have yet failed to attribute this to any distinct lipid synthesis pathway.

It is tempting to speculate that seipin may attract NL molecules, such as TAG, via the help of its ER luminal hydrophobic helices and help concentrate TAG lenses in the ER during the very early stages of LD biogenesis. Once the LD is formed, seipin remains at the contact, with the contact site potentially acting as a valve, releasing TAG from the ER into the LD. Thus, in the absence of seipin, some LDs will spontaneously bud out of the ER due to aberrantly high ER TAG concentration, as suggested by us and others (Cartwright et al., 2015; Salo et al., 2016), whilst others will aberrantly ripen within the ER to form supersized LDs. As the earliest stages of

LD assembly are currently below the resolution limits of even our most powerful microscopes, detailed simulations in combination with cell-free *in vitro* work would be required to test this model further. Furthermore, understanding the native lipid environment of seipin, perhaps using immune-purification together with sensitive lipidomics, would greatly facilitate our understanding of the lipogenic subdomain seipin may form.

A major unresolved issue is how stable is the conformation of the seipin oligomer *in vivo*. Seipin motility in the ER is stabilized at ER-LD necks compared to its non-LD associated cousins, but whether these seemingly different subpopulations also experience structural alterations is unknown. Furthermore, the reason for the decreased motility of LD-associated seipins at the molecular level is unclear. Examination of the structures of these subpopulations separately using affinity purification and cryo-EM, or microscopy approaches sensitive to conformational changes, such as single molecule FRET, could be employed to investigate this further.

Our data, together with the recent structural insights into seipin and the high resolution images of a ER-LD neck by cryo-EM (Mahamid et al., 2019; Salo et al., 2019; Sui et al., 2018), suggest that seipin at the ER-LD neck may simultaneously be embedded in the ER bilayer (via its TM helices) and the LD monolayer (via its luminal hydrophobic helices and, possibly, cytoplasmic amphipathic helices), where it may form a disk-like structure from wherein the LD buds (**Figure 13**). Here, the TM helices could function, perhaps together with as-yet-unidentified interactors, to control the flow of lipids via the ER bilayer to the LD. An intriguing notion is that at this site, seipin could experience conformational changes induced by the alterations of the membrane tension of the LD. In other words, "filling-up" of the LD core with NL may induce a slight "bulging" of the LD monolayer towards the lumen, which could loosen seipin structure so that more PLs could diffuse to the LD surface, relieving the membrane tension. Thus, at the molecular level, seipin would function to link ER and LD PL pools and control their trafficking according to the needs of the LD. This speculative notion would require advanced simulations in combination with ways to measure precisely the intracellular lipid flows at the ER-LD contact (see below).

Besides providing insight into seipin function, our work suggests that the LDs and ER could be considered as a joint system. Lipid fluxes via the connecting ER bilayer appear to contribute to LD-LD communication. For example, during early LD biogenesis, NLs are likely synthesized at highly dispersed sites along the ER. Upon rising local concentrations, a NL nucleates at a site marked by seipin and starts to grow. The flux of NL to the growing LD, enhanced by seipin, may thus reduce *nearby* TAG concentration in the ER, disfavoring the formation of other LDs nearby, as observed in study III. Similarly, in a setting with different sized LDs connected to the ER, seipin facilitates their growth, but upon its acute removal, the growth of the smaller LD is disfavored. These findings suggest that adaptations of phase theory could be utilized in future work to understand the ER-LD nexus.

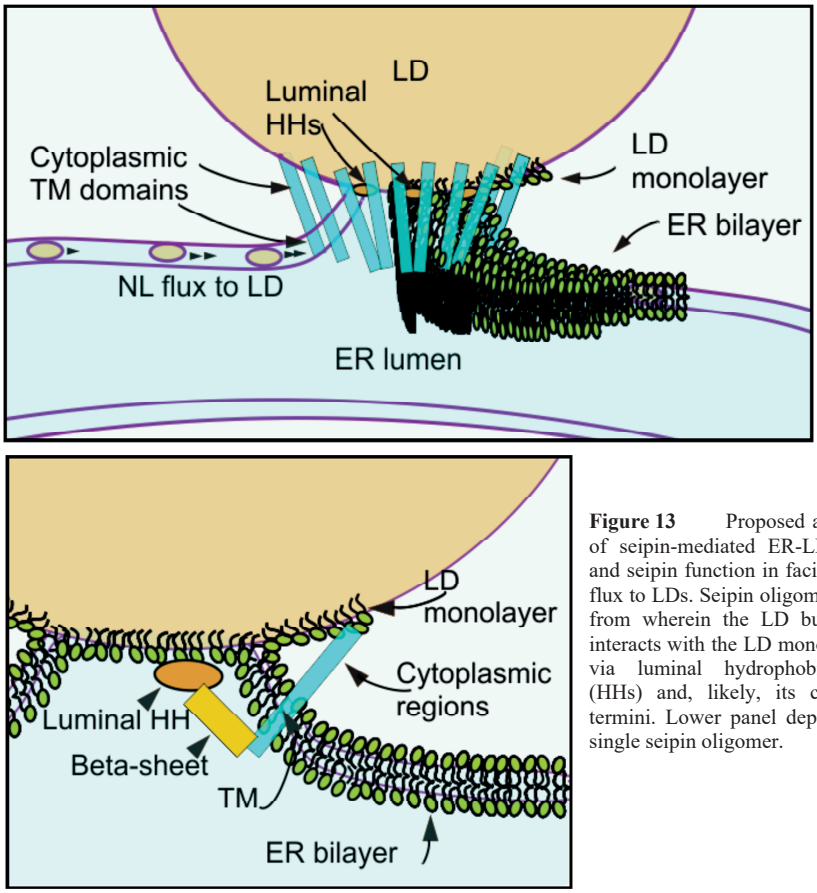

Figure 13 Proposed architecture of seipin-mediated ER-LD contacts and seipin function in facilitating NL flux to LDs. Seipin oligomer is a disk from wherein the LD buds, and it interacts with the LD monolayer both via luminal hydrophobic helices (HHs) and, likely, its cytoplasmic termini. Lower panel depicts only a single seipin oligomer.

Precise measurements of these aforementioned lipid fluxes between the ER and LDs would be of great interest in future work. This would require development of additional imaging techniques, as current methodology (for example, using BPY-labelled lipids), suffers from potential artifacts caused by the label. Label-free techniques, such as CARS, on the other hand, currently lack the required sensitivity to examine these minute lipid fluxes. Considering the rapid pace of advancement in imaging and labeling techniques, such measurements will likely be possible in the near future.

Finally, examining seipin function more closely in the context of its arguably most important function, adipogenesis, will be of utmost importance in the future. With the rapid advancement of CRISPR-mediated gene editing technologies and adipocyte cultures and organoids, it would be highly interesting to observe seipin localization, dynamics and function in developing and mature adipocytes. Indeed, adaption of the AID technique to rapidly remove seipin at specific stages of adipogenesis or in mature

adipocytes would likely bring valuable insight into seipin function and adipocyte biology. Furthermore, whilst our data suggest a single seipin foci at a forming nascent LD, it would be interesting to examine the relationship of seipin to the giant LDs of unilocular LDs of adipocytes. As these form via Fsp27-facilitated fusion, one would expect multiple, perhaps even hundreds, of seipin-mediated ER-LD necks at these LDs, but this notion has thus far not been tested experimentally. Nevertheless, as seipin appears to be crucial in aliquoting fat between the ER and LDs, more insight into seipin function in adipose tissue could also lead to advances in taggling one of the most rapidly increasing epidemics of our time, obesity.

9 ACKNOWLEDGEMENTS

This work was carried out in the laboratory of Academy Professor Elina Ikonen, Department of Anatomy, Department of Anatomy, Faculty of Medicine and Stem cells and Metabolism Research Unit, University of Helsinki and Minerva Foundation for Medical Research, Helsinki, Finland. I am thankful for the excellent facilities and atmosphere of the unit. I thank the Doctoral Programme in Biomedicine (DPBM) for support. I would also like to thank funding sources: DPBM, Finnish Medical Foundation, Maud Kuistila Memorial Foundation, Paulo Foundation, Emil Aaltonen Foundation, Alfred Kordelin Foundation and Biomedicum Helsinki Foundation. I am also grateful to the Academy of Finland for support for the ProLipids Center of Excellence in Biomembrane Research 2014-2019.

I would first like to thank my thesis supervisors, Prof. Elina Ikonen and Doc. Maarit Hölttä-Vuori. I am deeply grateful to Elina for providing me with the opportunity to work in her fantastic research group and allowing me to pursue fascinating research questions with the best possible support. Furthermore, I thank Elina for her excellent mentoring, trust and countless hours of interesting discussions and Maarit for her outstanding support, teaching and mentoring.

I wish to express my gratitude to Prof. Robert V. Farese, Jr. from Harvard Medical School for accepting our invitation to be my Opponent and Prof. Matti Airaksinen for acting as Custos at my PhD Dissertation. Prof. Eeva-Liisa Eskelinen from the University of Turku and Prof. Pedro Carvalho from the University of Oxford are warmly thanked for reviewing my thesis and providing insightful critique. I am also grateful to my thesis committee members Prof. Johana Arola and Doc. Carina Holmberg-Still for all the valuable comments and discussions.

I wish to express my gratitude to all my co-authors and scientific collaborators for their invaluable contributions. I am especially grateful for the fruitful collaboration with Adjunct Prof. Eija Jokitalo and her team members, especially Helena Vihinen and Ilya Belevich. I am also very grateful for the fantastic collaboration with Dr. Abdou Rachid Thiam and Alexandre Santinho from his lab. I would also like to thank Professor Christoph Thiele, Dr. Pentti Somerharju, Dr. Peter Horvath and Dr. Hongxia Zhao for introducing me to new techniques and Dr. Jocelyne Magré, Prof. Corinne Vigouroux and Maximiliano Suster for collaboration.

I would like to thank all co-authors in the Ikonen laboratory, especially Dr. Shiqian Li, whose wizardery in the realm of genome editing continues to amaze me and whose insight has been crucial for many of these projects. I also thank Yuki, Abel, Simon, Johan and Leena for their scientific contributions and teachings. Finally, I am also extremely grateful to the technical assistance, teachings and kindness provided by Anna Uro, Pipsa Kaipainen and Katharina Ven.

I would like to acknowledge support provided by the HiLife Light and Electron microscopy, Functional genomics and Flow cytometry units. I am especially grateful

for the expertise and patience of imaging specialists Mikko, Antti, Kirstin, Jussi and Marja.

I thank all past and present members of the Ikonen laboratory for their help and discussions, and for creating an inspiring working environment. I thank Kohta, Xin, Kecheng, Kristiina, Heljä, Juho, Lauri, Tomas, Andrea, Burcin, Wei, Boris, Aikki, Maurice, Matts, Mikko, Maarit N and Vilja. I also thank all the members of the ProLipids Center of Excellence and Minerva Foundation for Medical Research for numerous fascinating discussions and meetings. I am especially grateful for Dr Johan Peränen, Prof. Pekka Lappalainen, Prof. Ilpo Vattulainen and Prof. Vesa Olkkonen for their insightful advice.

I would like to thank all my friends for their support during the years. I am especially grateful to my bandmates Saara, Ville, Otto, Timo, Rami, Lauri, Jami, Ella, Santtu, Henri, Kalle, Otso, Leo, Elias and Juuso. I also thank Sampo, Jussi, Nalle, Rayan, Niko, Arto, Jarno, Matti, Kimmo, Ilona, Jenny, Satu, Riitta, Outi, Aino, Suvi, Sini, Toni and Inga for friendship. I also thank the kind colleagues at Malmi Hospital and Malmi Health Center and the people of the Hedman and Tjaderhäne research groups.

I would like to thank all my family members. I would especially like to thank my mother, Professor Tuula Salo, my father, Professor Heikki Salo and their spouses, Professor Leo Tjäderhane and Dr. Eija Laurikainen, for their continued support. I thank my grandparents and cousins for their warm support throughout the years. I also thank Emmi's parents, Marjo and Topi.

Finally, I thank my Emmi for her love and support.

10 REFERENCES

Agarwal, A.K., and Garg, A. (2002). A novel heterozygous mutation in peroxisome proliferator-activated receptor-gamma gene in a patient with familial partial lipodystrophy. J. Clin. Endocrinol. Metab. *87*, 408–411.

Agarwal, A.K., Arioglu, E., de Almeida, S., Akkoc, N., Taylor, S.I., Bowcock, A.M., Barnes, R.I., and Garg, A. (2002). AGPAT2 is mutated in congenital generalized lipodystrophy linked to chromosome 9q34. Nat. Genet. *31*, 21–23.

Agarwal, A.K., Fryns, J.P., Auchus, R.J., and Garg, A. (2003a). Zinc metalloproteinase ZMPSTE24, is mutated in mandibuloacral dysplasia. Hum. Mol. Genet. *12*, 1995–2001.

Agarwal, A.K., Simha, V., Oral, E.A., Moran, S.A., Gorden, P., O'Rahilly, S., Zaidi, Z., Gurakan, F., Arslanian, S.A., Klar, A., et al. (2003b). Phenotypic and Genetic Heterogeneity in Congenital Generalized Lipodystrophy. J. Clin. Endocrinol. Metab. *88*, 4840–4847.

Aitchison, A.J., Arsenault, D.J., and Ridgway, N.D. (2015). Nuclear-localized CTP:phosphocholine cytidylyltransferase α regulates phosphatidylcholine synthesis required for lipid droplet biogenesis. Mol. Biol. Cell *26*, 2927–2938.

Amine, M., Simon, L., Sabri, L., Rial, A., Bergeron, K.F., Ralston, J.C., Mutch, D.M., Mounier, C., and Diacylglycerol, D.A.G. (2017). Hepatic BSCL2 (Seipin) Deficiency Disrupts Lipid Droplet Homeostasis and Increases Lipid Metabolism via SCD1 Activity. Lipids *52*, 129–150.

Anand, P., Cermelli, S., Li, Z., Kassan, A., Bosch, M., Sigua, R., Huang, L., Ouellette, A.J., Pol, A., Welte, M.A., et al. (2012). A novel role for lipid droplets in the organismal antibacterial response. Elife *2012*, 1–18.

Angermüller, S., and Fahimi, H.D. (1982). Imidazole-buffered osmium tetroxide: an excellent stain for visualization of lipids in transmission electron microscopy. Histochem. J. *14*, 823–835.

Araújo-Vilar, D., Domingo-Jiménez, R., Ruibal, Á., Aguiar, P., Ibáñez-Micó, S., Garrido-Pumar, M., Martínez-Olmos, M.Á., López-Soler, C., Guillín-Amarelle, C., González-Rodríguez, M., et al. (2018). Association of metreleptin treatment and dietary intervention with neurological outcomes in Celia's encephalopathy. Eur. J. Hum. Genet. *26*, 396–406.

Auer-Grumbach, M., Schlotter-Weigel, B., Lochmüller, H., Strobl-Wildemann, G., Auer-Grumbach, P., Fischer, R., Offenbacher, H., Zwick, E.B., Robl, T., Hartl, G., et al. (2005). Phenotypes of the N88S Berardinelli-Seip congenital lipodystrophy 2 mutation. Ann. Neurol. *57*, 415–424.

De Azevedo Medeiros, L.B., Cândido Dantas, V.K., Craveiro Sarmento, A.S., Agnez-Lima, L.F., Meireles, A.L., Xavier Nobre, T.T., De Lima, J.G., and De Melo Campos, J.T.A. (2017). High prevalence of Berardinelli-Seip Congenital Lipodystrophy in Rio Grande do Norte State, Northeast Brazil. Diabetol. Metab. Syndr. *9*, 1–6.

Bailey, A.P., Koster, G., Guillermier, C., Hirst, E.M.A., MacRae, J.I., Lechene, C.P., Postle, A.D., and Gould, A.P. (2015). Antioxidant Role for Lipid Droplets in a Stem Cell Niche of Drosophila. Cell *163*, 340–353.

Barbosa, A.D., Sembongi, H., Su, W.-M., Abreu, S., Reggiori, F., Carman, G.M., and Siniossoglou, S. (2015). Lipid partitioning at the nuclear envelope controls membrane biogenesis. Mol. Biol. Cell *26*, 3641–3657.

Barisch, C., and Soldati, T. (2017). Breaking fat! How mycobacteria and other intracellular pathogens manipulate host lipid droplets. Biochimie *141*, 54–61.

Barneda, D., and Christian, M. (2017). Lipid droplet growth: regulation of a dynamic organelle. Curr. Opin. Cell Biol. *47*, 9–15.

Barneda, D., Planas-iglesias, J., Gaspar, M.L., Mohammadyani, D., Prasannan, S., Dormann, D., Han, G., Jesch, S.A., Carman, G.M., Kagan, V., et al. (2015). The brown adipocyte protein CIDEA promotes lipid droplet fusion via a phosphatidic acid-binding amphipathic helix. Elife.

Becuwe, M., Bond, L.M., Mejhert, N., Boland, S., Shane, D., Cicconet, M., Liu, X.N., Graham, M.M., Tobias, C., and Jr, R.V.F. (2018). FIT2 is a lipid phosphate phosphatase crucial for endoplasmic reticulum homeostasis. Biorxiv.

Beller, M., Sztalryd, C., Southall, N., Bell, M., Jäckle, H., Auld, D.S., and Oliver, B. (2008). COPI Complex Is a Regulator of Lipid Homeostasis. PLoS Biol. *6*, 14.

Berardinelli, W. (1954). An undiagnosed endocrinometabolic syndrome: report of 2 cases. J. Clin. Endocrinol. Metab. *14*, 193–204.

Bersuker, K., and Olzmann, J.A. (2017). Establishing the lipid droplet proteome: Mechanisms of lipid droplet protein targeting and degradation. Biochim. Biophys. Acta - Mol. Cell Biol. Lipids *1862*, 1166–1177.

Bersuker, K., Peterson, C.W.H., To, M., Sahl, S.J., Savikhin, V., Grossman, E.A., Nomura, D.K., and Olzmann, J.A. (2018). A Proximity Labeling Strategy Provides Insights into the Composition and Dynamics of Lipid Droplet Proteomes. Dev. Cell *44*, 97-112.e7.

Bi, J., Wang, W., Liu, Z., Huang, X., Jiang, Q., Liu, G., Wang, Y., and Huang, X. (2014). Seipin promotes adipose tissue fat storage through the ER Ca^{2+}-ATPase SERCA. Cell Metab. *19*, 861–871.

Binns, D., Lee, S., Hilton, C.L., Jiang, Q.-X., and Goodman, J.M. (2010). Seipin is a discrete homooligomer. Biochemistry *49*,

10747–10755.
Blackstone, C. (2018). Converging cellular themes for the hereditary spastic paraplegias. Curr. Opin. Neurobiol. *51*, 139–146.
Blaner, W.S., O'Byrne, S.M., Wongsiriroj, N., Kluwe, J., D'Ambrosio, D.M., Jiang, H., Schwabe, R.F., Hillman, E.M.C., Piantedosi, R., and Libien, J. (2009). Hepatic stellate cell lipid droplets: A specialized lipid droplet for retinoid storage. Biochim. Biophys. Acta - Mol. Cell Biol. Lipids *1791*, 467–473.
Bligh, E.G. and Dyer, W.J. (1959). A RAPID METHOD OF TOTAL LIPID EXTRACTION AND PURIFICATION. Can. J. Biochem. Physiol. *37*, 911–917.
Bosma, M., Dapito, D.H., Drosatos-Tampakaki, Z., Huiping-Son, N., Huang, L.S., Kersten, S., Drosatos, K., and Goldberg, I.J. (2014). Sequestration of fatty acids in triglycerides prevents endoplasmic reticulum stress in an in vitro model of cardiomyocyte lipotoxicity. Biochim. Biophys. Acta - Mol. Cell Biol. Lipids *1841*, 1648–1655.
Boström, P., Andersson, L., Rutberg, M., Perman, J., Lidberg, U., Johansson, B.R., Fernandez-Rodriguez, J., Ericson, J., Nilsson, T., Borén, J., et al. (2007). SNARE proteins mediate fusion between cytosolic lipid droplets and are implicated in insulin sensitivity. Nat. Cell Biol. *9*, 1286–1293.
Boutet, E., El Mourabit, H., Prot, M., Nemani, M., Khallouf, E., Colard, O., Maurice, M., Durand-Schneider, A.-M., Chrétien, Y., Grès, S., et al. (2009). Seipin deficiency alters fatty acid Delta9 desaturation and lipid droplet formation in Berardinelli-Seip congenital lipodystrophy. Biochimie *91*, 796–803.
Brasaemle, D.L., and Wolins, N.E. (2006). Isolation of Lipid Droplets from Cells by Density Gradient Centrifugation. Curr. Protoc. Cell Biol. *29*, 3.15.1–3.15.12.
Brasaemle, D.L., Barber, T., Wolins, N.E., Serrero, G., Blanchette-mackie, E.J., and Londos, C. (1997). Adipose differentiation-related protein is an ubiquitously expressed lipid storage droplet- associated protein. J. Lipid Res. *38*, 2249–2263.
Broekema, M.F., Savage, D.B., Monajemi, H., and Kalkhoven, E. (2019). Gene-gene and gene-environment interactions in lipodystrophy: Lessons learned from natural PPARγ mutants. Biochim. Biophys. Acta - Mol. Cell Biol. Lipids *1864*, 715–732.
Bulankina, A. V., Deggerich, A., Wenzel, D., Mutenda, K., Wittmann, J.G., Rudolph, M.G., Burger, K.N.J., and Höning, S. (2009). TIP47 functions in the biogenesis of lipid droplets. J. Cell Biol. *185*, 641–655.
Cai, Y., Goodman, J.M., Pyc, M., Mullen, R.T., Dyer, J.M., and Chapman, K.D. (2015). Arabidopsis SEIPIN Proteins Modulate Triacylglycerol Accumulation and Influence Lipid Droplet Proliferation. Plant Cell *9*, 2616–2636.
Cao, H. (2000). Nuclear lamin A/C R482Q mutation in Canadian kindreds with Dunnigan-type familial partial lipodystrophy. Hum. Mol. Genet. *9*, 109–112.
Cao, H., Alston, L., Ruschman, J., and Hegele, R.A. (2008). Heterozygous CAV1 frameshift mutations (MIM 601047) in patients with atypical partial lipodystrophy and hypertriglyceridemia. Lipids Health Dis. *7*, 1–5.
Cao, Z., Hao, Y., Lee, Y.Y., Wang, P., Li, X., Xie, K., Lam, W.J., Qiu, Y., Shui, G., Liu, P., et al. (2019). Dietary fatty acids promote lipid droplet diversity through seipin enrichment in an ER subdomain. Nat. Commun. *10*, 2902.
Carr, A., Samaras, K., Thorisdottir, A., Chisholm, D., and Cooper, D. (1999). Diagnosis, prediction, and natural course of HIV-1 protease-inhibitor- associated lipodystrophy, hyperlipidaemia, and diabetes mellitus: a cohort study. Lancet *353*, 2093–2099.
Cartwright, B.R., and Goodman, J.M. (2012). Seipin: from human disease to molecular mechanism. J. Lipid Res. *53*, 1042–1055.
Cartwright, B.R., Binns, D.D., Hilton, C.L., Han, S., Gao, Q., and Goodman, J.M. (2015). Seipin performs dissectible functions in promoting lipid droplet biogenesis and regulating droplet morphology. Mol. Biol. Cell *26*, 726–739.
De Carvalho, C.C.C.R., and Caramujo, M.J. (2018). The various roles of fatty acids. Molecules *23*, 2583.
Castro, I.G., Eisenberg-Bord, M., Persiani, E., Rochford, J.J., Schuldiner, M., and Bohnert, M. (2019). Promethin Is a Conserved Seipin Partner Protein. Cells *8*, 268.
Chang, H., Di, T., Wang, Y., Zeng, X., Li, G., Wan, Q., Yu, W., and Chen, L. (2019). Seipin deletion in mice enhances phosphorylation and aggregation of tau protein through reduced neuronal PPARγ and insulin resistance. Neurobiol. Dis. *127*, 350–361.
Chang, T.Y., Li, B.L., Chang, C.C.Y., and Urano, Y. (2009). Acyl-coenzyme A:cholesterol acyltransferases. Am. J. Physiol. - Endocrinol. Metab. *297*, 1–9.
Chen, X., and Goodman, J.M. (2017). The collaborative work of droplet assembly. Biochim. Biophys. Acta - Mol. Cell Biol. Lipids *1862*, 1205–1211.
Chen, W., Yechoor, V.K., Chang, B.H.-J., Li, M. V, March, K.L., and Chan, L. (2009). The human lipodystrophy gene product Berardinelli-Seip congenital lipodystrophy 2/seipin plays a key role in adipocyte differentiation. Endocrinology *150*, 4552–4561.
Chen, W., Chang, B., Saha, P., Hartig, S.M., Li, L., Reddy, V.T., Yang, Y., Yechoor, V., Mancini, M. a, and Chan, L. (2012). Berardinelli-seip congenital lipodystrophy 2/seipin is a cell-autonomous regulator of lipolysis essential for adipocyte differentiation. Mol. Cell. Biol. *32*, 1099–1111.
Chen, W., Zhou, H., Saha, P., Li, L., and Chan, L. (2014). Molecular mechanisms underlying fasting modulated liver insulin sensitivity and metabolism in male lipodystrophic Bscl2/seipin-deficient mice. Endocrinology *155*, 4215–4225.
Chen, Y., Wei, L., Tian, J., Wang, Y.H., Liu, G., and Wang, C. (2016). Seinpin knockout exacerbates cerebral ischemia/reperfusion damage in mice. Biochem. Biophys. Res. Commun. *474*, 377–383.

Chitraju, C., Mejhert, N., Haas, J.T., Diaz-Ramirez, L.G., Grueter, C.A., Imbriglio, J.E., Pinto, S., Koliwad, S.K., Walther, T.C., and Farese, R. V. (2017). Triglyceride Synthesis by DGAT1 Protects Adipocytes from Lipid-Induced ER Stress during Lipolysis. Cell Metab. *26*, 407-418.e3.

Chorlay, A., and Thiam, A.R. (2018). An Asymmetry in Monolayer Tension Regulates Lipid Droplet Budding Direction. Biophys. J. *114*, 631–640.

Chorlay, A., Monticelli, L., Veríssimo Ferreira, J., Ben M'barek, K., Ajjaji, D., Wang, S., Johnson, E., Beck, R., Omrane, M., Beller, M., et al. (2019). Membrane Asymmetry Imposes Directionality on Lipid Droplet Emergence from the ER. Dev. Cell *50*, 25-42.e7.

Choudhary, V., Ojha, N., Golden, A., and Prinz, W. a (2015). A conserved family of proteins facilitates nascent lipid droplet budding from the ER. J. Cell Biol. *211*, 261–271.

Choudhary, V., Golani, G., Joshi, A.S., Cottier, S., Schneiter, R., Prinz, W.A., and Kozlov, M.M. (2018). Architecture of Lipid Droplets in Endoplasmic Reticulum Is Determined by Phospholipid Intrinsic Curvature. Curr. Biol. *28*, 915-926.e9.

Congyan, Z., Li, Y., Ding, Y., Wang, Y., Lan, L., Ma, Q., Chi, X., Wei, P., Zhao, Y., Steinbüchel, A., et al. (2017). Bacterial lipid droplets bind to DNA via an intermediary protein that enhances survival under stress. Nat. Commun. *8*, 15979.

Coradetti, S.T., Pinel, D., Geiselman, G.M., Ito, M., Mondo, S.J., Reilly, M.C., Cheng, Y.F., Bauer, S., Grigoriev, I. V., Gladden, J.M., et al. (2018). Functional genomics of lipid metabolism in the oleaginous yeast Rhodosporidium toruloides. Elife *7*, 1–55.

Cui, X., Wang, Y., Tang, Y., Liu, Y., Zhao, L., Deng, J., Xu, G., Peng, X., Ju, S., Liu, G., et al. (2011). Seipin ablation in mice results in severe generalized lipodystrophy. Hum. Mol. Genet. *20*, 3022–3030.

Datta, S., Liu, Y., Hariri, H., Bowerman, J., and Henne, W.M. (2019). Cerebellar ataxia disease-associated Snx14 promotes lipid droplet growth at ER-droplet contacts. J. Cell Biol. *218*, 1335–1351.

Deslandes, F., Thiam, A.R., and Forêt, L. (2017). Lipid Droplets Can Spontaneously Bud Off from a Symmetric Bilayer. Biophys. J. *113*, 15–18.

Ding, L., Yang, X., Tian, H., Liang, J., Zhang, F., Wang, G., Wang, Y., Ding, M., Shui, G., and Huang, X. (2018). Seipin regulates lipid homeostasis by ensuring calcium-dependent mitochondrial metabolism. EMBO J. *37*, 1–17.

Dollet, L., Magré, J., Cariou, B., and Prieur, X. (2014). Function of seipin: New insights from Bscl2/seipin knockout mouse models. Biochimie *96*, 166–172.

Dwianingsih, E.K., Takeshima, Y., Itoh, K., Yamauchi, Y., Awano, H., Malueka, R.G., Nishida, A., Ota, M., Yagi, M., and Matsuo, M. (2010). A Japanese child with asymptomatic elevation of serum creatine kinase shows PTRF-CAVIN mutation matching with congenital generalized lipodystrophy type 4. Mol. Genet. Metab. *101*, 233–237.

Eastman, S.W., Yassaee, M., and Bieniasz, P.D. (2009). A role for ubiquitin ligases and Spartin/SPG20 in lipid droplet turnover. J. Cell Biol. *184*, 881–894.

Ebihara, C., Ebihara, K., Aizawa-Abe, M., Mashimo, T., Tomita, T., Zhao, M., Gumbilai, V., Kusakabe, T., Yamamoto, Y., Aotani, D., et al. (2015). Seipin is necessary for normal brain development and spermatogenesis in addition to adipogenesis. Hum. Mol. Genet. *24*, 4238–4249.

Ebihara, K., Kusakabe, T., Masuzaki, H., Kobayashi, N., Tanaka, T., Chusho, H., Miyanaga, F., Miyazawa, T., Hayashi, T., Hosoda, K., et al. (2004). Gene and Phenotype Analysis of Congenital Generalized Lipodystrophy in Japanese: A Novel Homozygous Nonsense Mutation in Seipin Gene. J. Clin. Endocrinol. Metab. *89*, 2360–2364.

Eisenberg-Bord, M., Mari, M., Weill, U., Rosenfeld-Gur, E., Moldavski, O., Castro, I.G., Soni, K.G., Harpaz, N., Levine, T.P., Futerman, A.H., et al. (2018). Identification of seipin-linked factors that act as determinants of a lipid droplet subpopulation. J. Cell Biol. *217*, 269–282.

Ellis, J.M., Frahm, J.L., Li, L.O., and Coleman, R.A. (2010). Acyl-coenzyme A synthetases in metabolic control. Curr. Opin. Lipidol. *21*, 212–217.

Falk, J., Rohde, M., Bekhite, M.M., Neugebauer, S., Hemmerich, P., Kiehntopf, M., Deufel, T., Hübner, C. a, and Beetz, C. (2014). Functional mutation analysis provides evidence for a role of REEP1 in lipid droplet biology. Hum. Mutat. *35*, 497–504.

Fanning, S., Haque, A., Imberdis, T., Baru, V., Barrasa, M.I., Nuber, S., Termine, D., Ramalingam, N., Ho, G.P.H., Noble, T., et al. (2019). Lipidomic Analysis of α-Synuclein Neurotoxicity Identifies Stearoyl CoA Desaturase as a Target for Parkinson Treatment. Mol. Cell *73*, 1001-1014.e8.

Farese, R. V, and Walther, T.C. (2009). Lipid Droplets Finally Get a Little R-E-S-P-E-C-T. Cell *139*, 855–860.

Fei, W., Shui, G., Gaeta, B., Du, X., Kuerschner, L., Li, P., Brown, a. J., Wenk, M.R., Parton, R.G., and Yang, H. (2008). Fld1p, a functional homologue of human seipin, regulates the size of lipid droplets in yeast. J. Cell Biol. *180*, 473–482.

Fei, W., Wang, H., Fu, X., Bielby, C., and Yang, H. (2009). Conditions of endoplasmic reticulum stress stimulate lipid droplet formation in Saccharomyces cerevisiae . Biochem. J. *424*, 61–67.

Fei, W., Zhong, L., Ta, M.T., Shui, G., Wenk, M.R., and Yang, H. (2011a). The size and phospholipid composition of lipid droplets can influence their proteome. Biochem. Biophys. Res. Commun. *415*, 455–462.

Fei, W., Li, H., Shui, G., Kapterian, T.S., Bielby, C., Du, X., Brown, A.J., Li, P., Wenk, M.R., Liu, P., et al. (2011b). Molecular characterization of seipin and its mutants: Implications for seipin in triacylglycerol synthesis. J. Lipid Res. *52*, 2136–2147.

Fei, W., Shui, G., Zhang, Y., Krahmer, N., Ferguson, C., Kapterian, T.S., Lin, R.C., Dawes, I.W., Brown, A.J., Li, P., et al. (2011c). A role for phosphatidic acid in the formation of "supersized" lipid droplets. PLoS Genet. *7*, e1002201.

Fuchs, C.D., Claudel, T., Kumari, P., Haemmerle, G., Pollheimer, M.J., Stojakovic, T., Scharnagl, H., Halilbasic, E., Gumhold, J., Silbert, D., et al. (2012). Absence of adipose triglyceride lipase protects from hepatic endoplasmic reticulum stress in mice. Hepatology *56*, 270–280.

Gandotra, S., Le Dour, C., Bottomley, W., Cervera, P., Giral, P., Reznik, Y., Charpentier, G., Auclair, M., Delépine, M., Barroso, I., et al. (2011). Perilipin deficiency and autosomal dominant partial lipodystrophy. N. Engl. J. Med. *364*, 740–748.

Gao, Q., and Goodman, J.M. (2015). The lipid droplet-a well-connected organelle. Front. Cell Dev. Biol. *3*, 49.

Gao, G., Chen, F.J., Zhou, L., Su, L., Xu, D., Xu, L., and Li, P. (2017a). Control of lipid droplet fusion and growth by CIDE family proteins. Biochim. Biophys. Acta - Mol. Cell Biol. Lipids *1862*, 1197–1204.

Gao, M., Wang, M., Guo, X., Qiu, X., Liu, L., Liao, J., Liu, J., Lu, G., Wang, Y., and Liu, G. (2015). Expression of seipin in adipose tissue rescues lipodystrophy, hepatic steatosis and insulin resistance in seipin null mice. Biochem. Biophys. Res. Commun. *460*, 143–150.

Gao, M., Huang, X., Song, B.-L., and Yang, H. (2019). The biogenesis of lipid droplets: Lipids take center stage. Prog. Lipid Res. *75*, 100989.

Gao, Q., Binns, D.D., Kinch, L.N., Grishin, N. V, Ortiz, N., Chen, X., and Goodman, J.M. (2017b). Pet10p is a yeast perilipin that stabilizes lipid droplets and promotes their assembly. J. Cell Biol. *216*, 3199–3217.

Garg, A. (2004). Acquired and Inherited Lipodystrophies. N. Engl. J. Med. *350*, 1220–1234.

Garg, A., and Agarwal, A.K. (2009). Lipodystrophies: Disorders of adipose tissue biology. Biochim. Biophys. Acta - Mol. Cell Biol. Lipids *1791*, 507–513.

Giménez-Andrés, M., Čopič, A., and Antonny, B. (2018). The many faces of amphipathic helices. Biomolecules *8*, 1–14.

Gluchowski, N.L., Becuwe, M., Walther, T.C., and Farese, R. V. (2017). Lipid droplets and liver disease: From basic biology to clinical implications. Nat. Rev. Gastroenterol. Hepatol. *14*, 343–355.

Gong, J., Sun, Z., Wu, L., Xu, W., Schieber, N., Xu, D., Shui, G., Yang, H., Parton, R.G., and Li, P. (2011). Fsp27 promotes lipid droplet growth by lipid exchange and transfer at lipid droplet contact sites. J. Cell Biol. *195*, 953–963.

Goodman, J.M. (2018). Understanding the Lipid Droplet Proteome and Protein Targeting. Dev. Cell *44*, 1–2.

Greenberg, A.S., Egan, J.J., Wek, S.A., Garty, N.B., Blanchette-Mackie, E.J., and Londos, C. (1991). Perilipin, a major hormonally regulated adipocyte-specific phosphoprotein associated with the periphery of lipid storage droplets. J. Biol. Chem. *266*, 11341–11346.

Greenwood, D.J., Dos Santos, M.S., Huang, S., Russell, M.R.G., Collinson, L.M., MacRae, J.I., West, A., Jiang, H., and Gutierrez, M.G. (2019). Subcellular antibiotic visualization reveals a dynamic drug reservoir in infected macrophages. Science (80-.). *364*, 1279–1282.

Grippa, A., Buxó, L., Mora, G., Funaya, C., Idrissi, F.-Z., Mancuso, F., Gomez, R., Muntanyà, J., Sabidó, E., and Carvalho, P. (2015). The seipin complex Fld1/Ldb16 stabilizes ER-lipid droplet contact sites. J. Cell Biol. *211*, 829–844.

Gross, D.A., Zhan, C., and Silver, D.L. (2011). Direct binding of triglyceride to fat storage-inducing transmembrane proteins 1 and 2 is important for lipid droplet formation. Proc. Natl. Acad. Sci. *108*, 19581–19586.

Guillén-Navarro, E., Sánchez-Iglesias, S., Domingo-Jiménez, R., Victoria, B., Ruiz-Riquelme, A., Rábano, A., Loidi, L., Beiras, A., González-Méndez, B., Ramos, A., et al. (2013). A new seipin-associated neurodegenerative syndrome. J. Med. Genet. 1–9.

Guo, J., Qiu, W., Soh, S.L.Y., Wei, S., Radda, G.K., Ong, W.-Y., Pang, Z.P., and Han, W. (2013). Motor neuron degeneration in a mouse model of seipinopathy. Cell Death Dis. *4*, e535.

Guo, Y., Walther, T.C., Rao, M., Stuurman, N., Goshima, G., Terayama, K., Wong, J.S., Vale, R.D., Walter, P., and Farese, R. V. (2008). Functional genomic screen reveals genes involved in lipid-droplet formation and utilization. Nature *453*, 657–661.

Haider, A., Wei, Y.C., Lim, K., Barbosa, A.D., Liu, C.H., Weber, U., Mlodzik, M., Oras, K., Collier, S., Hussain, M.M., et al. (2018). PCYT1A Regulates Phosphatidylcholine Homeostasis from the Inner Nuclear Membrane in Response to Membrane Stored Curvature Elastic Stress. Dev. Cell *45*, 481-495.e8.

Hamilton, J.A., Miller, K.W., and Small, D.M. (1983). Solubilization of Triolein and Cholesteryl Oleate in Egg Phosphatidylcholine Vesicles. J. Biol. Chem. *258*, 12821–12826.

Han, S., Binns, D.D., Chang, Y.-F., and Goodman, J.M. (2015). Dissecting seipin function: the localized accumulation of phosphatidic acid at ER/LD junctions in the absence of seipin is suppressed by Sei1pΔNterm only in combination with Ldb16p. BMC Cell Biol. *16*, 29.

Hapala, I., Marza, E., and Ferreira, T. (2011). Is fat so bad? Modulation of endoplasmic reticulum stress by lipid droplet formation. Biol. Cell *103*, 271–285.

Hariri, H., Rogers, S., Ugrankar, R., Liu, Y.L., Feathers, J.R., and Henne, W.M. (2017). Lipid droplet biogenesis is spatially coordinated at ER–vacuole contacts under nutritional stress. EMBO Rep. *19*, 57–72.

Hartman, I.Z., Liu, P., Zehmer, J.K., Luby-Phelps, K., Jo, Y., Anderson, R.G.W., and DeBose-Boyd, R.A. (2010). Sterol-induced dislocation of 3-Hydroxy-3-methylglutaryl coenzyme a reductase from endoplasmic reticulum membranes into the cytosol

through a subcellular compartment resembling lipid droplets. J. Biol. Chem. *285*, 19288–19298.

Hayashi, Y.K., Matsuda, C., Ogawa, M., Goto, K., Tominaga, K., Mitsuhashi, S., Park, Y.E., Nonaka, I., Hino-Fukuyo, N., Haginoya, K., et al. (2009). Human PTRF mutations cause secondary deficiency of caveolins resulting in muscular dystrophy with generalized lipodystrophy. J. Clin. Invest. *119*, 2623–2633.

Hayes, M.J., Choudhary, V., Ojha, N., Shin, J.J., Han, G.-S., Carman, G.M., Loewen, C.J., Prinz, W.A., and Levine, T.P. (2018). Fat storage-inducing transmembrane (FIT or FITM) proteins are related to lipid phosphatase/phosphotransferase enzymes. Microb. Cell *5*, 88–103.

Henne, M., Goodman, J.M., and Hariri, H. (2020). Spatial compartmentalization of lipid droplet biogenesis. Biochim. Biophys. Acta - Mol. Cell Biol. Lipids *1865*, 158499.

Henne, W.M., Reese, M.L., and Goodman, J.M. (2018). The assembly of lipid droplets and their roles in challenged cells. EMBO J. *37*, e98947.

Henneberry, A.L., Wright, M.M., and Mcmaster, C.R. (2002). The Major Sites of Cellular Phospholipid Synthesis and Molecular Determinants of Fatty Acid and Lipid Head Group Specificity. Mol. Biol. Cell *13*, 3148–3161.

Herms, A., Bosch, M., Reddy, B.J.N., Schieber, N.L., Fajardo, A., Rupérez, C., Fernández-Vidal, A., Ferguson, C., Rentero, C., Tebar, F., et al. (2015). AMPK activation promotes lipid droplet dispersion on detyrosinated microtubules to increase mitochondrial fatty acid oxidation. Nat. Commun. *6*, 7176.

Hetz, C. (2012). The unfolded protein response: Controlling cell fate decisions under ER stress and beyond. Nat. Rev. Mol. Cell Biol. *13*, 89–102.

Heybrock, S., Kanerva, K., Meng, Y., Ing, C., Liang, A., Xiong, Z.-J., Weng, X., Ah Kim, Y., Collins, R., Trimble, W., et al. (2019). Lysosomal integral membrane protein-2 (LIMP-2/SCARB2) is involved in lysosomal cholesterol export. Nat. Commun. *10*, 3521.

Hölttä-Vuori, M., Salo, V.T. V, Nyberg, L., Brackmann, C., Enejder, A., Panula, P., and Ikonen, E. (2010). Zebrafish: gaining popularity in lipid research. Biochem. J. *429*, 235–242.

Hölttä-Vuori, M., Salo, V.T., Ohsaki, Y., Suster, M.L., and Ikonen, E. (2013). Alleviation of seipinopathy-related ER stress by triglyceride storage. Hum. Mol. Genet. *22*, 1157–1166.

Horchani, H., De Saint-Jean, M., Barelli, H.L., and Antonny, B. (2014). Interaction of the Spo20 membrane-sensor motif with phosphatidic acid and other anionic lipids, and influence of the membrane environment. PLoS One *9*, 1–22.

Ikonen, E. (2018). Mechanisms of cellular cholesterol compartmentalization: recent insights. Curr. Opin. Cell Biol. *53*, 77–83.

Ioannou, M.S., Jackson, J., Sheu, S.H., Chang, C.L., Weigel, A. V., Liu, H., Pasolli, H.A., Xu, C.S., Pang, S., Matthies, D., et al. (2019). Neuron-Astrocyte Metabolic Coupling Protects against Activity-Induced Fatty Acid Toxicity. Cell *177*, 1522-1535.e14.

Ito, D., and Suzuki, N. (2007). Molecular pathogenesis of seipin/BSCL2-related motor neuron diseases. Ann. Neurol. *61*, 237–250.

Ito, D., and Suzuki, N. (2009). Seipinopathy: a novel endoplasmic reticulum stress-associated disease. Brain *132*, 8–15.

Ito, D., Yagi, T., Ikawa, M., and Suzuki, N. (2012). Characterization of inclusion bodies with cytoprotective properties formed by seipinopathy-linked mutant seipin. Hum. Mol. Genet. *21*, 635–646.

Jackson, C.L. (2019). Lipid droplet biogenesis. Curr. Opin. Cell Biol. *59*, 88–96.

Jacquier, N., Choudhary, V., Mari, M., Toulmay, A., Reggiori, F., and Schneiter, R. (2011). Lipid droplets are functionally connected to the endoplasmic reticulum in Saccharomyces cerevisiae. J. Cell Sci. *124*, 2424–2437.

Jambunathan, S., Yin, J., Khan, W., Tamori, Y., and Puri, V. (2011). FSP27 promotes lipid droplet clustering and then fusion to regulate triglyceride accumulation. PLoS One *6*, 1–12.

Jeninga, E.H., de Vroede, M., Hamers, N., Breur, J.M.P.J., Verhoeven-Duif, N.M., Berger, R., and Kalkhoven, E. (2012). A Patient with Congenital Generalized Lipodystrophy Due To a Novel Mutation in BSCL2: Indications for Secondary Mitochondrial Dysfunction. In JIMD Reports - Case and Research Reports, 2012/1, (Berlin, Heidelberg: Springer Berlin Heidelberg), pp. 47–54.

Jessica M. Kornke, M.M.A. (2017). Fat-containing cells are eliminated during Dictyostelium development. Biol. Open 1–11.

Jiang, M., Gao, M., Wu, C., He, H., Guo, X., Zhou, Z., Yang, H., Xiao, X., Liu, G., and Sha, J. (2014). Lack of testicular seipin causes teratozoospermia syndrome in men. Proc. Natl. Acad. Sci. *111*, 7054–7059.

Jiao, Y., Ahmed, U., Sim, M.F.M., Bejar, A., Zhang, X., Talukder, M.M.U., Rice, R., Flannick, J., Podgornaia, A.I., Reilly, D.F., et al. (2019). Discovering metabolic disease gene interactions by correlated effects on cellular morphology. Mol. Metab. *24*, 108–119.

Joshi, A.S., Nebenfuehr, B., Choudhary, V., Satpute-Krishnan, P., Levine, T.P., Golden, A., and Prinz, W.A. (2018). Lipid droplet and peroxisome biogenesis occur at the same ER subdomains. Nat. Commun. *9*, 2940.

Joubert, M., Jagu, B., Montaigne, D., Marechal, X., Tesse, A., Ayer, A., Dollet, L., Le May, C., Toumaniantz, G., Manrique, A., et al. (2017). The sodium-glucose cotransporter 2 inhibitor dapagliflozin prevents cardiomyopathy in a diabetic lipodystrophic mouse model. Diabetes *66*, 1030–1040.

Jüngst, C., Klein, M., and Zumbusch, A. (2013). Long-term live cell microscopy studies of lipid droplet fusion dynamics in

adipocytes. J. Lipid Res. *54*, 3419–3429.
Kamiyama, D., Sekine, S., Barsi-Rhyne, B., Hu, J., Chen, B., Gilbert, L.A., Ishikawa, H., Leonetti, M.D., Marshall, W.F., Weissman, J.S., et al. (2016). Versatile protein tagging in cells with split fluorescent protein. Nat. Commun. *7*, 1–9.
Kassan, A., Herms, A., Fernández-Vidal, A., Bosch, M., Schieber, N.L., Reddy, B.J.N., Fajardo, A., Gelabert-Baldrich, M., Tebar, F., Enrich, C., et al. (2013). Acyl-CoA synthetase 3 promotes lipid droplet biogenesis in ER microdomains. J. Cell Biol. *203*, 985–1001.
Khandelia, H., Duelund, L., Pakkanen, K.I., and Ipsen, J.H. (2010). Triglyceride blisters in lipid bilayers: Implications for lipid droplet biogenesis and the mobile lipid signal in cancer cell membranes. PLoS One *5*, 1–8.
Kim, C.A., Delépine, M., Boutet, E., El Mourabit, H., Le Lay, S., Meier, M., Nemani, M., Bridel, E., Leite, C.C., Bertola, D.R., et al. (2008). Association of a homozygous nonsense caveolin-1 mutation with berardinelli-seip congenital lipodystrophy. J. Clin. Endocrinol. Metab. *93*, 1129–1134.
Kim, J.I., Park, J., Ji, Y., Jo, K., Han, S.M., Sohn, J.H., Shin, K.C., Han, J.S., Jeon, Y.G., Nahmgoong, H., et al. (2019). During Adipocyte Remodeling, Lipid Droplet Configurations Regulate Insulin Sensitivity through F-Actin and G-Actin Reorganization. Mol. Cell. Biol. *39*.
Kimmel, A.R., and Sztalryd, C. (2014). Perilipin 5, a lipid droplet protein adapted to mitochondrial energy utilization. Curr. Opin. Lipidol. *25*, 110–117.
Kimura, H., Arasaki, K., Ohsaki, Y., Fujimoto, T., Ohtomo, T., Yamada, J., and Tagaya, M. (2018). Syntaxin 17 promotes lipid droplet formation by regulating the distribution of acyl-CoA synthetase 3. J. Lipid Res. *59*, 805–819.
Klemm, R.W., Norton, J.P., Cole, R. a, Li, C.S., Park, S.H., Crane, M.M., Li, L., Jin, D., Boye-Doe, A., Liu, T.Y., et al. (2013). A conserved role for atlastin GTPases in regulating lipid droplet size. Cell Rep. *3*, 1465–1475.
Kobayashi, K., Takahashi, Y., and Shibasaki, S. (1973). Cytological Studies of Fat-storing Cells in the Liver of Rats given Large Doses of Viatmin A. Nature *244*, 47–49.
Kohlwein, S.D. (2010). Obese and anorexic yeasts: Experimental models to understand the metabolic syndrome and lipotoxicity. Biochim. Biophys. Acta - Mol. Cell Biol. Lipids *1801*, 222–229.
Korobchevskaya, K., Lagerholm, B.C., Colin-York, H., and Fritzsche, M. (2017). Exploring the potential of Airyscan microscopy for live cell imaging. Photonics *4*, 41.
Kory, N., Farese, R. V., and Walther, T.C. (2016). Targeting Fat: Mechanisms of Protein Localization to Lipid Droplets. Trends Cell Biol. *26*, 535–546.
Kraemer, F.B., and Shen, W.J. (2002). Hormone-sensitive lipase: control of intracellular tri-(di-)acylglycerol and cholesteryl ester hydrolysis. J. Lipid Res. *43*, 1585–1594.
Krahmer, N., Guo, Y., Wilfling, F., Hilger, M., Lingrell, S., Heger, K., Newman, H.W., Schmidt-Supprian, M., Vance, D.E., Mann, M., et al. (2011). Phosphatidylcholine synthesis for lipid droplet expansion is mediated by localized activation of CTP:phosphocholine cytidylyltransferase. Cell Metab. *14*, 504–515.
Krahmer, N., Farese, R. V., and Walther, T.C. (2013a). Balancing the fat: Lipid droplets and human disease. EMBO Mol. Med. *5*, 905–915.
Krahmer, N., Hilger, M., Kory, N., Wilfling, F., Stoehr, G., Mann, M., Farese, R. V, and Walther, T.C. (2013b). Protein correlation profiles identify lipid droplet proteins with high confidence. Mol. Cell Proteomics *12*, 1115–1126.
Kuerschner, L., Moessinger, C., and Thiele, C. (2008). Imaging of lipid biosynthesis: how a neutral lipid enters lipid droplets. Traffic *9*, 338–352.
Kumar, N., Leonzino, M., Hancock-Cerutti, W., Horenkamp, F.A., Li, P., Lees, J.A., Wheeler, H., Reinisch, K.M., and De Camilli, P. (2018). VPS13A and VPS13C are lipid transport proteins differentially localized at ER contact sites. J. Cell Biol. *217*, 3625–3639.
Lass, A., Zimmermann, R., Haemmerle, G., Riederer, M., Schoiswohl, G., Schweiger, M., Kienesberger, P., Strauss, J.G., Gorkiewicz, G., and Zechner, R. (2006). Adipose triglyceride lipase-mediated lipolysis of cellular fat stores is activated by CGI-58 and defective in Chanarin-Dorfman Syndrome. Cell Metab. *3*, 309–319.
Laufman, O., Perrino, J., and Andino, R. (2019). Viral Generated Inter-Organelle Contacts Redirect Lipid Flux for Genome Replication. Cell 1–15.
Lee, J.-Y., Cortese, M., Haselmann, U., Tabata, K., Romero-Brey, I., Funaya, C., Schieber, N.L., Qiang, Y., Bartenschlager, M., Kallis, S., et al. (2019). Spatiotemporal Coupling of the Hepatitis C Virus Replication Cycle by Creating a Lipid Droplet-Proximal Membranous Replication Compartment. Cell Rep. *27*, 3602-3617.e5.
Lemmon, M.A. (2008). Membrane recognition by phospholipid-binding domains. Nat. Rev. Mol. Cell Biol. *9*, 99–111.
Li, H., Fong, C., Chen, Y., Cai, G., and Yang, M. (2010). Beta-adrenergic signals regulate adipogenesis of mouse mesenchymal stem cells via cAMP/PKA pathway. Mol. Cell. Endocrinol. *323*, 201–207.
Li, Q., Li, Y., Zhang, Z., Kang, H., Zhang, L., Zhang, Y., and Zhou, L. (2019a). SEIPIN overexpression in the liver may alleviate hepatic steatosis by influencing the intracellular calcium level. Mol. Cell. Endocrinol. *488*, 70–78.
Li, Q., Li, Y., Zhang, Z., Kang, H., Zhang, L., Zhang, Y., and Zhou, L. (2019b). SEIPIN overexpression in the liver may alleviate

hepatic steatosis by influencing the intracellular calcium level. Mol. Cell. Endocrinol. *488*, 70–78.

Li, S., Prasanna, X., Salo, V.T., Vattulainen, I., and Ikonen, E. (2019c). An efficient auxin-inducible degron system with low basal degradation in human cells. Nat. Methods *16*, 866–869.

Li, Z., Thiel, K., Thul, P.J., Beller, M., Kühnlein, R.P., and Welte, M. a (2012). Lipid Droplets Control the Maternal Histone Supply of Drosophila Embryos. Curr. Biol. 2104–2113.

Liao, J., Liu, X., Gao, M., Wang, M., Wang, Y., Wang, F., Huang, W., and Liu, G. (2018). Dyslipidemia, steatohepatitis and atherogenesis in lipodystrophic apoE deficient mice with Seipin deletion. Gene *648*, 82–88.

Libbing, C.L., McDevitt, A.R., Azcueta, R.-M.P., Ahila, A., and Mulye, M. (2019). Lipid Droplets: A Significant but Understudied Contributor of Host–Bacterial Interactions. Cells *8*, 354.

Lippincott-Schwartz, J., Snapp, E., and Kenworthy, A. (2001). Studying protein dynamics in living cells. Nat. Rev. Mol. Cell Biol. *2*, 444–456.

Listenberger, L.L., Han, X., Lewis, S.E., Cases, S., Farese, R. V., Ory, D.S., and Schaffer, J.E. (2003). Triglyceride accumulation protects against fatty acid-induced lipotoxicity. Proc. Natl. Acad. Sci. *100*, 3077–3082.

Liu, L., Jiang, Q., Wang, X., Zhang, Y., Lin, R.C.Y., Lam, S.M., Shui, G., Zhou, L., Li, P., Wang, Y., et al. (2014). Adipose-specific knockout of Seipin/Bscl2 results in progressive lipodystrophy. Diabetes *63*, 2320–2331.

Lohmann, D., Spandl, J., Stevanovic, A., Schoene, M., Philippou-Massier, J., and Thiele, C. (2013). Monoubiquitination of Ancient Ubiquitous Protein 1 Promotes Lipid Droplet Clustering. PLoS One *8*, 1–11.

Lundin, C., Nordström, R., Wagner, K., Windpassinger, C., Andersson, H., von Heijne, G., and Nilsson, I. (2006). Membrane topology of the human seipin protein. FEBS Lett. *580*, 2281–2284.

Lv, X., Liu, J., Qin, Y., Liu, Y., Jin, M., Dai, J., Chua, B.T., Yang, H., and Li, P. (2018). Identification of gene products that control lipid droplet size in yeast using a high-throughput quantitative image analysis. Biochim. Biophys. Acta - Mol. Cell Biol. Lipids *1864*, 113–127.

Ben M'barek, K., Ajjaji, D., Chorlay, A., Vanni, S., Forêt, L., and Thiam, A.R. (2017). ER Membrane Phospholipids and Surface Tension Control Cellular Lipid Droplet Formation. Dev. Cell *41*, 591-604.e7.

Magré, J., Delépine, M., Khallouf, E., Gedde-Dahl, T., Van Maldergem, L., Sobel, E., Papp, J., Meier, M., Mégarbané, a, Bachy, a, et al. (2001). Identification of the gene altered in Berardinelli-Seip congenital lipodystrophy on chromosome 11q13. Nat. Genet. *28*, 365–370.

Mahamid, J., Tegunov, D., Maiser, A., Arnold, J., Leonhardt, H., Plitzko, J.M., and Baumeister, W. (2019). Liquid-crystalline phase transitions in lipid droplets are related to cellular states and specific organelle association. Proc. Natl. Acad. Sci. *116*, 201903642.

Van Maldergem, L., Magré, J., Khallouf, T.E., Gedde-Dahl, T., Delépine, M., Trygstad, O., Seemanova, E., Stephenson, T., Albott, C.S., Bonnici, F., et al. (2002). Genotype-phenotype relationships in Berardinelli-Seip congenital lipodystrophy. J. Med. Genet. *39*, 722–733.

Markgraf, D.F., Klemm, R.W., Junker, M., Hannibal-Bach, H.K., Ejsing, C.S., and Rapoport, T. a (2014). An ER protein functionally couples neutral lipid metabolism on lipid droplets to membrane lipid synthesis in the ER. Cell Rep. *6*, 44–55.

Martin, S., and Parton, R. (2006). Lipid droplets: a unified view of a dynamic organelle. Nat. Rev. Mol. Cell Biol. *7*, 373–378.

Martin, S., Driessen, K., Nixon, S.J., Zerial, M., and Parton, R.G. (2005). Regulated localization of Rab18 to lipid droplets: Effects of lipolytic stimulation and inhibition of lipid droplet catabolism. J. Biol. Chem. *280*, 42325–42335.

McFie, P.J., Banman, S.L., and Stone, S.J. (2018). Diacylglycerol acyltransferase-2 contains a c-terminal sequence that interacts with lipid droplets. Biochim. Biophys. Acta - Mol. Cell Biol. Lipids *1863*, 1068–1081.

Mcilroy, G.D., Suchacki, K., Roelofs, A.J., Yang, W., Fu, Y., Bai, B., Wallace, R.J., De Bari, C., Cawthorn, W.P., Han, W., et al. (2018). Adipose specific disruption of seipin causes early-onset generalised lipodystrophy and altered fuel utilisation without severe metabolic disease. Mol. Metab. *10*, 55–65.

Melo, R.C.N., and Dvorak, A.M. (2012). Lipid body-phagosome interaction in macrophages during infectious diseases: host defense or pathogen survival strategy? PLoS Pathog. *8*, e1002729.

Melvin, A., Stears, A., and Savage, D.B. (2019). Recent developments in lipodystrophy. Curr. Opin. Lipidol. *30*, 284–290.

Miranda, D.M., Wajchenberg, B.L., Calsolari, M.R., Aguiar, M.J., Silva, J.M.C.L., Ribeiro, M.G., Fonseca, C., Amaral, D., Boson, W.L., Resende, B.A., et al. (2009). Novel mutations of the BSCL2 and AGPAT2 genes in 10 families with Berardinelli-Seip congenital generalized lipodystrophy syndrome. Clin. Endocrinol. (Oxf). *71*, 512–517.

Mishra, S., Khaddaj, R., Cottier, S., Stradalova, V., Jacob, C., and Schneiter, R. (2016). Mature lipid droplets are accessible to ER luminal proteins. J. Cell Sci. *129*, 3803–3815.

Miyanari, Y., Atsuzawa, K., Usuda, N., Watashi, K., Hishiki, T., Zayas, M., Bartenschlager, R., Wakita, T., Hijikata, M., and Shimotohno, K. (2007). The lipid droplet is an important organelle for hepatitis C virus production. Nat. Cell Biol. *9*, 1089–1097.

Miyoshi, H., Souza, S.C., Zhang, H.H., Strissel, K.J., Christoffolete, M.A., Kovsan, J., Rudich, A., Kraemer, F.B., Bianco, A.C., Obin, M.S., et al. (2006). Perilipin promotes hormone-sensitive lipase-mediated adipocyte lipolysis via phosphorylation-dependent and -independent mechanisms. J. Biol. Chem. *281*, 15837–15844.

Moessinger, C., Kuerschner, L., Spandl, J., Shevchenko, A., and Thiele, C. (2011). Human lysophosphatidylcholine acyltransferases 1 and 2 are located in lipid droplets where they catalyze the formation of phosphatidylcholine. J. Biol. Chem. *286*, 21330–21339.

Moessinger, C., Klizaite, K., Steinhagen, A., Philippou-Massier, J., Shevchenko, A., Hoch, M., Ejsing, C.S., and Thiele, C. (2014). Two different pathways of phosphatidylcholine synthesis, the Kennedy Pathway and the Lands Cycle, differentially regulate cellular triacylglycerol storage. BMC Cell Biol. *15*, 43.

Moldavski, O., Amen, T., Levin-Zaidman, S., Eisenstein, M., Rogachev, I., Brandis, A., Kaganovich, D., and Schuldiner, M. (2015). Lipid Droplets Are Essential for Efficient Clearance of Cytosolic Inclusion Bodies. Dev. Cell *33*, 603–610.

Molenaar, M.R., Vaandrager, A.B., and Helms, J.B. (2017). Some lipid droplets are more equal than others: Different metabolic lipid droplet pools in hepatic stellate cells. Lipid Insights *10*, 10–12.

Mori, E., Fujikura, J., Noguchi, M., Nakao, K., Matsubara, M., Sone, M., Taura, D., Kusakabe, T., Ebihara, K., Tanaka, T., et al. (2016). Impaired adipogenic capacity in induced pluripotent stem cells from lipodystrophic patients with BSCL2 mutations. Metabolism. *65*, 543–556.

Morishita, H., Zhao, Y.G., Tamura, N., and Nishimura, T. (2019). A critical role of VMP1 in lipoprotein secretion. Elife *8*, 1–24.

Murphy, S., Martin, S., and Parton, R.G. (2010). Quantitative analysis of lipid droplet fusion: inefficient steady state fusion but rapid stimulation by chemical fusogens. PLoS One *5*, e15030.

Nguyen, T.B., Louie, S.M., Daniele, J.R., Tran, Q., Dillin, A., Zoncu, R., Nomura, D.K., and Olzmann, J.A. (2017). DGAT1-Dependent Lipid Droplet Biogenesis Protects Mitochondrial Function during Starvation-Induced Autophagy. Dev. Cell *42*, 9-21.e5.

Nishimura, K., Fukagawa, T., Takisawa, H., Kakimoto, T., and Kanemaki, M. (2009). An auxin-based degron system for the rapid depletion of proteins in nonplant cells. Nat. Methods *6*, 917–922.

Nishiyama, A., Yagi, M., Awano, H., Okizuka, Y., Maeda, T., Yoshida, S., Takeshima, Y., and Matsuo, M. (2009). Two Japanese infants with congenital generalized lipodystrophy due to BSCL2 mutations. Pediatr. Int. *51*, 775–779.

Ohsaki, Y., Cheng, J., Suzuki, M., Fujita, A., and Fujimoto, T. (2008). Lipid droplets are arrested in the ER membrane by tight binding of lipidated apolipoprotein B-100. J. Cell Sci. *121*, 2415–2422.

Ohsaki, Y., Kawai, T., Yoshikawa, Y., Cheng, J., Jokitalo, E., and Fujimoto, T. (2016). PML isoform II plays a critical role in nuclear lipid droplet formation. *212*.

Olzmann, J.A., and Carvalho, P. (2019). Dynamics and functions of lipid droplets. Nat. Rev. Mol. Cell Biol. *20*, 137–155.

Olzmann, J.A., and Kopito, R.R. (2011). Lipid droplet formation is dispensable for endoplasmic reticulum-associated degradation. J. Biol. Chem. *286*, 27872–27874.

Olzmann, J. a, Richter, C.M., and Kopito, R.R. (2013). Spatial regulation of UBXD8 and p97/VCP controls ATGL-mediated lipid droplet turnover. Proc. Natl. Acad. Sci. *110*.

Ozeki, S., Cheng, J., Tauchi-Sato, K., Hatano, N., Taniguchi, H., and Fujimoto, T. (2005). Rab18 localizes to lipid droplets and induces their close apposition to the endoplasmic reticulum-derived membrane. J. Cell Sci. *118*, 2601–2611.

Paar, M., Jüngst, C., Steiner, N. a, Magnes, C., Sinner, F., Kolb, D., Lass, A., Zimmermann, R., Zumbusch, A., Kohlwein, S.D., et al. (2012). Remodeling of lipid droplets during lipolysis and growth in adipocytes. J. Biol. Chem. *287*, 11164–11173.

Pagac, M., Cooper, D.E., Qi, Y., Lukmantara, I.E., Mak, H.Y., Wu, Z., Tian, Y., Liu, Z., Lei, M., Du, X., et al. (2016). SEIPIN Regulates Lipid Droplet Expansion and Adipocyte Development by Modulating the Activity of Glycerol-3-phosphate Acyltransferase. Cell Rep. *17*, 1546–1559.

Palomer, X., Pizarro-Delgado, J., Barroso, E., and Vázquez-Carrera, M. (2018). Palmitic and Oleic Acid: The Yin and Yang of Fatty Acids in Type 2 Diabetes Mellitus. Trends Endocrinol. Metab. *29*, 178–190.

Papadopoulos, C., Orso, G., Mancuso, G., Herholz, M., Gumeni, S., Tadepalle, N., Jüngst, C., Tzschichholz, A., Schauss, A., Höning, S., et al. (2015). Spastin binds to lipid droplets and affects lipid metabolism. PLoS Genet. *11*, e1005149.

Payne, F., Lim, K., Girousse, A., Brown, R.J., Kory, N., Robbins, A., Xue, Y., Sleigh, A., Cochran, E., Adams, C., et al. (2014). Mutations disrupting the Kennedy phosphatidylcholine pathway in humans with congenital lipodystrophy and fatty liver disease. Proc. Natl. Acad. Sci. U. S. A. *111*, 8901–8906.

Payne, V.A., Grimsey, N., Tuthill, A., Virtue, S., Gray, S.L., Nora, E.D., Semple, R.K., Rahilly, S.O., and Rochford, J.J. (2008). The Human Lipodystrophy Gene BSCL2 / Seipin May Be Essential for Normal Adipocyte Differentiation. Diabetes *57*, 2055–60,2008.

Pennetta, G., and Welte, M.A. (2018). Emerging Links between Lipid Droplets and Motor Neuron Diseases. Dev. Cell *45*, 427–432.

Penno, A., Hackenbroich, G., and Thiele, C. (2013). Phospholipids and lipid droplets. Biochim. Biophys. Acta - Mol. Cell Biol. Lipids *1831*, 589–594.

Pereira-Dutra, F.S., Teixeira, L., Souza Costa, M.F., and Bozza, P.T. (2019). Fat, fight, and beyond: The multiple roles of lipid droplets in infections and inflammation. J. Leukoc. Biol. JLB.4MR0119-035R.

Péterfy, M., Phan, J., Xu, P., and Reue, K. (2001). Lipodystrophy in the fld mouse results from mutation of a new gene encoding a nuclear protein, lipin. Nat. Genet. *27*, 121–124.

Petschnigg, J., Wolinski, H., Kolb, D., Zelling, G., Kurat, C.F., Natter, K., and Kohlwein, S.D. (2009). Good fat, essential cellular requirements for triacylglycerol synthesis to maintain membrane homeostasis in yeast. J. Biol. Chem. *284*, 30981–30993.

Pezeshkian, W., Chevrot, G., and Khandelia, H. (2017). The role of Caveolin-1 in Lipid Droplets and their Biogenesis. Chem. Phys. Lipids.

Pfisterer, S.G., Gateva, G., Horvath, P., Pirhonen, J., Salo, V.T., Karhinen, L., Varjosalo, M., Ryhänen, S.J., Lappalainen, P., and Ikonen, E. (2017). Role for formin-like 1-dependent acto-myosin assembly in lipid droplet dynamics and lipid storage. Nat. Commun. *8*, 14858.

Pinder, J., Salsman, J., and Dellaire, G. (2015). Nuclear domain "knock-in" screen for the evaluation and identification of small molecule enhancers of CRISPR-based genome editing. Nucleic Acids Res. *43*, 9379–9392.

Ploegh, H.L. (2007). A lipid-based model for the creation of an escape hatch from the endoplasmic reticulum. Nature *448*, 435–438.

Pol, A., Gross, S.P., and Parton, R.G. (2014). Review: biogenesis of the multifunctional lipid droplet: lipids, proteins, and sites. J. Cell Biol. *204*, 635–646.

Poppelreuther, M., Sander, S., Minden, F., Dietz, M.S., Exner, T., Du, C., Zhang, I., Ehehalt, F., Knüppel, L., Domschke, S., et al. (2018). The metabolic capacity of lipid droplet localized acyl-CoA synthetase 3 is not sufficient to support local triglyceride synthesis independent of the endoplasmic reticulum in A431 cells. Biochim. Biophys. Acta - Mol. Cell Biol. Lipids *1863*, 614–624.

Prieur, X., Dollet, L., Takahashi, M., Nemani, M., Pillot, B., Le May, C., Mounier, C., Takigawa-Imamura, H., Zelenika, D., Matsuda, F., et al. (2013). Thiazolidinediones partially reverse the metabolic disturbances observed in Bscl2/seipin-deficient mice. Diabetologia *56*, 1813–1825.

Pyc, M., Cai, Y., Greer, M.S., Yurchenko, O., Chapman, K.D., Dyer, J.M., and Mullen, R.T. (2017). Turning Over a New Leaf in Lipid Droplet Biology. Trends Plant Sci. *22*, 596–609.

Qi, Y., Sun, L., and Yang, H. (2017). Lipid Droplet Growth and Adipocyte Development: Mechanistically Distinct Processes Connected by Phospholipids. Biochim. Biophys. Acta - Mol. Cell Biol. Lipids *1862*, 1273–1283.

Qiu, B., Ackerman, D., Sanchez, D.J., Li, B., Ochocki, J.D., Grazioli, A., Bobrovnikova-Marjon, E., Alan Diehl, J., Keith, B., and Celeste Simon, M. (2016). HIF2α-dependent lipid storage promotes endoplasmic reticulum homeostasis in clear-cell renal cell carcinoma. Cancer Discov. *5*, 653–667.

Radulovic, M., Knittelfelder, O., Cristobal-Sarramian, A., Kolb, D., Wolinski, H., and Kohlwein, S.D. (2013). The emergence of lipid droplets in yeast: Current status and experimental approaches. Curr. Genet. *59*, 231–242.

Rambold, A.S., Cohen, S., and Lippincott-Schwartz, J. (2015). Fatty Acid Trafficking in Starved Cells: Regulation by Lipid Droplet Lipolysis, Autophagy, and Mitochondrial Fusion Dynamics. Dev. Cell *32*, 678–692.

Ran, F.A., Hsu, P.D., Wright, J., Agarwala, V., Scott, D. a, and Zhang, F. (2013). Genome engineering using the CRISPR-Cas9 system. Nat. Protoc. *8*, 2281–2308.

Rao, K., Stone, M.C., Weiner, A.T., Gheres, K.W., Zhou, C., Deitcher, D.L., Levitan, E.S., and Rolls, M.M. (2016). Spastin, atlastin, and ER relocalization are involved in axon but not dendrite regeneration. Mol. Biol. Cell *27*, 3245–3256.

Renvoisé, B., Malone, B., Falgairolle, M., Munasinghe, J., Stadler, J., Sibilla, C., Park, S.H., and Blackstone, C. (2016). Reep1 null mice reveal a converging role for hereditary spastic paraplegia proteins in lipid droplet regulation. Hum. Mol. Genet. *25*, 5111–5125.

Robenek, H., Hofnagel, O., Buers, I., Robenek, M.J., Troyer, D., and Severs, N.J. (2006). Adipophilin-enriched domains in the ER membrane are sites of lipid droplet biogenesis. J. Cell Sci. *119*, 4215–4224.

Romanauska, A., and Köhler, A. (2018). The Inner Nuclear Membrane Is a Metabolically Active Territory that Generates Nuclear Lipid Droplets. Cell *174*, 700–715.

Rothbauer, U., Zolghadr, K., Tillib, S., Nowak, D., Schermelleh, L., Gahl, A., Backmann, N., Conrath, K., Muyldermans, S., Cardoso, M.C., et al. (2006). Targeting and tracing antigens in live cells with fluorescent nanobodies. Nat. Methods *3*, 887–889.

Rowe, E.R., Mimmack, M.L., Barbosa, A.D., Haider, A., Isaac, I., Ouberai, M.M., Thiam, A.R., Patel, S., Saudek, V., Siniossoglou, S., et al. (2016). Conserved amphipathic helices mediate lipid droplet targeting of perilipins 1-3. J. Biol. Chem. *291*, 6664–6678.

Rubio-Cabezas, O., Puri, V., Murano, I., Saudek, V., Semple, R.K., Dash, S., Hyden, C.S.S., Bottomley, W., Vigouroux, C., Magré, J., et al. (2009). Partial lipodystrophy and insulin resistant diabetes in a patient with a homozygous nonsense mutation in CIDEC. EMBO Mol. Med. *1*, 280–287.

Ruggiano, A., Mora, G., Buxó, L., and Carvalho, P. (2016). Spatial control of lipid droplet proteins by the ERAD ubiquitin ligase Doa10. EMBO J. *35*, 1644–1655.

Ruiz-Riquelme, A., Sánchez-Iglesias, S., Rábano, A., Guillén-Navarro, E., Domingo-Jiménez, R., Ramos, A., Rosa, I., Senra, A., Nilsson, P., García, Á., et al. (2015). Larger aggregates of mutant seipin in Celia's Encephalopathy, a new protein misfolding

neurodegenerative disease. Neurobiol. Dis. *83*, 44–53.
Salo, V.T., and Ikonen, E. (2019). Moving out but keeping in touch: contacts between endoplasmic reticulum and lipid droplets. Curr. Opin. Cell Biol. *57*, 64–70.
Salo, V.T., and Ikonen, E. (2020). Kuinka solut varastoivat rasvaa? Duodecim *136*, 487–95.
Salo, V., Li, S., Vihinen, H., Hölttä-Vuori, M., Szkalisity, A., Horvath, P., Belevich, I., Peränen, J., Thiele, C., Somerharju, P., et al. (2019). Seipin facilitates triglyceride flow to lipid droplet and counteracts droplet ripening via ER contact. Dev. Cell *50*, 1–16.
Salo, V.T., Belevich, I., Li, S., Karhinen, L., Vihinen, H., Vigouroux, C., Magré, J., Thiele, C., Hölttä-Vuori, M., Jokitalo, E., et al. (2016). Seipin regulates ER–lipid droplet contacts and cargo delivery. EMBO J. *24*, 2699–2716.
Sánchez-Iglesias, S., Unruh-Pinheiro, A., Guillín-Amarelle, C., González-Méndez, B., Ruiz-Riquelme, A., Rodríguez-Cañete, B.L., Rodríguez-García, S., Guillén-Navarro, E., Domingo-Jiménez, R., and Araújo-Vilar, D. (2016). Skipped BSCL2 transcript in celia's encephalopathy (PELD): New insights on fatty acids involvement, senescence and adipogenesis. PLoS One *11*, 1–13.
Sánchez-Iglesias, S., Crocker, M., O'Callaghan, M., Darling, A., García-Cazorla, A., Domingo-Jiménez, R., Castro, A., Fernández-Pombo, A., Ruibal, Á., Aguiar, P., et al. (2019). Celia's encephalopathy and c.974dupG in BSCL2 gene: a hidden change in a known variant. Neurogenetics *20*, 73–82.
Sarmento, A.S.C., De Azevedo Medeiros, L.B., Agnez-Lima, L.F., Lima, J.G., and De Melo Campos, J.T.A. (2018). Exploring seipin: From biochemistry to bioinformatics predictions. Int. J. Cell Biol. *2018*, 5207608.
Schott, M.B., Weller, S.G., Schulze, R.J., Krueger, E.W., Drizyte-Miller, K., Casey, C.A., and McNiven, M.A. (2019). Lipid droplet size directs lipolysis and lipophagy catabolism in hepatocytes. J. Cell Biol. *218*, 3320–3335.
Schroeder, B., Schulze, R.J., Weller, S.G., Sletten, A.C., Casey, C.A., and McNiven, M.A. (2015). The small GTPase Rab7 as a central regulator of hepatocellular lipophagy. Hepatology *61*, 1896–1907.
Schuldiner, M., and Bohnert, M. (2017). A different kind of love - lipid droplet contact sites. Biochim. Biophys. Acta - Mol. Cell Biol. Lipids *1862*, 1188–1196.
Schulze, R.J., Sathyanarayan, A., and Mashek, D.G. (2017). Breaking fat: The regulation and mechanisms of lipophagy. Biochim. Biophys. Acta - Mol. Cell Biol. Lipids *1862*, 1178–1187.
Schweiger, M., Schreiber, R., Haemmerle, G., Lass, A., Fledelius, C., Jacobsen, P., Tornqvist, H., Zechner, R., and Zimmermann, R. (2006). Adipose triglyceride lipase and hormone-sensitive lipase are the major enzymes in adipose tissue triacylglycerol catabolism. J. Biol. Chem. *281*, 40236–40241.
Seip, M. (1959). Lipodystrophy and gigantism with associated endocrine manifestations. A new diencephalic syndrome? Acta Paediatr. *48*.
Senkal, C.E., Salama, M.F., Snider, A.J., Allopenna, J.J., Rana, N.A., Koller, A., Hannun, Y.A., and Obeid, L.M. (2017). Ceramide Is Metabolized to Acylceramide and Stored in Lipid Droplets. Cell Metab. *25*, 686–697.
Seo, A.Y., Lau, P.W., Feliciano, D., Sengupta, P., Le Gros, M.A., Cinquin, B., Larabell, C.A., and Lippincott-Schwartz, J. (2017). AMPK and vacuole-associated Atg14p orchestrate μ-lipophagy for energy production and long-term survival under glucose starvation. Elife *6*, 1–27.
Shastry, S., Delgado, M.R., Dirik, E., Turkmen, M., Agarwal, A.K., and Garg, A. (2010). Congenital generalized lipodystrophy, type 4 (CGL4) associated with myopathy due to novel PTRF mutations. Am. J. Med. Genet. Part A *152*, 2245–2253.
Shpilka, T., Welter, E., Borovsky, N., Amar, N., Mari, M., and Reggiori, F. (2015). Lipid droplets and their component triglycerides and steryl esters regulate autophagosome biogenesis. EMBO J. *34*, 2117–2131.
Sim, M.F.M., Dennis, R.J., Aubry, E.M., Ramanathan, N., Sembongi, H., Saudek, V., Ito, D., O'Rahilly, S., Siniossoglou, S., and Rochford, J.J. (2012). The human lipodystrophy protein seipin is an ER membrane adaptor for the adipogenic PA phosphatase lipin 1. Mol. Metab. *2*, 38–46.
Sim, M.F.M., Talukder, M.M.U., Dennis, R.J., O'Rahilly, S., Edwardson, J.M., and Rochford, J.J. (2013). Analysis of naturally occurring mutations in the human lipodystrophy protein seipin reveals multiple potential pathogenic mechanisms. Diabetologia *56*, 2498–2506.
Simha, V., and Garg, A. (2003). Phenotypic Heterogeneity in Body Fat Distribution in Patients with Congenital Generalized Lipodystrophy Caused by Mutations in the AGPAT2 or Seipin Genes. J. Clin. Endocrinol. Metab. *88*, 5433–5437.
Singh, R., Kaushik, S., Wang, Y., Xiang, Y., Novak, I., Komatsu, M., Tanaka, K., Cuervo, A.M., and Czaja, M.J. (2009). Autophagy regulates lipid metabolism. Nature *458*, 1131–1135.
Skinner, J.R., Shew, T.M., Schwartz, D.M., Tzekov, A., Lepus, C.M., Abumrad, N.A., and Wolins, N.E. (2009). Diacylglycerol Enrichment of Endoplasmic Reticulum or Lipid Droplets Recruits Perilipin 3 / TIP47 during Lipid Storage. *284*, 30941–30948.
Slayton, M., Gupta, A., Balakrishnan, B., and Puri, V. (2019). CIDE Proteins in Human Health and Disease. Cells *8*, 238.
Sosa, B.A., Rothballer, A., Kutay, U., and Schwartz, T.U. (2012). LINC complexes form by binding of three KASH peptides to domain interfaces of trimeric SUN proteins. Cell *149*, 1035–1047.
Spandl, J., White, D.J., Peychl, J., and Thiele, C. (2009). Live cell multicolor imaging of lipid droplets with a new dye, LD540. Traffic *10*, 1579–1584.

Stone, S.J., Levin, M.C., Zhou, P., Han, J., Walther, T.C., and Farese, R. V (2009). The endoplasmic reticulum enzyme DGAT2 is found in mitochondria-associated membranes and has a mitochondrial targeting signal that promotes its association with mitochondria. J. Biol. Chem. *284*, 5352–5361.

Subramanian, V., Rotlienberg, A., Gomez, C., Cohen, A.W., Garcia, A., Bhattacharyya, S., Shapiro, L., Dolios, G., Wang, R., Lisanti, M.P., et al. (2004). Perilipin A mediates the reversible binding of CGI-58 to lipid droplets in 3T3-L1 adipocytes. J. Biol. Chem. *279*, 42062–42071.

Sui, X., Arlt, H., Kelly, B., Zong, L., Frank, D., Debora, M., Maofu, L., Jr, R.V.F., and Walther, T.C.. (2018). Cryo-electron microscopy structure of the lipid droplet-formation protein seipin. J. Cell Biol. *217*, 4080–4091.

Sun, X., Zhang, A., Baker, B., Sun, L., Howard, A., Buswell, J., Maurel, D., Masharina, A., Johnsson, K., Noren, C.J., et al. (2011). Development of SNAP-tag fluorogenic probes for wash-free fluorescence imaging. ChemBioChem *12*, 2217–2226.

Suzuki, M., Murakami, T., Cheng, J., Kano, H., Fukata, M., and Fujimoto, T. (2015). ELMOD2 is anchored to lipid droplets by palmitoylation and regulates adipocyte triglyceride lipase recruitment. Mol. Biol. Cell *26*, 2333–2342.

Sztalryd, C., and Brasaemle, D.L. (2017). The perilipin family of lipid droplet proteins: Gatekeepers of intracellular lipolysis. Biochim. Biophys. Acta - Mol. Cell Biol. Lipids *1862*, 1221–1232.

Sztalryd, C., Xu, G., Dorward, H., Tansey, J.T., Contreras, J.A., Kimmel, A.R., and Londos, C. (2003). Perilipin A is essential for the translocation of hormone-sensitive lipase during lipolytic activation. J. Cell Biol. *161*, 1093–1103.

Szymanski, K.M., Binns, D., Bartz, R., Grishin, N. V, Li, W., Agarwal, A.K., Garg, A., Anderson, R.G.W., and Goodman, J.M. (2007). The lipodystrophy protein seipin is found at endoplasmic reticulum lipid droplet junctions and is important for droplet morphology. Proc. Natl. Acad. Sci. U. S. A. *104*, 20890–20895.

Takeuchi, K., and Reue, K. (2009). Biochemistry, physiology, and genetics of GPAT, AGPAT, and lipin enzymes in triglyceride synthesis. Am. J. Physiol. - Endocrinol. Metab. *296*.

Talukder, M.M.U., Sim, M.F.M., O'Rahilly, S., Edwardson, J.M., and Rochford, J.J. (2015). Seipin oligomers can interact directly with AGPAT2 and lipin 1, physically scaffolding critical regulators of adipogenesis. Mol. Metab. *4*, 199–209.

Tan, K., Kimber, W.A., Luan, J., Soos, M.A., Semple, R.K., Wareham, N.J., O'Rahilly, S., and Barroso, I. (2007a). Analysis of genetic variation in Akt2/PKB-β in severe insulin resistance, lipodystrophy, type 2 diabetes, and related metabolic phenotypes. Diabetes *56*, 714–719.

Tan, X., Calderon-Villalobos, L.I.A., Sharon, M., Zheng, C., Robinson, C. V., Estelle, M., and Zheng, N. (2007b). Mechanism of auxin perception by the TIR1 ubiquitin ligase. Nature *446*, 640–645.

Targett-Adams, P., Chambers, D., Gledhill, S., Hope, R.G., Coy, J.F., Girod, A., and McLauchlan, J. (2003). Live cell analysis and targeting of the lipid droplet-binding adipocyte differentiation-related protein. J. Biol. Chem. *278*, 15998–16007.

Tauchi-Sato, K., Ozeki, S., Houjou, T., Taguchi, R., and Fujimoto, T. (2002). The surface of lipid droplets is a phospholipid monolayer with a unique Fatty Acid composition. J. Biol. Chem. *277*, 44507–44512.

Teixeira, V., Johnsen, L., Martínez-Montañés, F., Grippa, A., Buxó, L., Idrissi, F.Z., Ejsing, C.S., and Carvalho, P. (2018). Regulation of lipid droplets by metabolically controlled Ldo isoforms. J. Cell Biol. *217*, 127–138.

Temprano, A., Sembongi, H., Han, G.S., Sebastián, D., Capellades, J., Moreno, C., Guardiola, J., Wabitsch, M., Richart, C., Yanes, O., et al. (2016). Redundant roles of the phosphatidate phosphatase family in triacylglycerol synthesis in human adipocytes. Diabetologia *59*, 1985–1994.

Tharp, K.M., Kang, M.S., Timblin, G.A., Dempersmier, J., Dempsey, G.E., Zushin, P.J.H., Benavides, J., Choi, C., Li, C.X., Jha, A.K., et al. (2018). Actomyosin-Mediated Tension Orchestrates Uncoupled Respiration in Adipose Tissues. Cell Metab. *27*, 602-615.e4.

Thiam, A.R., and Beller, M. (2017). The why, when and how of lipid droplet diversity. J. Cell Sci. *130*, 315–324.

Thiam, A.R., and Forêt, L. (2016). The physics of lipid droplet nucleation, growth and budding. Biochim. Biophys. Acta - Mol. Cell Biol. Lipids *1861*, 715–722.

Thiam, A.R., Farese, R. V, and Walther, T.C. (2013a). The biophysics and cell biology of lipid droplets. Nat. Rev. Mol. Cell Biol. *14*, 775–786.

Thiam, A.R., Antonny, B., Wang, J., Delacotte, J., Wilfling, F., Walther, T.C., Beck, R., Rothman, J.E., and Pincet, F. (2013b). COPI buds 60-nm lipid droplets from reconstituted water-phospholipid-triacylglyceride interfaces, suggesting a tension clamp function. Proc. Natl. Acad. Sci. U. S. A. *110*, 13244–13249.

Thiele, C., Papan, C., Hoelper, D., Kusserow, K., Gaebler, A., Schoene, M., Piotrowitz, K., Lohmann, D., Spandl, J., Stevanovic, A., et al. (2012). Tracing fatty acid metabolism by click chemistry. ACS Chem. Biol. *7*, 2004–2011.

Tian, Y., Bi, J., Shui, G., Liu, Z., Xiang, Y., Liu, Y., Wenk, M.R., Yang, H., and Huang, X. (2011). Tissue-autonomous function of Drosophila seipin in preventing ectopic lipid droplet formation. PLoS Genet. *7*, e1001364.

To, M., Peterson, C.W.H., Roberts, M.A., Counihan, J.L., Wu, T.T., Forster, M.S., Nomura, D.K., and Olzmann, J.A. (2017). Lipid disequilibrium disrupts ER proteostasis by impairing ERAD substrate glycan trimming and dislocation. Mol. Biol. Cell *28*, 270–284.

Tsuji, T., Cheng, J., Tatematsu, T., Ebata, A., Kamikawa, H., Fujita, A., Gyobu, S., Segawa, K., Arai, H., Taguchi, T., et al.

(2019). Predominant localization of phosphatidylserine at the cytoplasmic leaflet of the ER, and its TMEM16K-dependent redistribution. Proc. Natl. Acad. Sci. 201822025.

U, C.L., Brasaemle, D.L., Schultz, C.J., Segrest, J.P., and Kimmel, A.R. (1999). Perilipins, ADRP, and other proteins that associate with intracellular neutral lipid droplets in animal cells. Semin Cell Dev Biol *10*, 51–58.

Valm, A.M., Cohen, S., Legant, W.R., Melunis, J., Hershberg, U., Wait, E., Cohen, A.R., Davidson, M.W., Betzig, E., and Lippincott-Schwartz, J. (2017). Applying Systems-level Spectral Imaging and Analysis to Reveal the Organelle Interactome. Nature *546*, 162–167.

Vance, J.E. (2015). Phospholipid Synthesis and Transport in Mammalian Cells. Traffic *16*, 1–18.

Velázquez, A.P., Tatsuta, T., Ghillebert, R., Drescher, I., and Graef, M. (2016). Lipid droplet-mediated ER homeostasis regulates autophagy and cell survival during starvation. J. Cell Biol. *212*, 621–631.

Victoria, B., Cabezas-Agrícola, J.M., González-Méndez, B., Lattanzi, G., Del Coco, R., Loidi, L., Barreiro, F., Calvo, C., Lado-Abeal, J., and Araújo-Vilar, D. (2010). Reduced adipogenic gene expression in fibroblasts from a patient with type 2 congenital generalized lipodystrophy. Diabet. Med. *27*, 1178–1187.

Vieyres, G., and Pietschmann, T. (2019). HCV Pit Stop at the Lipid Droplet: Refuel Lipids and Put on a Lipoprotein Coat before Exit. Cells *8*, 233.

Vigouroux, C., Caron-Debarle, M., Le Dour, C., Magré, J., and Capeau, J. (2011). Molecular mechanisms of human lipodystrophies: From adipocyte lipid droplet to oxidative stress and lipotoxicity. Int. J. Biochem. Cell Biol. *43*, 862–876.

Walther, T., and Farese, R. V (2012). Lipid droplets and cellular lipid metabolism. Annu. Rev. Biochem. 687–714.

Walther, T., Chung, J., and Farese, R. V (2017). Lipid Droplet Biogenesis. Annu. Rev. Cell Dev. Biol. *33*, 491–510.

Wang, C.-W., Miao, Y.-H., and Chang, Y.-S. (2014). Control of lipid droplet size in budding yeast requires the collaboration between Fld1 and Ldb16. J. Cell Sci. *127*, 1214–1228.

Wang, H., Sreenivasan, U., Sreenevasan, U., Hu, H., Saladino, A., Polster, B.M., Lund, L.M., Gong, D., Stanley, W.C., and Sztalryd, C. (2011). Perilipin 5, a lipid droplet-associated protein, provides physical and metabolic linkage to mitochondria. J. Lipid Res. *52*, 2159–2168.

Wang, H., Becuwe, M., Housden, B.E., Chitraju, C., Porras, A.J., Graham, M.M., Liu, X.N., Thiam, A.R., Savage, D.B., Agarwal, A.K., et al. (2016a). Seipin is required for converting nascent to mature lipid droplets. Elife *5*, 133–150.

Wang, H., Airola, M. V., and Reue, K. (2017). How lipid droplets "TAG" along: Glycerolipid synthetic enzymes and lipid storage. Biochim. Biophys. Acta - Mol. Cell Biol. Lipids *1862*, 1131–1145.

Wang, L., Hong, J., Wu, Y., Liu, G., Yu, W., and Chen, L. (2018a). Seipin deficiency in mice causes loss of dopaminergic neurons via aggregation and phosphorylation of α-synuclein and neuroinflammation. Cell Death Dis. *9*, 440.

Wang, M., Gao, M., Liao, J., Qi, Y., Du, X., Wang, Y., Li, L., Liu, G., and Yang, H. (2016b). Adipose tissue deficiency results in severe hyperlipidemia and atherosclerosis in the low-density lipoprotein receptor knockout mice. Biochim. Biophys. Acta - Mol. Cell Biol. Lipids *1861*, 410–418.

Wang, S., Idrissi, F.Z., Hermansson, M., Grippa, A., Ejsing, C.S., and Carvalho, P. (2018b). Seipin and the membrane-shaping protein Pex30 cooperate in organelle budding from the endoplasmic reticulum. Nat. Commun. *9*, 1–12.

Weber-Boyvat, M., Kentala, H., Peränen, J., and Olkkonen, V.M. (2015). Ligand-dependent localization and function of ORP-VAP complexes at membrane contact sites. Cell. Mol. Life Sci. *72*, 1967–1987.

Wee, K., Yang, W., Sugii, S., and Han, W. (2014). Towards a mechanistic understanding of lipodystrophy and seipin functions. Biosci. Rep. *34*, 583–591.

Wei, S., Soh, S.L.Y., Qiu, W., Yang, W., Seah, C.J.Y., Guo, J., Ong, W.Y., Pang, Z.P., and Han, W. (2013). Seipin regulates excitatory synaptic transmission in cortical neurons. J. Neurochem. *124*, 478–489.

Welte, M. a (2015). Expanding roles for lipid droplets. Curr. Biol. *25*, R470-81.

Wilfling, F., Wang, H., Haas, J.T., Krahmer, N., Gould, T.J., Uchida, A., Cheng, J.-X., Graham, M., Christiano, R., Fröhlich, F., et al. (2013). Triacylglycerol synthesis enzymes mediate lipid droplet growth by relocalizing from the ER to lipid droplets. Dev. Cell *24*, 384–399.

Wilfling, F., Thiam, A.R., Olarte, M.-J., Wang, J., Beck, R., Gould, T.J., Allgeyer, E.S., Pincet, F., Bewersdorf, J., Farese, R. V, et al. (2014). Arf1/COPI machinery acts directly on lipid droplets and enables their connection to the ER for protein targeting. Elife *3*, e01607.

Windpassinger, C., Auer-Grumbach, M., Irobi, J., Patel, H., Petek, E., Hörl, G., Malli, R., Reed, J.A., Dierick, I., Verpoorten, N., et al. (2004). Heterozygous missense mutations in BSCL2 are associated with distal hereditary motor neuropathy and Silver syndrome. Nat. Genet. *36*, 271–276.

Wolinski, H., Kolb, D., Hermann, S., Koning, R.I., and Kohlwein, S.D. (2011). A role for seipin in lipid droplet dynamics and inheritance in yeast. J. Cell Sci. *124*, 3894–3904.

Wolinski, H., Hofbauer, H.F., Hellauer, K., Cristobal-Sarramian, A., Kolb, D., Radulovic, M., Knittelfelder, O.L., Rechberger, G.N., and Kohlwein, S.D. (2015). Seipin is involved in the regulation of phosphatidic acid metabolism at a subdomain of the nuclear envelope in yeast. Biochim. Biophys. Acta - Mol. Cell Biol. Lipids *1851*, 1450–1464.

Wu, Y.R., Hung, S.I., Chang, Y.C., Chen, S.T., Lin, Y.L., and Chung, W.H. (2009). Complementary mutations in seipin gene in a patient with Berardinelli-Seip congenital lipodystrophy and dystonia: Phenotype variability suggests multiple roles of seipin gene. J. Neurol. Neurosurg. Psychiatry *80*, 1180–1181.

Xu, D., Li, Y., Wu, L., Li, Y., Zhao, D., Yu, J., Huang, T., Ferguson, C., Parton, R.G., Yang, H., et al. (2018). Rab18 promotes lipid droplet (LD) growth by tethering the ER to LDs through SNARE and NRZ interactions. J. Cell Biol. *217*, 975–995.

Xu, N., Zhang, S.O., Cole, R. a, McKinney, S. a, Guo, F., Haas, J.T., Bobba, S., Farese, R. V, and Mak, H.Y. (2012). The FATP1-DGAT2 complex facilitates lipid droplet expansion at the ER-lipid droplet interface. J. Cell Biol. *198*, 895–911.

Xu, S., Benoff, B., Liou, H.L., Lobel, P., and Stock, A.M. (2007). Structural basis of sterol binding by NPC2, a lysosomal protein deficient in Niemann-Pick type C2 disease. J. Biol. Chem. *282*, 23525–23531.

Yagi, T., Ito, D., Nihei, Y., Ishihara, T., and Suzuki, N. (2011). N88S seipin mutant transgenic mice develop features of seipinopathy/BSCL2-related motor neuron disease via endoplasmic reticulum stress. Hum. Mol. Genet. *20*, 3831–3840.

Yamaguchi, T., Omatsu, N., Matsushita, S., and Osumi, T. (2004). CGI-58 Interacts with Perilipin and Is Localized to Lipid Droplets. J. Biol. Chem. *279*, 30490–30497.

Yan, R., Qian, H., Lukmantara, I., Gao, M., Du, X., Yan, N., and Yang, H. (2018). Human SEIPIN Binds Anionic Phospholipids. Dev. Cell *47*, 1–9.

Yang, W., Thein, S., Guo, X., Xu, F., Venkatesh, B., Sugii, S., Radda, G.K., and Han, W. (2013). Seipin differentially regulates lipogenesis and adipogenesis through a conserved core sequence and an evolutionarily acquired C-terminus. Biochem. J. *452*, 37–44.

Yang, W., Thein, S., Wang, X., Bi, X., Ericksen, R.E., Xu, F., and Han, W. (2014). BSCL2/seipin regulates adipogenesis through actin cytoskeleton remodelling. Hum. Mol. Genet. *23*, 502–513.

Yen, C.L.E., Stone, S.J., Koliwad, S., Harris, C., and Farese, R. V. (2008). DGAT enzymes and triacylglycerol biosynthesis. J. Lipid Res. *49*, 2283–2301.

Young, P.A., Senkal, C.E., Suchanek, A.L., Grevengoed, T.J., Lin, D.D., Zhao, L., Crunk, A.E., Klett, E.L., Füllekrug, J., Obeid, L.M., et al. (2018). Long-chain acyl-CoA synthetase 1 interacts with key proteins that activate and direct fatty acids into niche hepatic pathways. J. Biol. Chem. *293*, 16724–16740.

Zanghellini, J., Wodlei, F., and von Grünberg, H.H. (2010). Phospholipid demixing and the birth of a lipid droplet. J. Theor. Biol. *264*, 952–961.

Zechner, R., Kienesberger, P.C., Haemmerle, G., Zimmermann, R., and Lass, A. (2009). Adipose triglyceride lipase and the lipolytic catabolism of cellular fat stores. J. Lipid Res. *50*, 3–21.

Zechner, R., Madeo, F., and Kratky, D. (2017). Cytosolic lipolysis and lipophagy: Two sides of the same coin. Nat. Rev. Mol. Cell Biol. *18*, 671–684.

Zeharia, A., Shaag, A., Houtkooper, R.H., Hindi, T., de Lonlay, P., Erez, G., Hubert, L., Saada, A., de Keyzer, Y., Eshel, G., et al. (2008). Mutations in LPIN1 Cause Recurrent Acute Myoglobinuria in Childhood. Am. J. Hum. Genet. *83*, 489–494.

Zhou, H., Lei, X., Benson, T., Mintz, J., Xu, X., Harris, R.B., Weintraub, N.L., Wang, X., and Chen, W. (2015). Berardinelli-Seip congenital lipodystrophy 2 regulates adipocyte lipolysis, browning, and energy balance in adult animals. J. Lipid Res. *56*, 1912–1925.

Zhou, H., Lei, X., Yan, Y., Lydic, T., Li, J., Weintraub, N.L., Su, H., and Chen, W. (2019). Targeting ATGL to rescue BSCL2 lipodystrophy and its associated cardiomyopathy. JCI Insight *4*, e129781.

Zimmermann, R., Haemmerle, G., Schoiswohl, G., Birner-gruenberger, R., Riederer, M., Lass, A., Neuberger, G., and Eisenhaber, F. (2004). Fat Mobilization in Adipose Tissue Is Promoted by Adipose Triglyceride Lipase. Science (80-.). *306*, 1383–1386.

Zolotov, S., Xing, C., Mahamid, R., Shalata, A., Sheikh-Ahmad, M., and Garg, A. (2017). Homozygous LIPE mutation in siblings with multiple symmetric lipomatosis, partial lipodystrophy, and myopathy. Am. J. Med. Genet. Part A *173*, 190–194.